THE THERMAL DECOMPOSITION OF THE METHOXYMETHYL AND ETHYL RADICALS

by

Leon F. Loucks

A thesis submitted in partial fulfillment
of the requirements for the degree of
Doctor of Philosophy
in the
Department of Chemistry
University of Ottawa
Ottawa, Canada
February, 1967

K. J. Laidler
Professor of Chemistry
Research Supervisor

Leon F. Loucks
Ph.D. Candidate

To My Wife

PREFACE

This thesis is divided into a chapter of general introduction and six chapters on experimental work.

The general introduction provides the elementary background for understanding the objectives of the research which follows, and acquaints the reader with the reasons for conducting the work. The introduction also describes the advantages and disadvantages of the design of experiments in this field of research.

Chapter II deals with the mercury-photosensitized decomposition of dimethyl ether at moderate temperatures. The overall reaction mechanism is considered and the results of the present investigation are compared with those of previous studies.

Chapter III considers the unimolecular decomposition of the methoxymethyl radical to give a formaldehyde molecule and a methyl radical. Although this reaction has been studied briefly before, in recent years there has arisen considerable controversy regarding the kinetic order of the reaction. The present study was undertaken to examine the kinetics of this unimolecular reaction and to establish the Arrhenius parameters of the limiting high-pressure and low-pressure rate constants.

Chapters IV and V deal with the combination of two methyl radicals and the combination of a methyl radical with a methoxymethyl radical. Radical combination reactions

have been considered by a number of authors, with the combination of methyl radicals receiving frequent attention. The kinetics of the combination reaction can change from second to third order as the pressure is lowered. This pressure dependence is the critical feature which is examined for both of the reactions, and from the results certain conclusions regarding the reverse reactions can be drawn.

Chapter VI describes the work conducted to establish the heat of formation of the methoxymethyl radical. No heat of formation for this radical has been reported in the literature. This severely limits the thermochemical calculations which can be made for reactions involving this radical. Kinetic measurements, combined with other heat of formation data and with appearance potential measurements, lead to an evaluation of the heat of formation of the methoxymethyl radical and to the assignment of certain bond dissociation energies.

Chapter VII deals with the unimolecular decomposition of the ethyl radical to give an ethylene molecule and a hydrogen atom. In recent years the kinetic order of this decomposition has been examined indirectly but not in sufficient detail to establish conclusively the pressure dependence of the first-order rate coefficient. The activation energy has also been open to question since the observed values have been somewhat lower than expected

from thermochemical calculations. The present work examines the effects of pressure and temperature on this decomposition and leads to a more complete assessment of the kinetic behavior of the reaction.

ACKNOWLEDGMENTS

This research was conducted under the supervision of Professor K. J. Laidler. The author is indebted to him for many constructive discussions, for his patient interest and for his sincere criticism. The author is particularly grateful for his prompt and meticulous examination of this manuscript during its preparation.

The author extends thanks to Drs. M. H. Back, J. L. Holmes, and R. A. Back for their help in the design of apparatus and experiments as well as for helpful discussions on the interpretation of results. The assistance of Drs. S. Marantz and G. T. Armstrong of the National Bureau of Standards is gratefully acknowledged for the determination of a heat of combustion. The author also thanks Dr. F. P. Lossing for making available some unpublished results.

The author wishes to acknowledge the receipt of a National Research Council studentship and a Province of Ontario fellowship.

The encouragement of my wife has been an invaluable asset throughout the course of this work. The author thanks her for this encouragement and for her enduring understanding.

TABLE OF CONTENTS

LIST OF TABLES

LIST OF FIGURES

LIST OF PLATES

ABSTRACT

The Mercury-photosensitized Decomposition of Dimethyl Ether

The mercury-photosensitized decomposition of dimethyl ether was investigated from 200° to 300°C and over the pressure range of 3 to 600 mm Hg. Measurements were made of the initial rates of formation of the products of reaction, which are CO, H_2, C_2H_6, CH_4, $CH_3OC_2H_5$ and $CH_3OCH_2CH_2OCH_3$. It is concluded that the primary step involves a C-H split; there is no evidence for a primary C-O split. Over the range 200 to 300°C the methoxymethyl radical, CH_3OCH_2, decomposed to give formaldehyde and a methyl radical, while at 30°C no decomposition of the CH_3OCH_2 radical was detected. The mass balance is consistent with the mechanism proposed. The homogeneity of the reaction conditions was examined by varying the concentration of mercury in the reaction vessel.

The Thermal Decomposition of the Methoxymethyl Radical

The decomposition of the methoxymethyl radical, generated in the mercury-photosensitized decomposition of dimethyl ether, has been investigated over the temperature range 200 to 300°C and the pressure range 3 to 600 mm Hg. The radical decomposes to give a formaldehyde molecule and a methyl radical. The effects of pressure and temperature on the first-order rate coefficient for the decomposition of the methoxymethyl radical have been examined in detail.

The rate coefficient shows a pressure dependence over the full pressure range studied. The order of the decomposition is about 1.4 at the middle of the pressure range studied, with a lower order at higher pressures and a higher order at lower pressures. At 100 mm Hg the observed activation energy for the decomposition of the methoxymethyl radical is 24.8 kcal per mole.

The first-order and second-order rate coefficients, k^{∞} and k^{0}, corresponding to the limiting conditions of high pressures and low pressures respectively, have been evaluated as

$$k^{\infty} = 2.0 \times 10^{13} e^{-25,500/RT} \text{ sec}^{-1}$$

$$k^{0} = 2.8 \times 10^{16} e^{-18,100/RT} \text{ cc mole}^{-1} \text{ sec}^{-1}.$$

Kassel integrations have been carried out for the methoxymethyl radical and have been fitted to the experimental data. It is concluded that 8 or 9 normal modes contribute to the energization of the radical. The rate coefficient is increased by the presence of carbon dioxide, but carbon dioxide has a lower efficiency than dimethyl ether for the transfer of energy in the energization process.

The concentration of mercury in the reaction zone, and the degree of homogeneity of Hg $^3P_1$ production associated with this concentration, considerably affect the rate of production of 1,2-dimethoxyethane but have no influence on the decomposition of the methoxymethyl radical.

The Combination of Methyl Radicals

As part of the study of the mercury-photosensitized decomposition of dimethyl ether, the combination of methyl radicals has been investigated in the temperature range 200 to 300°C and at pressures between 3 and 300 mm Hg. For pressures of less than 100 mm the second-order rate constant for the combination of methyl radicals shows a pressure dependence. The pressure dependence agrees qualitatively with that observed by others, but occurs at somewhat higher pressures. Calculations for the Kassel equation using the Arrhenius parameters for ethane decomposition and fitted to the pressure dependence of the methyl radical combination show that the number of effective modes for ethane decomposition is 8 or 9. Carbon dioxide was found to be a quite ineffective third body for energy-transfer.

The Combination of Methyl Radicals with Methoxymethyl Radicals

The results for the mercury-photosensitized decomposition of dimethyl ether have been analyzed in order to obtain information about the combination of methyl radicals with methoxymethyl radicals in the temperature range 200 to 300°C and at pressures from 3 to 600 mm Hg. The combination of these radicals becomes pressure dependent at pressures less than about 15 mm. Kassel integrations based on the rate constant

$$k^{\infty} = 4.8 \times 10^{15} e^{-78,200/RT} \text{ sec}^{-1}$$

for the unimolecular decomposition of methyl ethyl ether at the C-C bond, and fitted to the observed pressure dependence of the combination reaction, leads to s=10 for these reactions.

The rate constant for the abstraction of a hydrogen atom by a methyl radical from dimethyl ether was found to be

$$k = 1.1 \times 10^{11} e^{-9,400/RT} \text{ cc mole}^{-1} \text{ sec}^{-1}.$$

Thermochemistry of the Methoxymethyl Radical

A kinetic study has been made of the pyrolysis of 1,2-dimethoxyethane, $CH_3OCH_2CH_2OCH_3$, using toluene as a radical scavenger. The initial step involves the C-C split, and there are no chains; the activation energy of 71.3 kcal per mole thus corresponds to the dissociation energy of the C-C bond. The heat of formation of $CH_3OCH_2CH_2OCH_3$ has been found to be -82.4 kcal per mole and these values lead to -5.6 for the heat of formation of the CH_3OCH_2 radical and to 90.5 for the dissociation energy of CH_3OCH_2-H.

Support for these values is provided by the results of a similar study with chloromethyl methyl ether, CH_3OCH_2Cl, for which the C-Cl bond is ruptured in the initial step. Activation energies of 69.3 and 69.9 kcal per mole were found with toluene and propylene as scavengers. With the use of appearance-potential data these values lead

to $D(CH_3OCH_2-H)$ = 92.9 and $\Delta H_f^o(CH_3OCH_2)$ = -3.2 kcal. per mole, with, however, a wider margin of error than for the results with $CH_3OCH_2CH_2OCH_3$.

The Thermal Decomposition of the Ethyl Radical

The kinetics of the thermal decomposition of the ethyl radical to give an ethylene molecule and a hydrogen atom was studied over the pressure range 4 to 650 mm Hg and the temperature range 400 to 500°C; the mercury-photosensitized decomposition of ethane was used to generate the ethyl radical. The unimolecular decomposition of the ethyl radical was found to be pressure-dependent over the entire range of pressures studied, with the order of reaction varying from 1.6 for the lowest pressures to 1.4 at the highest pressures. The extrapolated high-pressure and low-pressure rate constants for the decomposition of the ethyl radical are given by:

$$k^\infty = 3.5 \times 10^{14}\ e^{-40,900/RT}\ sec^{-1}$$

$$k^o = 6.8 \times 10^{17}\ e^{-31,800/RT}\ cc\ mole^{-1}\ sec^{-1},$$

A best fit of the Kassel equation to the observed pressure dependence shows that s = 8 for this reaction.

The results lead to a value of 98.1 kcal. per mole for the bond dissociation energy $D(C_2H_5-H)$. The heat of formation of the ethyl radical was calculated to be 30.0 and 26.2 kcal. per mole for 0°K and 25°C respectively.

CHAPTER I

GENERAL INTRODUCTION

The study of unimolecular reactions has received increasingly more attention in recent years. The most easily accessible of unimolecular reactions are the thermal isomerization reactions such as the isomerization of cyclopropane to propylene. A number of isomerizations have been studied in detail. Other unimolecular reactions, such as chain-initiating steps and certain chain-propagating steps, are of more consequence in developing an understanding of complex reaction mechanisms. It is only in recent years that techniques have become available to study the individual steps of a reaction mechanism and to examine the effects of temperature, pressure and foreign gases on the individual steps. In some cases it is now possible to observe the kinetic behavior of a unimolecular reaction which is one step of an overall mechanism.

A characteristic feature of unimolecular reactions is the pressure-dependence of the first-order rate coefficient when studies are made at low pressures. The first-order kinetics are found to fail at low pressures, and at sufficiently low pressures second-order kinetics are observed. This behavior was first explained by Lindemann with the proposal that for molecules obtaining energy for reaction through collisions with other molecules the rate

of energization will become a second-order process at low pressures. The reactions can be shown in the following scheme:

$$[1] \qquad A + A \underset{k_{-1}}{\overset{k_1}{\rightleftharpoons}} A^* + A$$

$$[2] \qquad A^* \xrightarrow{k_2} P$$

Here A represents a molecule of reactant, A^* represents a molecule of reactant with sufficient energy to decompose, and P represents the products of a unimolecular decomposition. The overall rate of decomposition is given by

$$[3] \qquad v_2 = k_2 [A^*]$$

The steady-state treatment for A^* leads to

$$[4] \qquad k_1[A]^2 - k_{-1}[A^*][A] - k_2[A^*] = 0$$

This can be rearranged to give an expression for $[A^*]$, and on substituting this expression in [3] one obtains

$$[5] \qquad v_2 = \frac{k_1 k_2 [A]^2}{k_{-1}[A] + k_2}$$

This expression qualitatively describes the observed pressure dependence since at high pressures, when $k_2 \ll k_{-1}[A]$, the kinetics are first-order, while at low pressures, when $k_{-1}[A] \ll k_2$, the kinetics are second-order.

The Lindemann treatment has provided a very successful basis for examining unimolecular reactions, but is found to fail on two accounts. The first failure of the Lindemann theory resulted from the use of simple collision theory to estimate k_1 from the expression

[6] $$k_1 = Z_1 e^{-E^*/RT}$$

This expression led to values of k_1 which were considerably too small. Hinshelwood recognized that the process of energization may be much faster for a complex molecule with a considerable number of vibrational degrees of freedom than for a simple molecule, since the energy can be distributed in many ways among the vibrational modes of the complex molecule. The expression for k_1 for a molecule having s modes of vibration is

[7] $$k_1 = \frac{Z_{-1}}{(s-1)!} \left(\frac{E^*}{RT}\right)^{s-1} e^{-E^*/RT}$$

where Z_{-1} is the collision frequency for the deactivation process. In application, it is found that agreement with experiment is obtained most frequently for a value of s near $\frac{3N-6}{2}$, i.e., only one half of the normal modes of vibration contribute to the energization process.

The second failure of the Lindemann theory is that the variation in the first-order rate coefficient with the pressure shows the wrong form. This effect is a result of an inadequate description of k_2 in the Lindemann theory. The theories of Kassel and of Rice and Ramsperger take into account the fact that highly energized excited species decompose more rapidly than a species that is just critically energized. In discussions of the Kassel theory it is convenient to consider the following reactions instead of reactions [1] and [2]:

[8] $$A + A \underset{k_{-1}}{\overset{k_1}{\rightleftharpoons}} A^* + A$$

[9] $$A^* \xrightarrow{k_2} A^\dagger$$

[10] $$A^\dagger \xrightarrow{k^\dagger} P$$

This scheme differentiates between an energized molecule (A^*) and an activated complex ($A^\dagger$), where an energized molecule has sufficient energy to become an activated complex, but does not have that energy distributed among the vibrational modes in the manner required for the activated complex. The energy in the energized molecule is assumed to be reshuffled on every vibration. The greater the energy of the energized molecule, the greater is the chance of redistributing this energy in the manner required for the activated complex. This leads to a higher rate of formation of the activated complex from highly energized molecules than from just critically energized molecules. The expression describing this behavior of k_2 is given by

[11] $$k_2 = k^\dagger \left(\frac{\epsilon - \epsilon^*}{\epsilon}\right)^{s-1}$$

where ϵ and ϵ^* are the energy of the energized molecules and the critical energy respectively, and s is the number of modes of vibration in the molecule. The rate constant for the decomposition of an activated complex is not dependent on the total energy of the activated complex since the complex is assumed to decompose during the period of the first vibration.

With this expression for k_2 and with the Hinshelwood expression for k_1, the final equation of the Kassel theory is obtained:

$$[12] \qquad k^1 = \frac{k^*}{(s-1)!} \int_{\epsilon^*}^{\infty} \frac{\left(\frac{\epsilon}{kT}\right)^{s-1} \left(\frac{\epsilon-\epsilon^*}{\epsilon}\right)^{s-1} e^{-\epsilon/kT} \frac{d\epsilon}{kT}}{1 + \frac{k^*}{k_{-1}[A]} \left(\frac{\epsilon-\epsilon^*}{\epsilon}\right)^{s-1}}$$

This equation gives the value of a first-order rate coefficient, k^1, for a given pressure [A], and for a chosen value of the parameter s. In applying the Kassel equation it is necessary to know *, the high-pressure activation energy, and k , the high-pressure limiting rate constant. It is then possible to fit the calculated values of k^1 to the observed values, through variation of the s parameter. The Kassel equation leads to an s value which is less than the total number of modes, and which is often about one half of the total number of modes. It may be recalled that Hinshelwood's expression for k_1 also led to low s values when fitted to experimental data.

Although the unimolecular decompositions of quite a number of molecules have been examined, there have been few detailed studies into the unimolecular decomposition of radicals. One of the chain-propagating steps in a chain reaction is frequently the unimolecular decomposition of a radical; an understanding of the unimolecular decomposition of the radical is basic to the understanding of the overall reaction mechanism. The decomposition of some radicals has

been examined over a wide enough temperature range to yield an activation energy for the reaction, but these studies have most frequently been made at only one pressure. The studies often involve an assumption regarding the kinetic order of the decomposition at this pressure. Although there may sometimes be sufficient reason for the assumption of a certain order of reaction, the orders of reaction for many radical decompositions are open to question until more pressure studies have been made. Radicals containing from 4 to 10 atoms are most likely to show variation in the order of reaction with pressure, in the pressure range 10-600 mm (most frequently used in pyrolysis and photolysis experiments). For larger species the pressure dependence will be observed at lower pressures, while smaller species will show second-order kinetics over this range of pressure, and the kinetics will change to first order only at several atmospheres pressure.

The rate constant for a radical decomposition is often difficult to isolate. Most frequently a rate-constant ratio has been considered. Various ratios have been considered by authors and have led to very different conclusions regarding the rate constant for the decomposition of the radical. An example is seen in the case of n-propyl radical, for which activation energies ranging from 20 to 38 kcal per mole were obtained in six separate studies.

One of the best rate-constant ratios to study for the decomposition of a radical can be derived from the following abbreviated scheme:

[13] $R \longrightarrow M + R'$

[14a] $2R \longrightarrow R_2$

[14b] $2R \longrightarrow RH + O$

In this scheme R represents the radical under study, R' a second radical, M a molecule produced in decomposition, R_2 the dimer of the radical combination and O the olefin produced by disproportionation. The rates of the various reactions are given by

[15] $v_{13} = k_{13}[R] = v_M$

[16a] $v_{14a} = k_{14a}[R]^2 = v_{R_2}$

[16b] $v_{14b} = k_{14b}[R]^2 = v_O$

It follows that

[17] $k_{13}/k_{14a}^{\frac{1}{2}} = v_{13}/v_{14a}^{\frac{1}{2}} = v_M/v_{R_2}^{\frac{1}{2}}$

The rate-constant ratio given in [17] has the following advantages over other rate-constant ratios. The ratio is derived from the cancellation of the radical concentration in the two rate expressions, and hence involves no assumptions about the radical concentration. The formation of M and of R_2 is almost always unambiguous in the reaction scheme, since these products cannot be formed through other reactions. No assumption for the disproportionation to combination ratio is required. The activation energy for the decomposition of the radical has greater precision than

other rate-constant ratios since the activation energy for combination is usually zero and thus requires no correction by difference from the activation energy observed for the ratio. The main disadvantage of this ratio is the difficulty involved in making quantitative measurements of the dimer. A corresponding ratio can be derived using the disproportionation products, but experimentally it is usually easier to measure the combination products.

Various methods have been used to generate radicals for the study of their thermal decomposition. These have generally been photolytic or sensitization methods; examples are the photolysis of *n*-butyraldehyde to produce n-propyl radicals and the thermally sensitized reaction of azomethane in the presence of propane to produce propyl radicals. Mercury-photosensitization is a useful means of producing radicals, where the radical required involves the loss of a hydrogen atom from the parent species. The usual primary step in mercury-photosensitization is the removal of a hydrogen atom from the parent molecule, by the Hg $^3P_1$ atom. Mercury-photosensitization has the advantage that a wide range of temperatures is available for the investigation. Sensitization by chemical means, such as by azomethane, limits the temperature range considerably. Furthermore mercury-photosensitization provides clean reaction conditions since no other radicals are added to the system. Photolytic and sensitization methods both

generate radicals other than the one under study and complicate the overall mechanism. The main disadvantage of mercury-photosensitization is the degree of conversion which can be used. Certain products, particularly olefins, which have high quenching cross-sections can be lost through further reaction by a mercury-photosensitized reaction. When using mercury-photosensitization to generate radicals, one must also consider the possibility of primary steps other than the removal of a hydrogen atom and the possible formation of hot radicals.

The studies described in this thesis were initiated to examine the thermal decomposition of two radicals over a wide range of pressure and temperature. The two radicals studied were the methoxymethyl radical and the ethyl radical, which are known to decompose to formaldehyde and a methyl radical, and to ethylene and a hydrogen atom respectively. For both radicals the activation energy and the pressure dependence of the first-order rate coefficient for the unimolecular decomposition were unsettled in view of discrepancies in the previous literature.

In the progress of the study on the thermal decomposition of the methoxymethyl radical, it became evident that the mercury-photosensitized decomposition of dimethyl ether provided a basis for the study of two radical combination reactions. These two reactions were the combina-

tion of two methyl radicals to form ethane, and the combination of a methyl radical with a methoxymethyl radical to form methyl ethyl ether. These reactions and the effects of pressure on them have been examined in detail.

A correlation of the observed activation energies with the thermochemistry of the corresponding reactions was not possible for reactions involving the methoxymethyl radical until the heat of formation of this radical was known. This heat of formation has been determined in order to provide a more complete basis for thermochemical discussion.

CHAPTER II

THE OVERALL REACTION MECHANISM FOR THE MERCURY-PHOTOSENSITIZED DECOMPOSITION OF DIMETHYL ETHER

INTRODUCTION

The mercury-photosensitized decomposition of dimethyl ether has previously been examined by Marcus, Darwent and Steacie (1), and by Pottie, Harrison and Lossing (2). The former authors studied the reaction over the temperature range of 25°C to 292°C at pressures of 28 mm Hg and 110 mm Hg. They concluded that the primary decomposition step was

$$Hg\ ^3P_1 + CH_3OCH_3 \longrightarrow CH_3OCH_2 + H + Hg\ ^1S_0$$

At 25°C the only subsequent reactions were

$$H + CH_3OCH_3 \longrightarrow H_2 + CH_3OCH_2$$

$$2CH_3OCH_2 \longrightarrow CH_3OCH_2CH_2OCH_3$$

At higher temperatures the methoxymethyl radical, CH_3OCH_2, decomposed by the reaction

$$CH_3OCH_2 \longrightarrow CH_3 + CH_2O$$

They found the activation energy for this decomposition to be 18.5 kcal. per mole at 28 mm and 20.0 kcal. per mole at 110 mm, on the assumption that methoxymethyl radicals combine with zero activation energy.

The latter authors studied the mercury-photosensitized decomposition of dimethyl ether in a fast flow

system coupled to a mass spectrometer. The effective ether pressure was about 0.010 mm Hg. The study was made at 55°C, and a high-intensity light source was used. Under these conditions a second primary decomposition,

$$Hg\ ^3P_1 + CH_3OCH_3 \longrightarrow CH_3 + OCH_3 + Hg\ ^1S_0$$

was found to occur. It was concluded that under these conditions this C-O split accounted for as much as 50% of the total initiation.

In the present investigation a more detailed study has been made of the mercury-photosensitized decomposition of dimethyl ether, particular attention being paid to the kinetics of the various elementary processes over a range of temperatures and pressures.

EXPERIMENTAL

Materials

The dimethyl ether used was obtained from the Matheson Company and was further purified by bulb to bulb distillation. The purified ether contained small quantities of carbon dioxide and methyl ethyl ether. For the measurement of methyl ethyl ether formed during reaction a small correction had to be made for the methyl ethyl ether in the reactant. No evidence of any other impurity was observed in chromatographic analysis of the dimethyl ether. The 1,2-dimethoxyethane used for calibrations of the chromatograph was obtained from the Aldrich Chemical Company.

Methyl ethyl ether was prepared by a Williamson synthesis using ethyl alcohol and methyl iodide.

Apparatus

The reaction was studied in a static system. A view of the apparatus is shown in Plate I. The essential features of the apparatus are shown schematically in Figure 1.

A cylindrical quartz reaction vessel, 4" in length and 2" in diameter was used; its volume was 166 cc. The furnace constructed around the reaction vessel had the following features. A cylindrical iron collar 9" long by 1/4" thick was placed around the reaction vessel to provide even heating. Outside the iron collar windings of resistance wire were placed in three zones along the length of the furnace so that heating could be controlled for each section. The heating of the two end zones was controlled by the adjustment of a Variac. The temperature of the central heating zone was controlled by a Thermo Electric temperature controller which was activated by means of a thermocouple (C_4) placed at the side of the reaction vessel.

The temperature of the reaction vessel was measured by means of chromel-alumel thermocouples (0°C reference), connected to a Croyden Type P-3 potentiometer. The temperature was observed for three thermocouples (C_1, C_2, C_3) throughout the reaction time. These thermocouples gave the temperature at both ends and at the middle of the

PLATE I

A view of the apparatus

Figure 1

A schematic diagram of the apparatus

M: Manometer

B: Storage bulb

V: Variac

T: Trap

S: Stopcock

D: Mercury diffusion pump

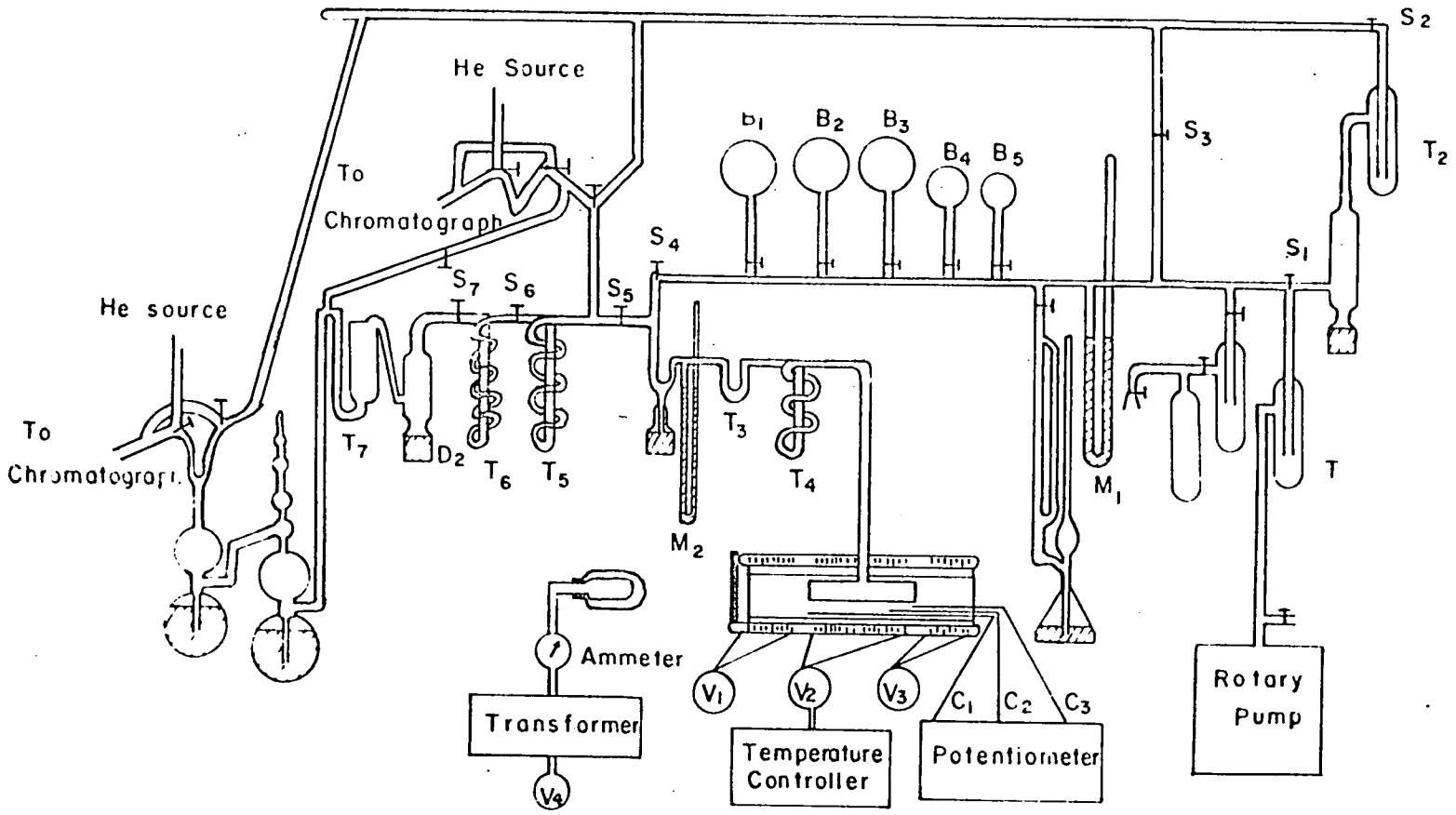
He Source
To
Chromatograph
He source
To
Chromatograph
S_2
S_3
S_4
S_5
S_6
S_7
S_1
T_2
T_7
D_2
T_6
T_5
T_3
T_4
M_2
M_1
T
B_1
B_2
B_3
B_4
B_5
Ammeter
Transformer
V_4
V_1
V_2
V_3
C_1
C_2
C_3
Temperature Controller
Potentiometer
Rotary Pump

reaction vessel. It was possible to maintain very constant temperature for C_2 and C_3 but the opening of the shutter caused some fluctuation in C_1 during the reaction. This was compensated for by adjusting the Variac controlling the temperature of this zone.

The mercury lamp was a low-pressure lamp and was maintained at 11" from the incident face of the reaction vessel. The lamp was warmed up for at least twenty minutes before use and was operated at room temperature. The lamp was operated at a current of 9.0 ma. This current was adjusted with a Variac (V_4) in the primary circuit of the transformer (output 2,000 v maximum) used to activate the mercury lamp.

The concentration of mercury in the reaction zone was controlled by the temperature of a spiral trap (T_4), containing mercury, in the lead to the reaction vessel. The concentration of mercury was assumed to correspond to the equilibrium vapor pressure of mercury at the temperature of the spiral trap. For much of the work, this trap was maintained at 0°C, but other temperatures ranging from -30°C to +20°C were also used to vary the concentration of mercury in the reaction zone.

Procedure and Analysis

Prior to each experiment a pressure of 2×10^{-5} mm or better was obtained. A sample of ether was admitted to the manifold from the reaction vessel and then trapped out

in a U-tube (T_3) after stopcock S_4 and the mercury cut-off were opened. The reaction vessel was then isolated by closing the mercury cut-off, and the ether was allowed to expand into the reaction vessel, with the ether passing through the mercury saturator trap (T_4). The reaction was started with the removal of the shutter and was stopped by switching off the mercury lamp. Conversions were kept low for all runs. The conversion was well under 1% except for runs at less than 10 mm pressure of reactant.

The products of reaction were separated into four fractions: (1) noncondensable, (2) condensables at -196°C (liquid nitrogen), (3) condensables at -160°C (isopentane slush) and (4) condensables at -127°C (n-propanol slush). The noncondensable products, which comprised hydrogen, carbon monoxide and methane, were collected with a Toepler pump. The trap at -196°C retained ethane, although occasionally a small correction had to be added for ethane which appeared in the noncondensable fraction. The -160° trap contained reactant and methyl ethyl ether while the trap at -127°C contained 1,2-dimethoxyethane with virtually no reactant or methyl ethyl ether. A mercury diffusion pump between the -160° trap and the -196° trap was used to pump reactant and products from the reaction vessel.

The products of reaction were analysed by a gas chromatograph having a hot filament detecting unit. All columns were 1/4 inch in diameter. Helium was the carrier

gas used for all chromatographic analyses, and all columns were thermostatted at 30°C. Methane, carbon monoxide and ethane were analysed using a twelve-foot column of 100-200 mesh silica gel. The fraction containing reactant and methyl ethyl ether was analysed on a forty-foot column of polypropylene glycol on 60-80 mesh Chromosorb P (20% load). The length of this column allowed the reactant to be eluted and the base line to return to good stability before the methyl ethyl ether appeared. 1,2-Dimethoxyethane was analysed on a ten-inch column of polypropylene glycol on 60-80 mesh Chromosorb P HMDS (20% load). Peak-height measurements provided good calibration curves for all products except 1,2-dimethoxyethane, for which it was necessary to make area measurements.

The low conversion necessitated high sensitivity for the gas chromatographic analysis. This sensitivity was obtained by preamplification of the signal, by means of a Leeds and Northrup microvolt amplifier, before it was put through a 10 mv. recorder. This high amplification requires minimal fluctuations of pressure between the helium source and the detector, in order to have a stable base line; this was accomplished by inserting Edwards VPC-1 pressure controllers in both the reference flow and the analysis flow of the chromatograph.

RESULTS AND DISCUSSION

The reaction was studied over the range of 200° to 300°C, and of 3 to 600 mm Hg pressure. The products found were hydrogen, carbon monoxide, methane, ethane, methyl ethyl ether (MEE) and 1,2-dimethoxyethane (dimer). Formaldehyde is certainly produced but its analysis, which is difficult and unreliable, was not attempted. Table I shows the rates of production of products for typical runs.

These results suggest the following reaction scheme:

[1] $Hg\ ^3P_1 + CH_3OCH_3 \longrightarrow CH_3OCH_2 + H + Hg\ ^1S_0$

[2] $2\ CH_3OCH_2 \longrightarrow CH_3OCH_2CH_2OCH_3$

[3] $CH_3OCH_2 \longrightarrow CH_3 + CH_2O$

[4] $CH_3 + CH_3OCH_3 \longrightarrow CH_4 + CH_3OCH_2$

[5] $2\ CH_3 \longrightarrow C_2H_6$

[6] $CH_3 + CH_3OCH_2 \longrightarrow CH_3OCH_2CH_3$

[7] $H + CH_3OCH_3 \longrightarrow H_2 + CH_3OCH_2$

[8] $CH_2O \longrightarrow CO + H_2$

Under the conditions of the present work there appears to be no C-O split in the primary step. The production of CH_3O would lead to the formation of methanol; the chromatograph had good sensitivity for methanol, but none was detected.

When the reaction was carried out at 30°C the only products were hydrogen and 1,2-dimethoxyethane; reaction [3] does not occur under these conditions. This result confirms

TABLE I.

Rates of Reaction for Typical Runs

Temp. °C	Pressure mm	Time of run sec	v_{H_2}	v_{CH_4}	v_{CO}	$v_{C_2H_6}$	v_{dimer}	v_{HEE}
200	75.0	600	4.65	1.585	0.048	0.116	2.530	0.837
225	69.2	450	4.89	5.389	0.124	0.465	1.693	1.426
248	61.0	300	5.16	10.74	0.281	0.753	0.747	1.699
270	61.0	240	6.17	22.19	0.690	1.996	0.389	2.021
300	57.5	150	6.14	40.77	1.321	2.811	0.151*	1.305

All rates are expressed in moles cc^{-1} sec^{-1} x 10^{12}

*Calculated

that methane results only from the decomposition of the methoxymethyl radical. It also provides further evidence that there is no C-O split in the primary step; if there were, the CH_3 radicals would produce either CH_4 or C_2H_6, neither of which was found at 30°C.

The carbon monoxide produced in the reaction is undoubtedly formed by the decomposition of formaldehyde. This process, represented by equation [8], certainly does not occur as an elementary process, but via HCO. It is easily verified that these processes do not interfere with the mass balances employed in the present work.

Dark reactions carried out at 248°C and 300°C confirmed that no significant thermal decomposition of the ether was occurring.

Mass Balance

The steady-state equations for H, CH_3 and CH_3OCH_2 are

$$v_1 = v_7$$

$$v_3 = v_4 + 2v_5 + v_6$$

$$v_1 + v_4 + v_7 = 2v_2 + v_3 + v_6$$

Elimination of v_1 and v_3 gives

$$v_7 = v_2 + v_5 + v_6$$

Since hydrogen is produced only by reaction [7] or by the decomposition of formaldehyde, in which case an equivalent amount of carbon monoxide is produced, v_7 is

equal to $v_{H_2} - v_{CO}$; therefore

$$v_{H_2} - v_{CO} = v_{dimer} + v_{C_2H_6} + v_{MEE}$$

A series of experiments was carried out to test this relationship, care being taken to avoid any loss of products. The products other than hydrogen were analysed by chromatography; the amount of hydrogen formed was obtained from the difference of the gas burette measurement of the total noncondensables and the chromatographic measurement of all other noncondensables in the sample. The results obtained at 200°C are shown in Table II, from which it is seen that the mass balance relationship is substantiated within the experimental error.

Homogeneity of Reaction

The question arises as to whether the mercury vapor concentration is such that there is very little drop in intensity as the light passes through the reaction vessel. In order to test this, measurements were made of the net termination rate, $v_{dimer} + v_{C_2H_6} + v_{MEE}$, (this is equal to the initiation rate) at various mercury vapor pressures. The temperature of the trap controlling the concentration of mercury vapor in the vessel was adjusted at temperatures from -30°C to +20°C, for various runs. The results are shown in Figure 2. It is to be seen that at temperatures above about 0°C the rate of termination has reached an upper limit, corresponding to total light absorption. At

TABLE II

Products of Reaction at 200°C

Pressure	Reaction Time	Moles of Product x 10^7						MEE+C_2H_6+dimer
mm	sec	CO	CH_4	H_2	MEE	C_2H_6	dimer	H_2-CO
20.3	1800	0.311	2.025	6.212	2.424	0.265	3.330	1.020
23.6	1200	0.102	1.414	2.663	1.357	0.234	0.872	0.962
22.7	1800	0.193	2.083	4.128	1.894	0.283	1.791	1.008
23.9	1200	0.138	1.550	3.200	1.537	0.226	1.125	0.943
17.7	1800	0.165	1.612	3.294	1.603	0.260	1.251	0.995
11.7	1200	0.105	1.680	3.100	1.505	0.167	1.297	0.991

Figure 2

Net rate of termination of the mercury-photosensitized decomposition of dimethyl ether as a function of the mercury vapor pressure. The trap temperatures are indicated.

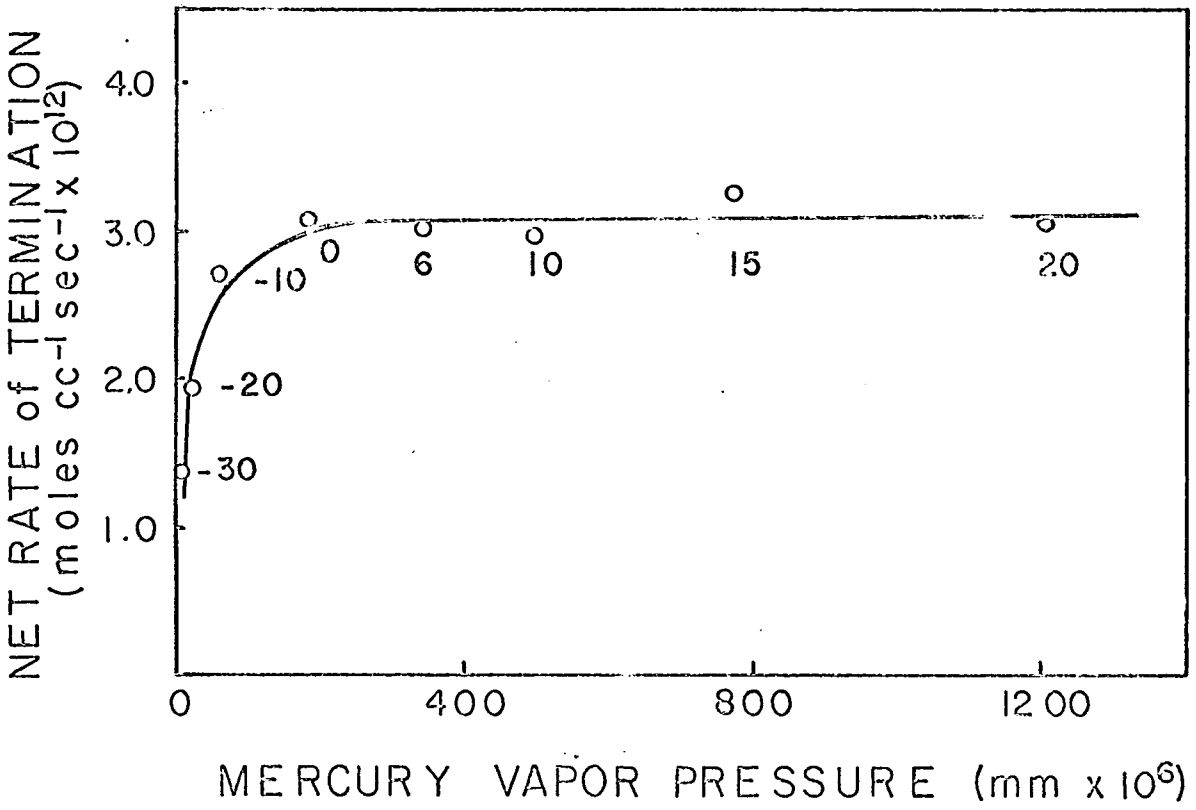
NET RATE of TERMINATION
(moles cc-1 sec-1 x 10^12)
4.0
3.0
2.0
1.0
-10
0
6
10
15
20
-20
-30
0
400
800
1200
MERCURY VAPOR PRESSURE (mm x 10^6)

-30°C the termination has fallen to a point where 50% absorption is occuring. In the work described in the following three chapters a correction has been made for this lack of homogeneity.

CHAPTER III

THE THERMAL DECOMPOSITION OF THE METHOXYMETHYL RADICAL

INTRODUCTION

A previous study of the mercury-photosensitized decomposition of dimethyl ether by Marcus, Darwent and Steacie (1) has led to the conclusion that the methoxymethyl radical, CH_3OCH_2, decomposes into a methyl radical and formaldehyde. At a pressure of 110 mm the activation energy was given as 20.0 kcal. per mole, while at 28 mm it was 18.5 kcal. per mole. From the above experimental data Trotman-Dickenson (3) calculated the frequency factor of this reaction to be about 10^{10} sec^{-1} for the decomposition in its first-order region. The low frequency factor and the decreased activation energy at lower pressure both suggest that the decomposition of the methoxymethyl radical is in its pressure-dependent region.

In the thermal decomposition of dimethyl ether the decomposition of the methoxymethyl radical is one of the chain-propagating steps. Benson and Jain (4) prefer to regard this decomposition as being second-order, while McKenney and Laidler (5) have suggested that this reaction is in its first-order region. Although the order of this reaction does not influence the overall order of dimethyl ether pyrolysis, clarification of the pressure dependence

of methoxymethyl radical decomposition is a matter of some interest.

In the present work the kinetics of the methoxymethyl radical decomposition have been deduced from the results of a study of the mercury-sensitized decomposition of dimethyl ether.

EXPERIMENTAL

The apparatus and experimental technique have been described in detail in Chapter II. The bulk of work was carried out using 0°C for the trap controlling the mercury concentration in the reaction vessel. However, for some of the later runs the temperature of the trap was varied from -30 to +20°C using an ethanol bath.

RESULTS AND DISCUSSION

The scheme of reactions describing the mercury-photosensitized decomposition of dimethyl ether was given in Chapter II; the same numbering of reactions [1] to [7] is used here. The present work has been centered on the kinetics of reaction [3] and has been accomplished by considering the rates of the individual steps [2] and [3],

[8] $$v_3 = k_3 [CH_2OCH_3]$$

[9] $$v_2 = k_2 [CH_2OCH_3]^2$$

whence

[10] $$\frac{v_3}{v_2^{1/2}} = \frac{k_3}{k_2^{1/2}}$$

Thus by measuring v_3 and v_2 the rate constant ratio $k_3/k_2^{1/2}$ may be evaluated. The rate of reaction [2] has been measured directly as the rate of production of 1,2-dimethoxyethane. The rate of reaction [3] has been measured as the sum of $v_{CH_4} + 2v_{C_2H_6} + v_{MEE}$. The steady-state condition for methyl radicals yields

[11] $$v_3 = v_4 + 2v_5 + v_6$$

Provided that all methyl radicals are produced by reaction [3] and are consumed in the production of CH_4, C_2H_6 and $CH_3CH_2OCH_3$, the relation

[12] $$v_3 = v_{CH_4} + 2v_{C_2H_6} + v_{CH_3CH_2OCH_3}$$

holds.

The rates of production of methane, ethane, methyl ethyl ether and 1,2-dimethoxyethane have been measured for the mercury-photosensitized decomposition of dimethyl ether. The reaction has been studied over the temperature range of 200° to 300°C and over a pressure range of 3 mm to 600 mm. The measured rates at various temperatures and pressures are shown in Appendix I.

Values of $k_3/k_2^{1/2}$ have been calculated using relationship [10]. Figure 3 shows a plot of log $k_3/k_2^{1/2}$ vs. log P, where P is the pressure of ether in the system. At each temperature there is a steady decrease in the log $k_3/k_2^{1/2}$ values as the values of log P decrease. In view of the large number of atoms in 1,2-dimethoxyethane, no pressure dependence of k_2 would be expected in this pressure

Figure 3

The pressure dependence of $k_3/k_2^{1/2}$ at five temperatures in the range 200° to 300°C.

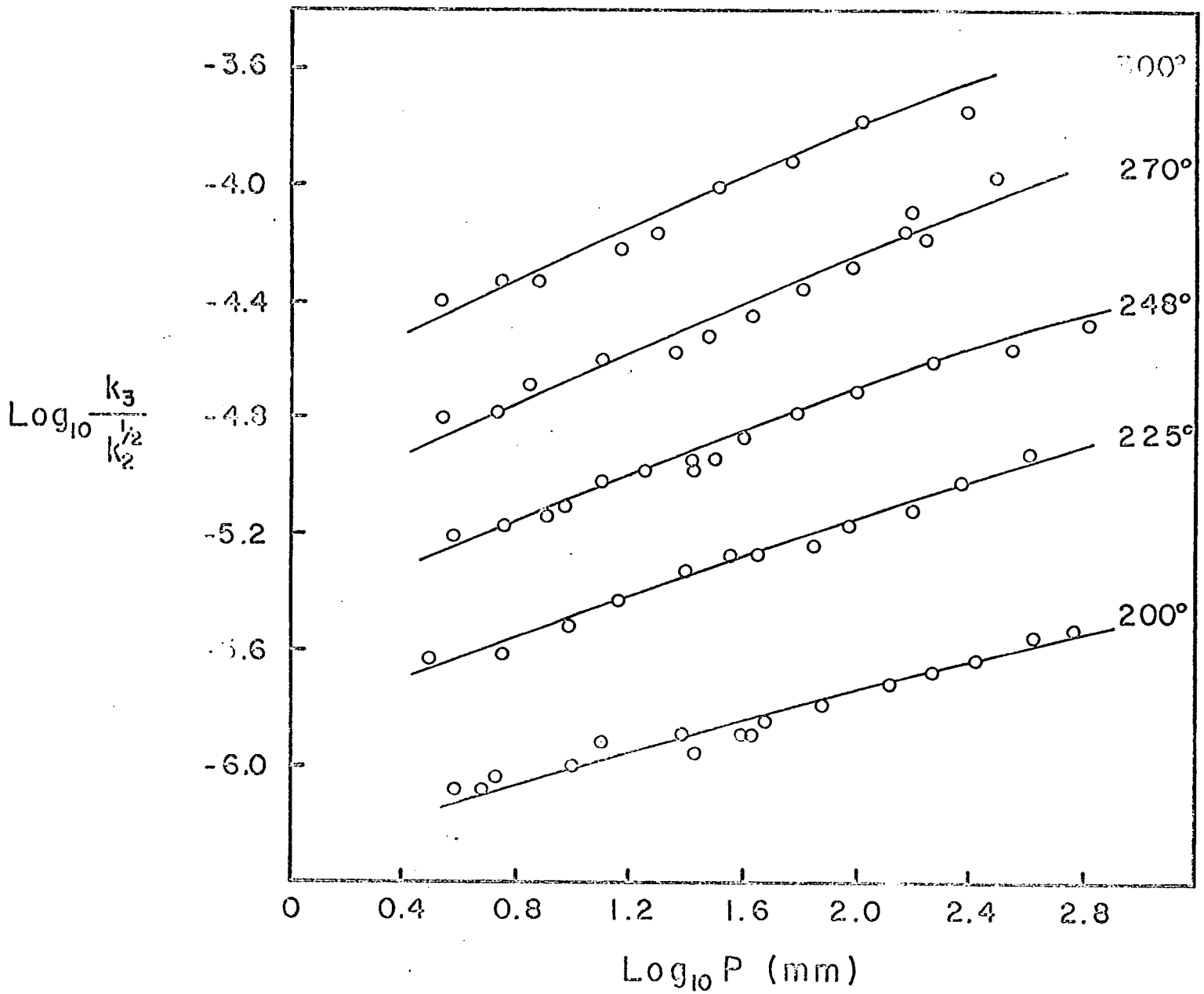
-3.6
-4.0
-4.4
-4.8
-5.2
-5.6
-6.0
$\log_{10} \frac{k_3}{k_2^{1/2}}$
300°
270°
248°
225°
200°
0
0.4
0.8
1.2
1.6
2.0
2.4
2.8
$\log_{10} P$ (mm)

region. The fall-off observed in Figure 3 is attributed to the pressure dependence of k_3. If the decomposition of methoxymethyl radical were first-order, the slope of log $k_3/k_2^{1/2}$ against log P would be zero; if the decomposition were in its second-order region the slope of the curve would be unity. From Figure 1 it is seen that the order of reaction lies between 1 and 2 over the entire pressure region for all temperatures investigated. At 248°C the order of reaction is about 1.4 in the middle of the pressure range studied.

Figure 4 shows an Arrhenius plot for the $k_3/k_2^{1/2}$ values interpolated from Figure 3 at a pressure corresponding to 100 mm ether. The activation energy for the decomposition of methoxymethyl radical is found to be 24.8 kcal. per mole at this pressure, on the assumption that the radicals combine with zero activation energy.

Of more importance are the Arrhenius parameters that correspond to the reaction in its first-order and second-order regions. From the Lindemann theory

[13] $$\frac{1}{k^1} = \frac{1}{k^\infty} + \frac{1}{k^0[A]}$$

where k^1 is the defined first-order rate coefficient, k^∞ is the first-order rate constant corresponding to the first-order decomposition obtained at sufficiently high pressures and k^0 is the second-order rate constant corresponding to the decomposition in its second-order region at sufficiently low pressures.

Figure 4

An Arrhenius plot for $k_3/k_2^{1/2}$ at 100 mm Hg pressure.

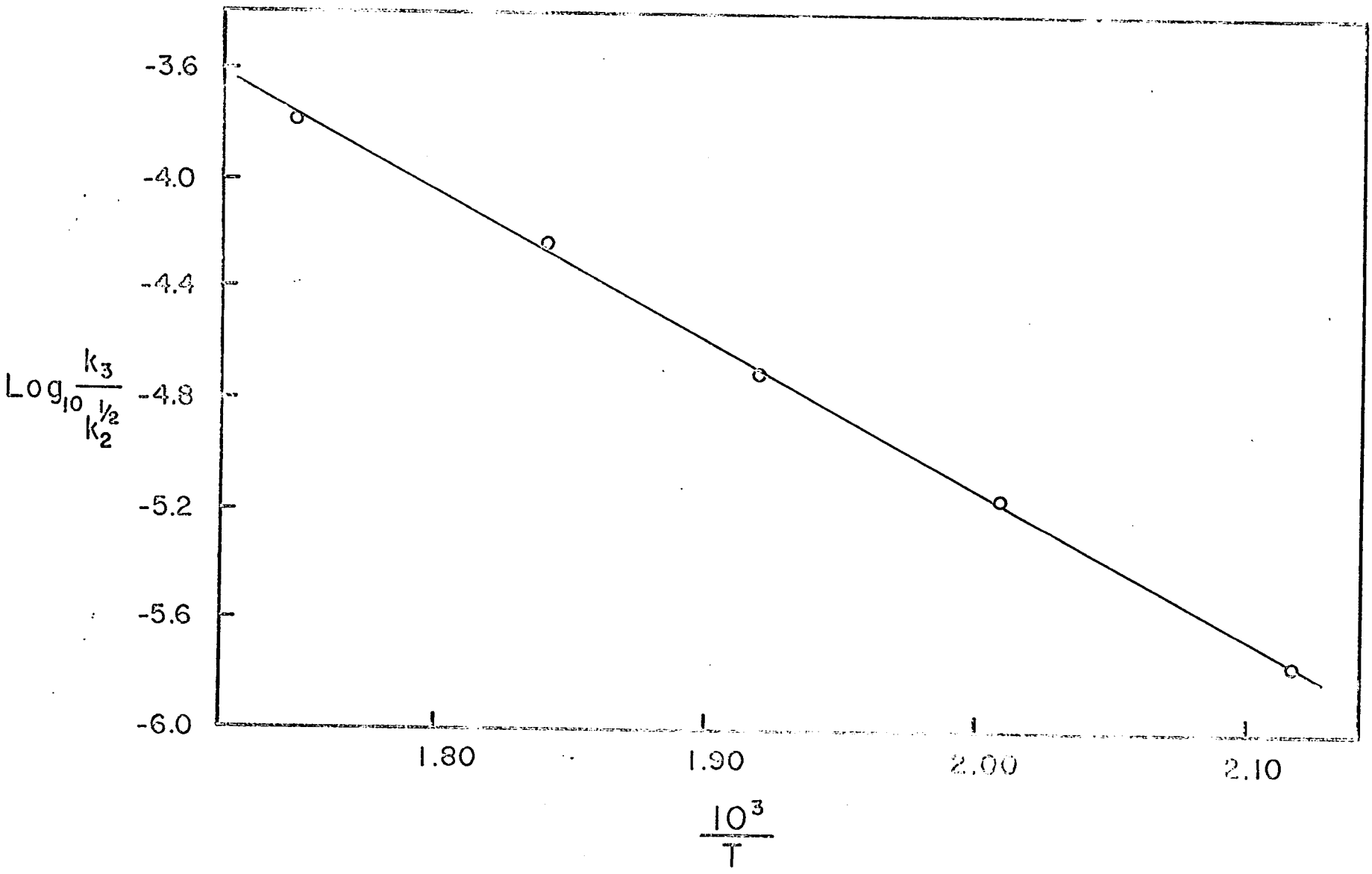
-3.6
-4.0
-4.4
-4.8
-5.2
-5.6
-6.0
$\log_{10} \frac{k_3}{k_2^{1/2}}$
1.80
1.90
2.00
2.10
$\frac{10^3}{T}$

Plots of $k_2^{1/2}/k_3$ against $\frac{1}{[A]}$ have been made to evaluate k_3^{∞} and k_3^{o}. A typical reciprocal plot is shown in Figure 5. It is seen that for high pressures the plot is not linear; the experimental points fall below the straight line. This corresponds to the deviation from Lindemann theory that arises because highly energized radicals decompose more rapidly than those which are just critically energized. The intercept taken from the reciprocal plot is the one estimated from the extension of the curved portion of the line and not from the extension of the straight line. The intercept yields $k_2^{1/2}/k_3^{\infty}$ values. The slope of the linear portion of Figure 5 yields values of $k_2^{1/2}/k_3^{o}$.

Arrhenius plots for $k_3^{o}/k_2^{1/2}$ and $k_3^{\infty}/k_2^{1/2}$ are shown in Figure 6. On the assumption that methoxymethyl radicals combine with zero activation energy, $E_3^{\infty} = 25.5$ kcal. per mole and $E_3^{o} = 18.1$ kcal. per mole. In order to evaluate the frequency factor it has been assumed that methoxymethyl radicals have the same frequency factor as methyl radicals for the combination reaction. The A factor for the methyl radical combination has been given by Shepp (6) to be 2.2×10^{13} cc mole^{-1} sec^{-1}. With this value for A_2, it is found that $A_3^{\infty} = 10^{13.0}$ sec^{-1} and $A_3^{o} = 10^{16.16}$ cc mole^{-1} sec^{-1}.

Thus

$$k_3^{\infty} = 1.0 \times 10^{13}\ e^{-25,500/RT}\ \text{sec}^{-1}$$

$$k_3^{o} = 1.4 \times 10^{16}\ e^{-18,100/RT}\ \text{cc mole}^{-1}\ \text{sec}^{-1}$$

Figure 5

Lindemann plot for data at 270°C. The slope of the linear portion gives $k_2^{1/2}/k_3^0$; the intercept obtained by extrapolation of the curve yields $k_2^{1/2}/k_3^\infty$.

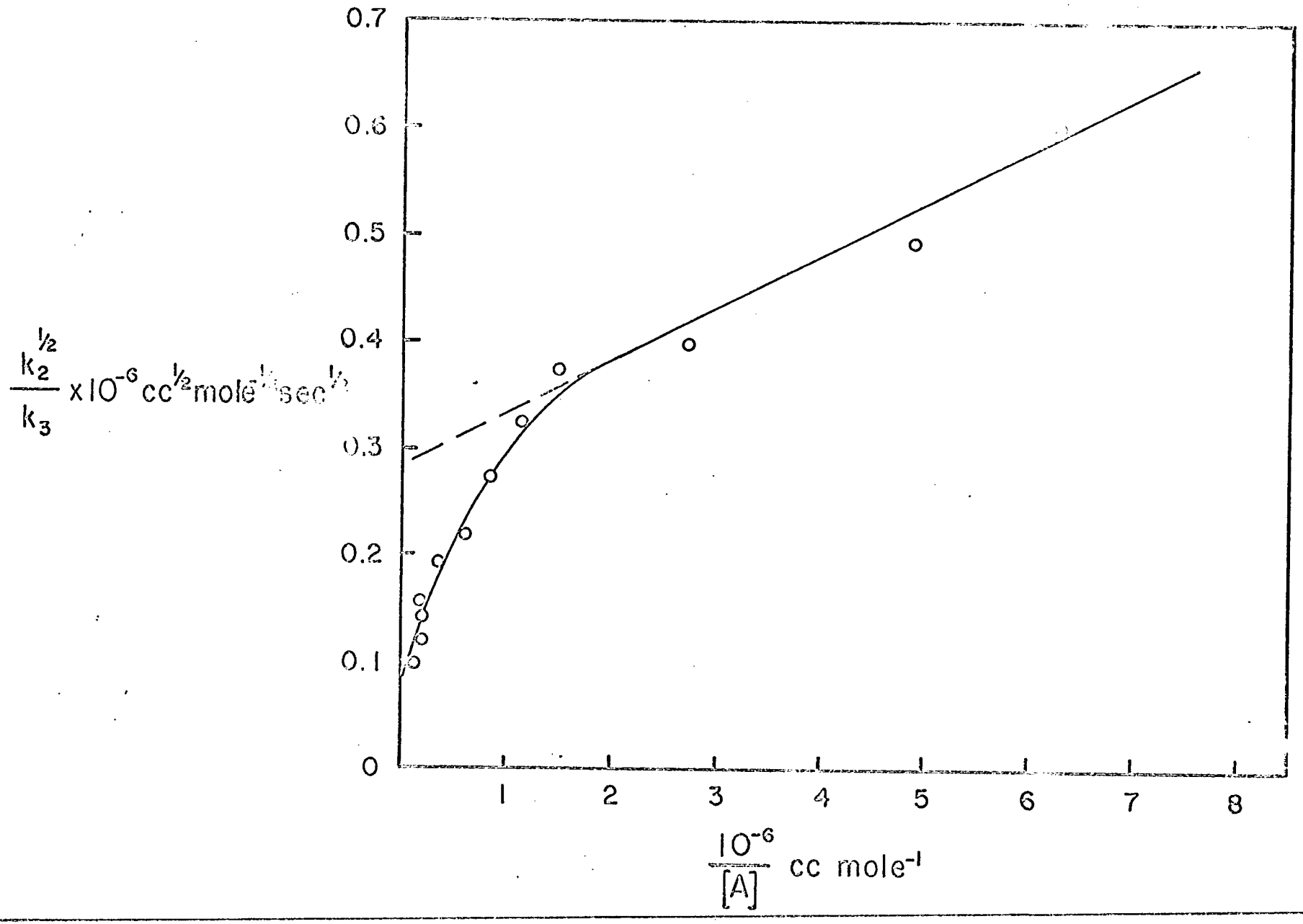
0.7
0.6
0.5
0.4
0.3
0.2
0.1
0
1
2
3
4
5
6
7
8
$\frac{k_2^{1/2}}{k_3}$ x10^{-6} cc$^{1/2}$mole$^{-1/2}$sec$^{1/2}$
$\frac{10^{-6}}{[A]}$ cc mole^{-1}

Figure 6

Arrhenius plots for $k_3^{\infty}/k_2^{1/2}$ and $k_3^{o}/k_2^{1/2}$.

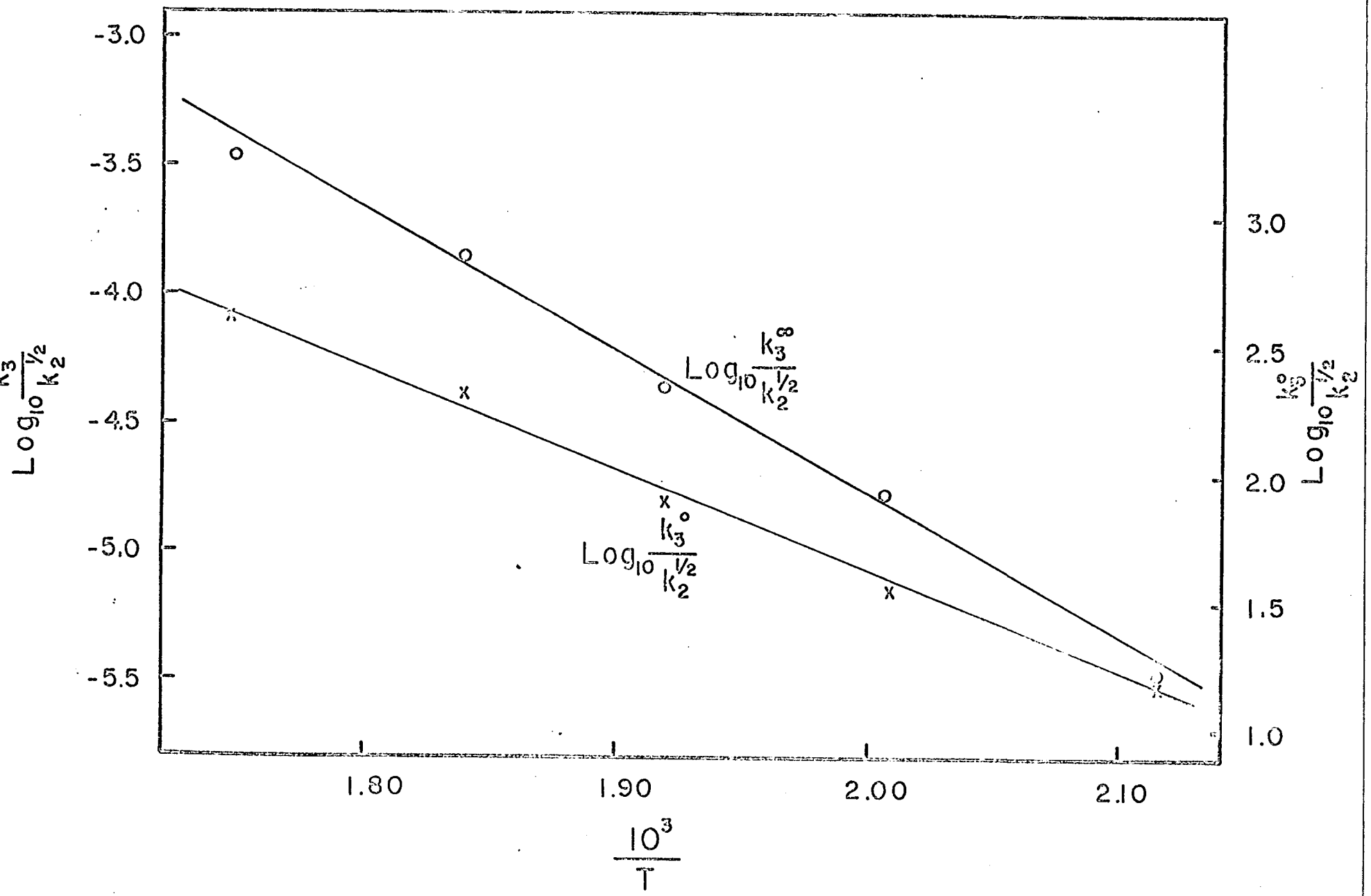
-3.0
-3.5
-4.0
-4.5
-5.0
-5.5
3.0
2.5
2.0
1.5
1.0
$\text{Log}_{10} \frac{k_3^\infty}{k_2^{1/2}}$
$\text{Log}_{10} \frac{k_3^\circ}{k_2^{1/2}}$
$\text{Log}_{10} \frac{k_3^\infty}{k_2^{1/2}}$
$\text{Log}_{10} \frac{k_3^\circ}{k_2^{1/2}}$
1.80
1.90
2.00
2.10
$\frac{10^3}{T}$

The assignment of E_3^0 = 18.1 kcal. per mole must be viewed with some caution since the slopes of the Lindemann plots were rather poorly defined. E_3^0 could be ±2 kcal. per mole from the value quoted. The value of E_3^∞ is quite well defined, however, since the extrapolation to the intercept was quite readily made. Furthermore it has already been observed that E_3 = 24.8 kcal. at 100 mm pressure and this sets a lower limit for E_3^∞. The E_3^∞ value of 25.5 kcal. per mole should be accurate within ±0.5 kcal. per mole.

From the assignment of E_3^∞ and E_3^0 it is possible to make an estimate of s, the number of normal modes contributing to the process of energization of the radical. From the Hinshelwood expression for energization it follows that

[14] $$E_\infty - E_0 = (s - 3/2)RT$$

For temperatures in the range studied this yields an s value between 8 and 9.

Application of the Kassel Equation

After k_3^∞ was evaluated it was possible to calculate Kassel integrals for the unimolecular decomposition of the methoxymethyl radical. The integrations were carried out on an IBM 1620 II computer. Calculations were made for each temperature studied and over a pressure range greater than studied experimentally. The Kassel integral may be written as

$$[15] \qquad k^1 = \frac{k^\dagger}{(s-1)!} \int_{\epsilon^*}^{\infty} \frac{\left(\frac{\epsilon}{kT}\right)^{s-1} \left(\frac{\epsilon-\epsilon^*}{\epsilon}\right)^{s-1} e^{-\epsilon/kT} \frac{d\epsilon}{kT}}{1 + \frac{k^\dagger}{k_{-1}[A]} \left(\frac{\epsilon-\epsilon^*}{\epsilon}\right)^{s-1}}$$

where k^1 is the defined first order rate coefficient and the other rate constants correspond to the following scheme:

$$A + A \underset{k_{-1}}{\overset{k_1}{\rightleftharpoons}} A^* + A$$

$$A^* \xrightarrow{k_2} A^\dagger$$

$$A^\dagger \xrightarrow{k^\dagger} \text{products}$$

In this scheme A^* is an energized molecule and $A^\dagger$ an activated complex; the latter is a complex passing smoothly into products while the former is characterized only by having sufficient energy to become an activated complex.

In Kassel integrations k_{-1} is normally taken to be the collision frequency for the deactivation process, and deactivation is assumed to occur on every collision. In the present work A^* is necessarily a methoxymethyl radical, while A is normally an ether molecule. For the calculation of the collision number $\frac{2M_A M_{A^*}}{M_A + M_{A^*}}$ was taken as 45.56. The collision diameters of both methoxymethyl radical and of dimethyl ether were taken to be 5.0 A° (3)(7).

The solid lines of Figure 7 show the dependence of the calculated Kassel rate constants on pressure, in terms of a log-log plot. These curves were calculated for s=7 and yielded the best fit to the experimental data, which are also shown in Figure 7.

Figure 7

Curves calculated from the Kassel equation for k_3 and fitted to the experimental data at five temperatures from 200 to 300°C. The Kassel integrations were performed with $s = 7$ and $\lambda = 1.0$.

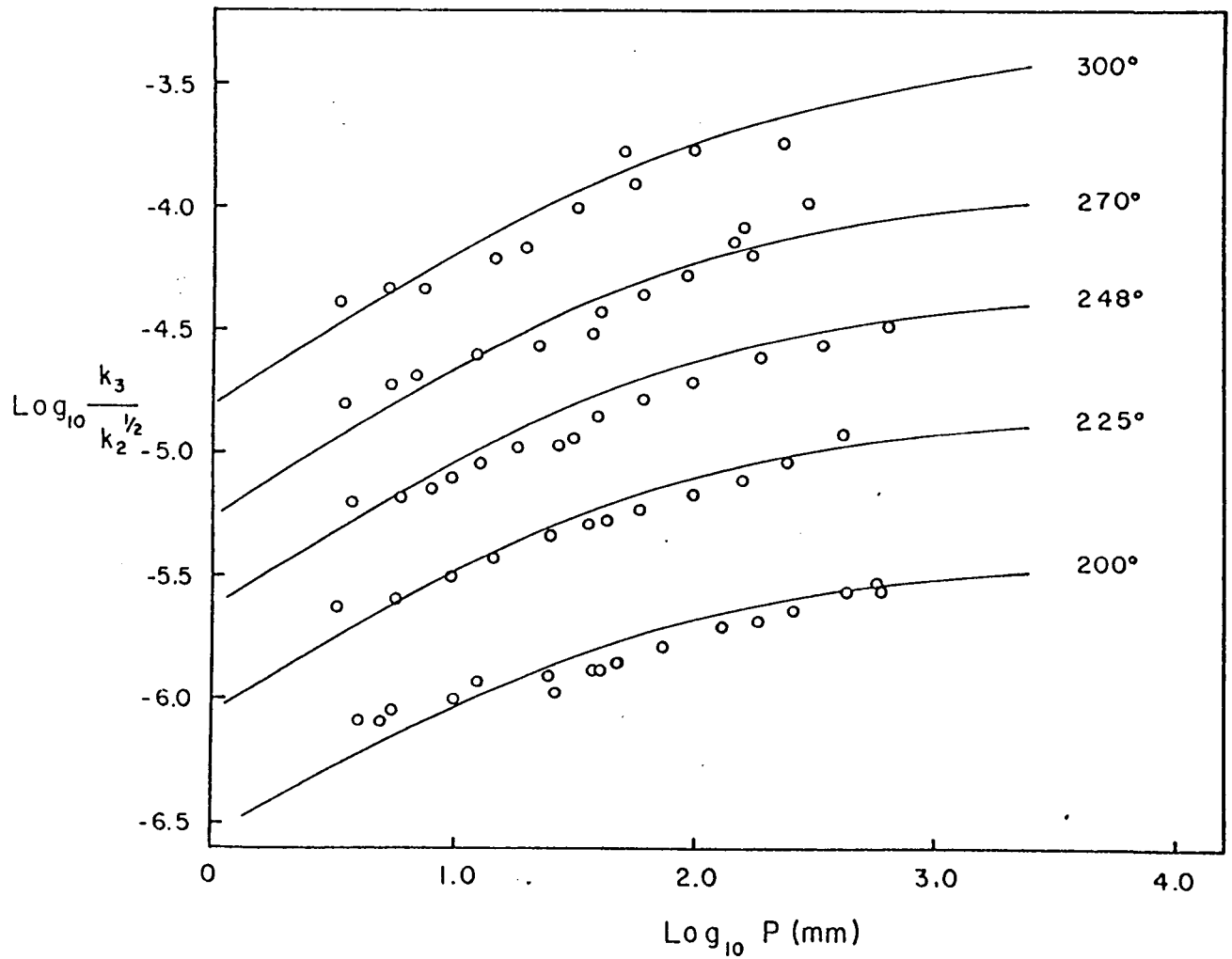
300°
270°
248°
225°
200°
-3.5
-4.0
-4.5
-5.0
-5.5
-6.0
-6.5
$\log_{10} \frac{k_3}{k_2^{1/2}}$
0
1.0
2.0
3.0
4.0
$\log_{10}$ P (mm)

The curvature found for s=7 seems rather sharper than indicated from the experimental data, although the fall-off occurred in the correct range of pressure. Higher values of s appear to have a curvature more in line with the experimental points, but the fall-off occurs at pressures much lower than found experimentally. In an attempt to fit the experimental data more exactly, the assumption of unit efficiency for the deactivation process has been examined. Although deactivation may occur on every collision for some processes, a collision-efficiency factor, λ , may have a value of less than unity for some deactivation reactions. Reactions involving a low critical ratio, such as the decomposition of the methoxymethyl radical ($E/RT = 25$), may be more susceptible to low collision efficiencies, for the deactivation process, than decompositions involving a high critical ratio. With this in mind Kassel integrations were carried out for $\lambda = 0.1$; such a value may be unrealistically low since this implies that only one collision in ten is effective in deactivation.

Figure 8 shows the Kassel curves calculated for $\lambda = 0.1$. These curves were obtained for a value of s=10. The fit to the curvature of the experimental points is only marginally better than obtained in Figure 7 for s=7 and $\lambda = 1.0$.

From the Kassel integrations it appears that s, the number of normal modes contributing to energization,

Figure 8

Curves calculated from the Kassel equation for k_3. The integrations were performed with s = 10 and $\lambda = 0.1$.

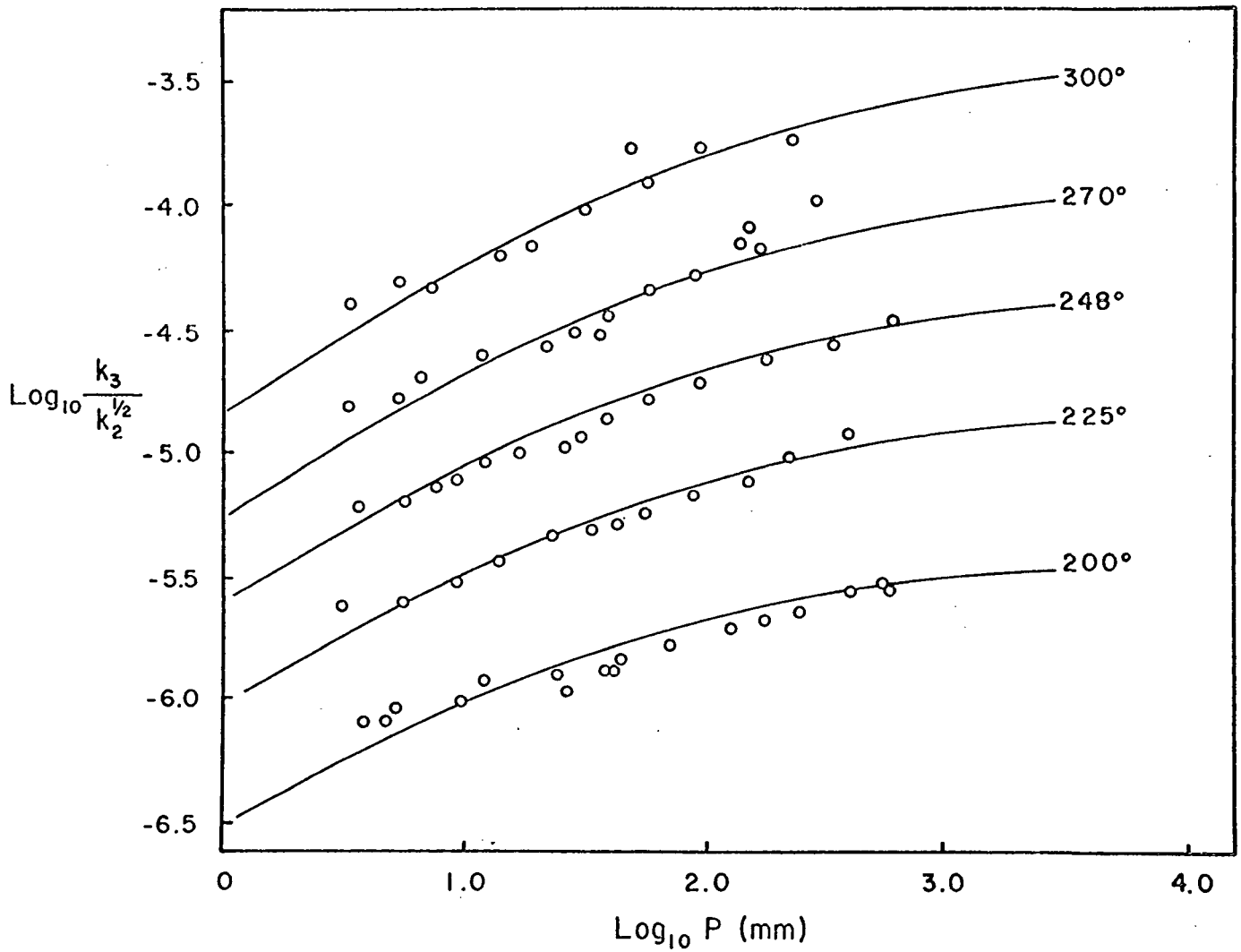
-3.5
-4.0
-4.5
-5.0
-5.5
-6.0
-6.5
$\text{Log}_{10}\frac{k_3}{k_2^{1/2}}$
300°
270°
248°
225°
200°
0
1.0
2.0
3.0
4.0
Log_{10} P (mm)

has a value no less than 7 and no greater than 10. This is in agreement with the value of 8 or 9 obtained from the activation energy difference. The value of s is frequently close to $\frac{3N-6}{2}$ where N is the number of atoms in the species decomposing. For the methoxymethyl radical, $\frac{3N-6}{2}$ is 9.

There are a number of modes which may be expected to contribute very little to the energization process which eventually ruptures the C-O bond in CH_3OCH_2. A linear activated complex for the decomposition of the methoxymethyl radical seems unlikely, since only when the methyl group has actually left would linearity be achieved. For a non-linear activated complex there would be two torsional modes and one bending mode, none of which will contribute to energization. In addition the methoxymethyl radical should exhibit five C-H stretching frequencies which would have high zero-point energy; the high-energy quanta required for energization of these C-H stretches may not be available. It is reasonable to exclude these eight modes when counting the modes which contribute to energization: this leaves ten normal modes, in agreement with the s values previously discussed.

It is significant that the experimental rate coefficients fall less sharply at lower pressures than is predicted theoretically. This effect may be related to the presence of hot radicals arising as a result of the excess energy provided in the mercury photosensitization. The

bond dissociation energy $D(CH_3OCH_2-H)$ is shown in Chapter VI to be 90.5 kcal. per mole, and the Hg $^3P_1$ contains 22.2 kcal. energy in excess of this. For reaction [1] this excess energy must reside in the fragments. The presence of some of this energy in the methoxymethyl radicals could lead to an enhanced rate of decomposition, even though the hot radicals have less than the critical energy required for decomposition. At high pressures the hot radicals may be thermalized rapidly, while at low pressures some of the hot radicals may decompose before being thermalized. This would account for the observed pressure dependence. Further support for such a postulate is seen in the fact that for the lowest temperature studied the anomalous pressure dependence was more pronounced than for the higher temperatures. This trend would also be accounted for by the decomposition of hot radicals, since at lower temperatures a larger fraction of the total methoxymethyl radicals are generated by the photosensitization step, due to shorter chain lengths.

Influence of Carbon Dioxide

The pressure dependence of k_3 has been tested by using CO_2 as an inert gas to increase the pressure at low pressures of ether. For a given pressure of ether in the presence of inert gas the rate coefficient should have a value greater than at the same pressure of ether with no inert gas. The rate coefficient should increase to the

value corresponding to an ether pressure equal to the total pressure developed by the ether plus the inert gas. Figure 9 shows the results obtained experimentally. The solid dots show the value of the rate constant obtained for that pressure of ether in the presence of CO_2. The crosses refer to the increase in the rate constant that would be obtained if CO_2 had the same efficiency for activation and deactivation as dimethyl ether. The methoxymethyl radical is not decomposing in the presence of a great abundance of other methoxymethyl radicals, but rather in the presence of dimethyl ether; dimethyl ether is thus the normal third body involved in activation and deactivation. When carbon dioxide is added, both carbon dioxide and dimethyl ether will act as third bodies. The efficiency of CO_2 in activation is expected to be less than the efficiency of a molecule such as dimethyl ether; hence it is expected that for runs carried out in the presence of CO_2 the rate constant would not be increased to the value corresponding to the total pressure. The distinct increases in the rate constant observed in Figure 9 support the pressure dependence of the methoxymethyl radical decomposition.

Homogeneity of Reaction

The homogeneity of the reaction conditions has been discussed in Chapter II. It was found that the use of a $0^{o}C$ trap to control the partial pressure of mercury vapor in the reaction vessel did not lead to a low enough partial

Figure 9

The influence of carbon dioxide and of light intensity on k_3 at 248°C.

- o : results with ether alone.
- ● : experimental values with ether-carbon dioxide mixtures.
- x : expected value if ether and carbon dioxide had equal energy-transfer efficiencies.
- △ : results with reduced light intensity.

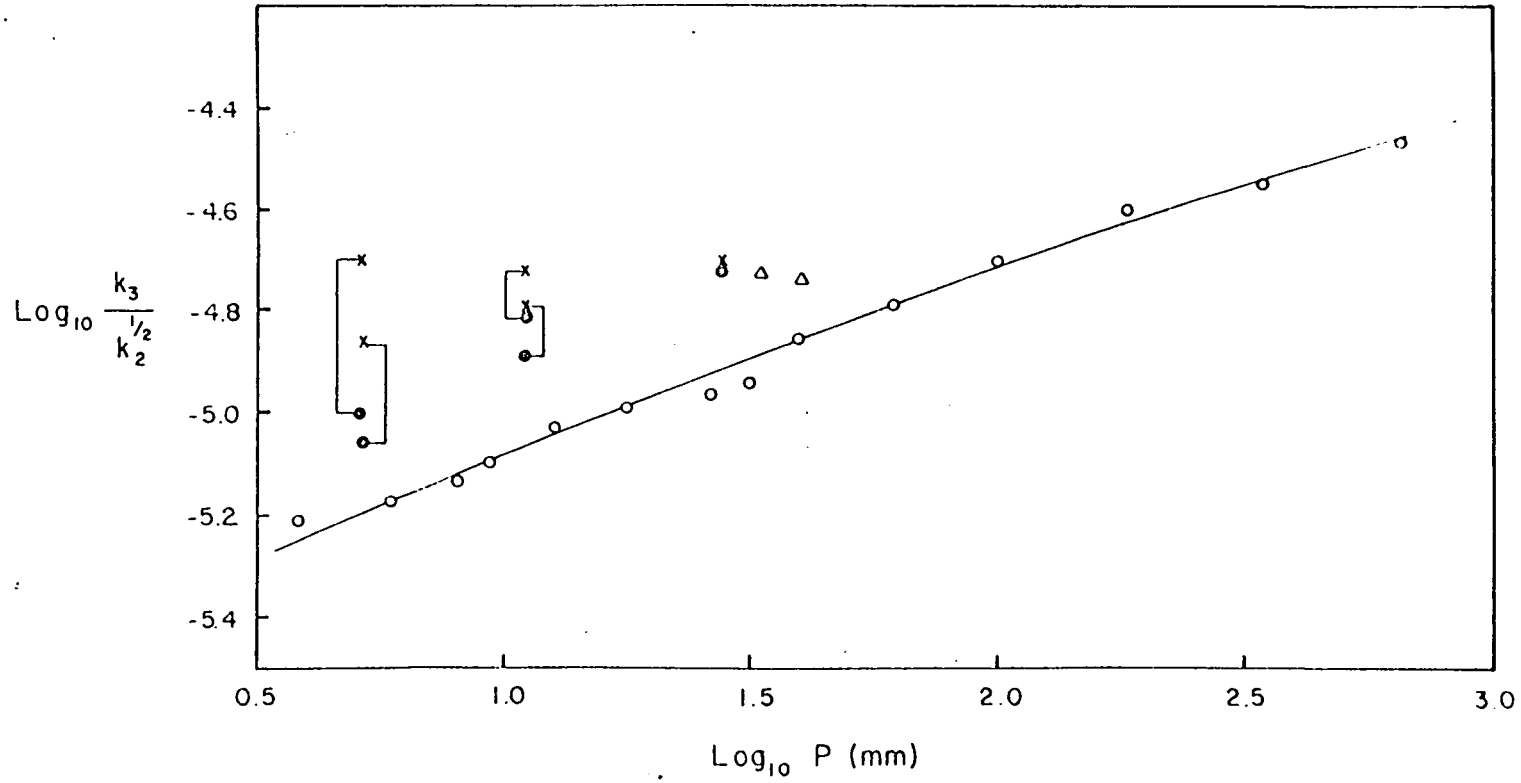
-4.4
-4.6
-4.8
-5.0
-5.2
-5.4
0.5
1.0
1.5
2.0
2.5
3.0
Log10 k3 / k2 1/2
Log10 P (mm)

pressure to assure the homogeneous production of Hg $^3P_1$ atoms. Since the bulk of the present work was carried out under the above conditions it was necessary to determine the effect of the possible non-homogeneity on the decomposition of the methoxymethyl radical. A number of runs were made with a trap at -30°C to control the mercury concentration. In Chapter II, it was concluded that nearly homogeneous conditions are obtained by using this procedure.

The use of the -30°C trap for the mercury had a distinct effect on the $k_3/k_2^{1/2}$ ratios. For all temperatures studied the ratio was increased by a factor of about 2. At 225°C the decomposition was reinvestigated over the full pressure region, while at 200, 248 and 270°C the decomposition was studied over a smaller range of pressure. Figure 10 shows the new experimental data superimposed on the curves found under the previous conditions. It is seen that the curve for 225°C has the same shape as previously found, and that the fall off is occurring in the same range of pressure. Enough data were obtained at the other temperatures to establish the position of the fall-off curve at a pressure of about 35 mm. Values of the rate constant were interpolated from both the old and new curves at a pressure of 35 mm. These values of log $k_3/k_2^{1/2}$ are shown in Arrhenius plots in Figure 11. It is seen that the activation energy has remained the same under the new conditions as under the old conditions. It is concluded that the effects of non-homo-

Figure 10

The variation of k_3 with pressure, for mercury concentration in the reaction zone controlled by a -30°C trap. The experimental points and dashed lines correspond to this condition. The solid curves are the same as shown in Figure 3 and were obtained with the mercury trap at 0°C.

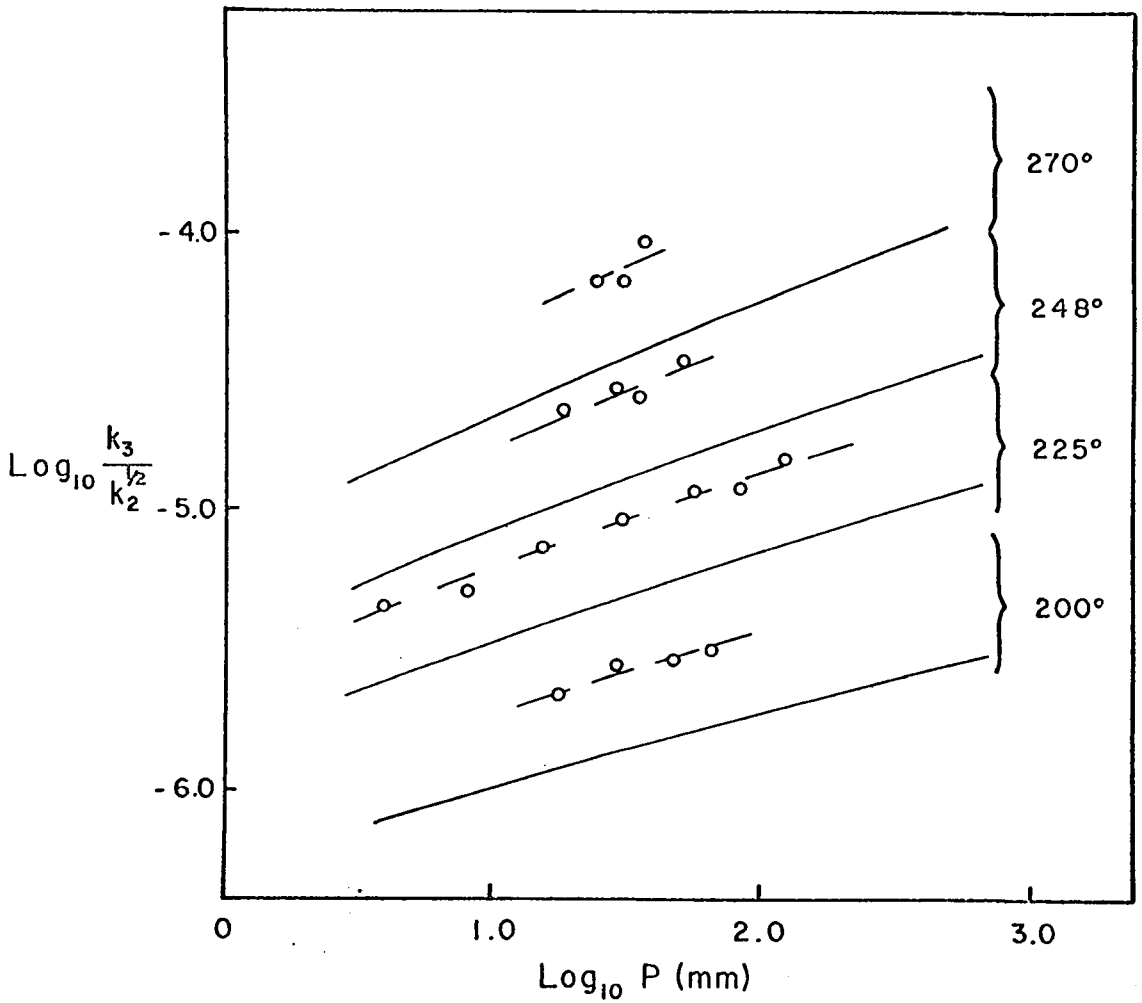
270°
248°
225°
200°
-4.0
-5.0
-6.0
$\text{Log}_{10} \frac{k_3}{k_2^{1/2}}$
0
1.0
2.0
3.0
Log_{10} P (mm)

Figure 11

Arrhenius plots for $k_3/k_2^{1/2}$ at 35 mm Hg pressure. The lower curve was obtained from data using a trap at 0°C to control the mercury concentration; the upper curve was obtained with a -30°C trap to control the mercury concentration.

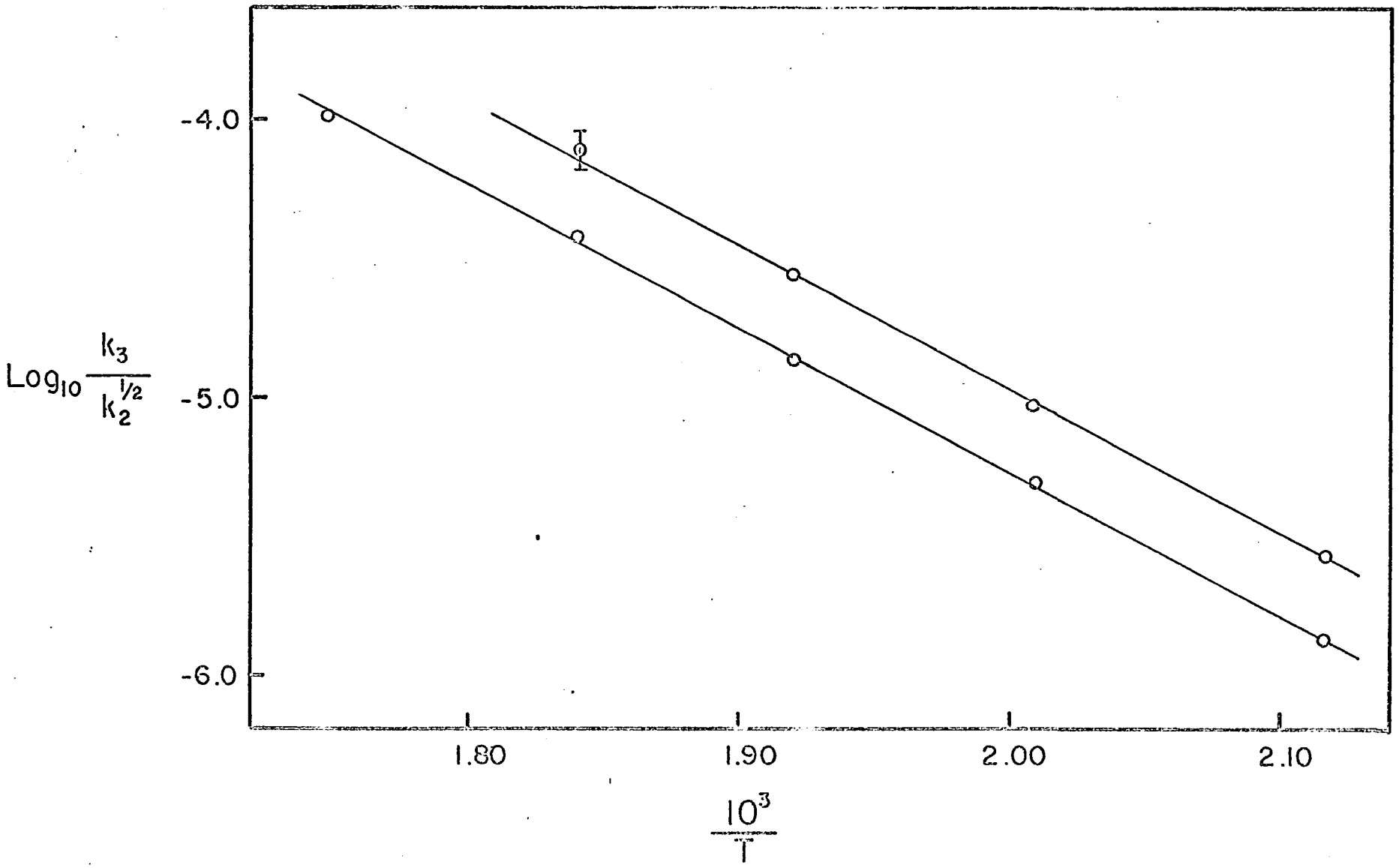
-4.0
-5.0
-6.0
$\log_{10} \frac{k_3}{k_2^{1/2}}$
1.80
1.90
2.00
2.10
$\frac{10^3}{T}$

geneity did not interfere with the conclusions drawn about the decomposition of the methoxymethyl radical. The increase in the ratio $k_3/k_2^{1/2}$ is thought to arise from the effect of non-homogeneity on the 1,2-dimethoxyethane formation. Under conditions of complete absorption the concentration of methoxymethyl radicals will be particularly high near the incident face of the reaction vessel. This will give rise to an abnormally favourable condition for combination of methoxymethyl radicals, leading to formation of 1,2-dimethoxyethane at rates greater than expected for a homogeneous reaction. This in turn causes $k_3/k_2^{1/2}$ ratios to be smaller than expected for homogeneous conditions.

Although it has been shown that with the mercury trap at 0°C, E_3 has not been affected by the non-homogeneity, one must also consider the effect on A_3. The log $k_3/k_2^{1/2}$ values for -30°C were all about 0.3 log units higher than obtained for 0°C. This change is therefore present in the Arrhenius plot, and has the effect of increasing the intercept by 0.3 log units. This requires that the A factors for the decomposition of methoxymethyl radical should be increased by $10^{0.3}$ giving

$$k_3^{\infty} = 2.0 \times 10^{13} e^{-25,500/RT} \text{ sec}^{-1}$$

$$k_3^{o} = 2.8 \times 10^{16} e^{-19,100/RT} \text{ cc mole}^{-1} \text{ sec}^{-1}.$$

Another test for homogeneity was conducted (using 0°C for the mercury trap) by reducing the light intensity by inserting a wire mesh between the light source and the

reaction vessel. Figure 9 shows that the $k_3/k_2^{1/2}$ ratio was increased under these conditions. This may also be explained in terms of the 1,2-dimethoxyethane production. Although complete absorption would still be occurring, the methoxymethyl radical concentration near the incident face of the reaction vessel would be substantially reduced so that 1,2-dimethoxyethane would be produced at a lower rate. The unimolecular decomposition would remain unaffected and hence the $k_3/k_2^{1/2}$ ratio would be expected to increase under the condition of lower light intensity.

Thermochemistry

The thermochemistry of the decomposition of the methoxymethyl radical gives support to the activation energy of 25.5 kcal. per mole found experimentally. Calculations have been made using the following ΔH_f° values for a standard state of 25°C: CH_3OCH_3 = -44.0 (8), CH_3 = 32.0 (9), and CH_2O = -27.7 (9) all in kcal. per mole. The heat of formation of the methoxymethyl radical is shown in Chapter VI to be -5.56 kcal. per mole.

Figure 12 shows the thermochemical relationships for the decomposition of the methoxymethyl radical. It is seen that the decomposition is endothermic to the extent of 9.9 kcal. per mole. The observed activation energy of 25.5 kcal. per mole is 15.6 kcal. per mole in excess of the endothermicity. This latter quantity is the activation energy for the exothermic back reaction, which is the

Figure 12

Energy diagram for the decomposition of the methoxymethyl radical to formaldehyde and a methyl radical.

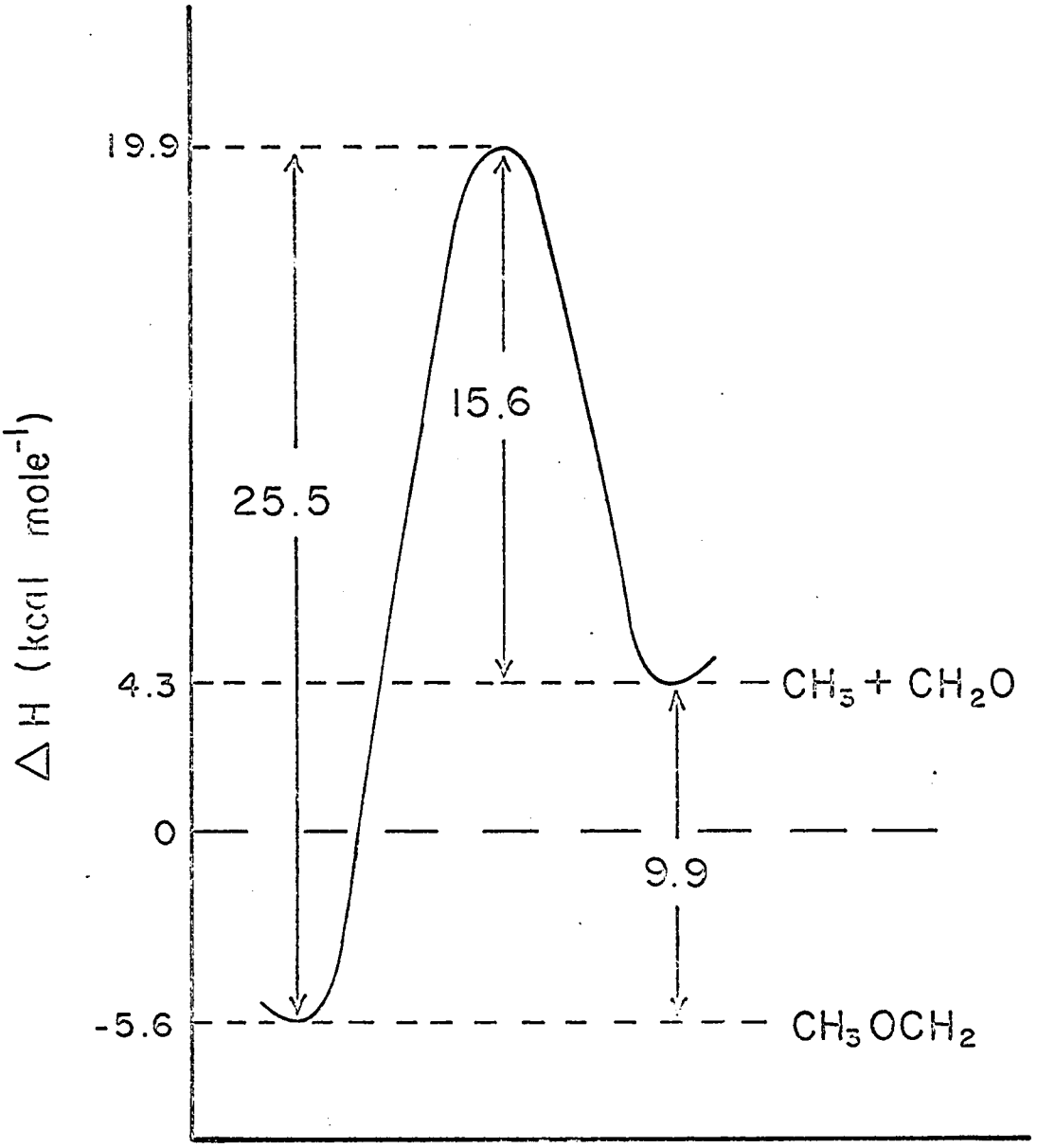
19.9
15.6
25.5
4.3
$CH_3 + CH_2O$
0
9.9
-5.6
CH_3OCH_2
ΔH (kcal mole^{-1})

addition of a methyl group to the carbonyl group of formaldehyde, with addition occurring at the oxygen atom. The reaction of methyl radicals with formaldehyde has been studied by Toby and Kutschke (10) and by Blake and Kutschke (11). The above back reaction was not observed, the only reaction being abstraction of a hydrogen atom by methyl radical. The activation energy for the abstraction reaction was found to be 6.2 and 6.6 kcal. per mole in the two studies. An activation energy of 15.6 kcal. per mole for the addition of a methyl radical to formaldehyde is sufficiently higher than the activation energy for abstraction to render the addition reaction unobservable.

CHAPTER IV

THE COMBINATION OF METHYL RADICALS

INTRODUCTION

Several investigations into the pressure dependence of the combination of methyl radicals have been conducted under various conditions. Kistiakowsky and Roberts (12) studied the combination of methyl radicals produced in the photolysis of acetone at temperatures in the 135 to 240°C range; in the pressure range 1 to 10 mm of acetone there was a pressure dependence of the second-order rate coefficient. Ingold and Lossing (13) and Ingold, Henderson, and Lossing (14) studied the combination of methyl radicals produced from mercury dimethyl at temperatures ranging from 160 to 1000°C, using a mass spectrometric technique. The pressure of the system was almost entirely that of the helium carrier gas. At 1000°C the combination of methyl radicals was observed to be pressure dependent in the pressure range 3.4 to 15.0 mm with an indication that there was pressure dependence at even higher pressures. Dodd and Steacie (15) examined the combination of methyl radicals at 247°C over the pressure range of 0.2 mm to 100 mm, the methyl radicals being produced by the photolysis of acetone. They showed that over this pressure range the order of reaction changes from second to third as the

pressure decreases, the fall-off being most rapid in the 1 to 10 mm range. The combination of methyl radicals has been studied by Toby and Weiss (16) for pressures ranging from 3 to 60 mm and at temperatures from 25 to 180°C, the photolysis of azomethane being used to produce methyl radicals. Pressure effects on the combination of methyl radicals were observed for pressures of azomethane below 20 mm.

In the present work, pressure effects on the kinetics of the combination of methyl radicals have been deduced from the results of the mercury-photosensitized decomposition of dimethyl ether at temperatures from 200 to 300°C.

EXPERIMENTAL

The apparatus and experimental technique have been described in detail in Chapter II.

RESULTS AND DISCUSSION

The reaction scheme for the mercury-photosensitized decomposition of dimethyl ether has been given in Chapter II. The same numbering for reactions [1]-[8] is used in this chapter.

In the temperature range 200 to 300°C the methoxymethyl radical decomposes to give a methyl radical and formaldehyde. The methyl radicals either combine to form ethane or abstract a hydrogen atom to give methane. The rates of these reactions are

[9] $$v_5 = k_5[CH_3]^2 = v_{C_2H_6}$$

[10] $$v_4 = k_4[CH_3][CH_3OCH_3] = v_{CH_4}$$

It follows that

[11] $$\frac{k_5^{1/2}}{k_4} = \frac{v_5^{1/2}[CH_3OCH_3]}{v_4} = \frac{v_{C_2H_6}^{1/2}[CH_3OCH_3]}{v_{CH_4}}$$

Figure 13 shows a plot of log $k_5^{1/2}/k_4$ against the logarithm of the pressure (P) in mm Hg. A fall-off in the rate coefficient is observed at the lower pressures, with the rate coefficient approaching a constant value for pressures above 100 mm. Since the function plotted contains $k_5^{1/2}$ in the numerator, a slope of zero is expected in the second-order region, while a slope of 0.5 would correspond to the reaction in its third-order region. For the lowest pressures studied the combination of methyl radicals is not yet completely third-order. It should be noted that fall-off in the rate coefficient appears to begin at pressures of about 100 mm. The present results are qualitatively in agreement with the work of Dodd and Steacie (15), in which, at similar temperatures, the fall-off was observed at somewhat lower pressures. Differences in the efficiency of dimethyl ether and acetone as third bodies for the combination of methyl radicals could account for the differences in fall-off pressures. Since, in the present work, the pressure dependence is observed at pressures higher than in Dodd and Steacie's work, it is concluded that dimethyl ether is a less efficient third

Figure 13

The pressure dependence of $k_5^{1/2}/k_4$ at five temperatures in the range 200 to 300°C.

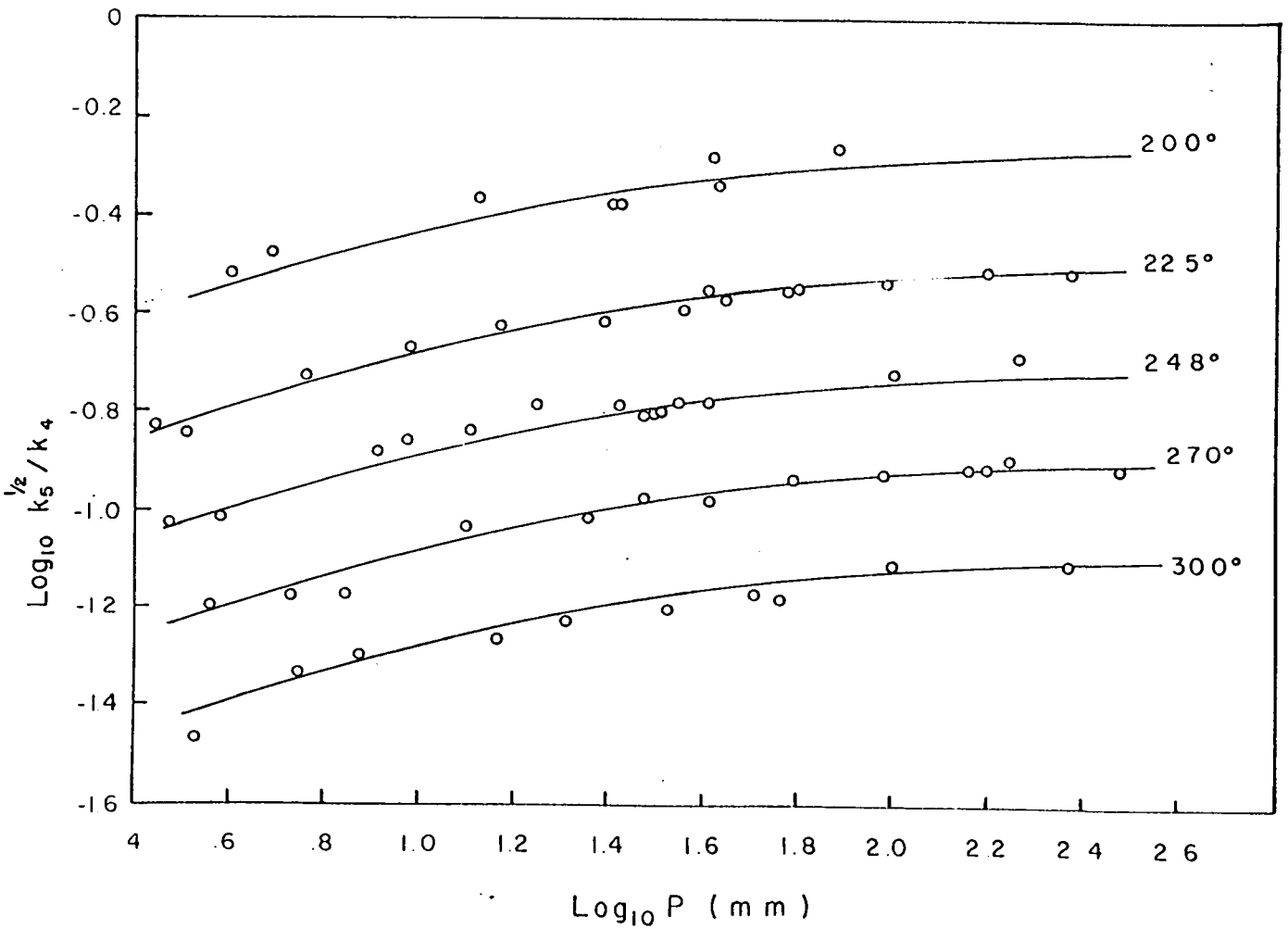
0
-0.2
-0.4
-0.6
-0.8
-1.0
-1.2
-1.4
-1.6
Log10 k5^1/2 / k4
200°
225°
248°
270°
300°
.4
.6
.8
1.0
1.2
1.4
1.6
1.8
2.0
2.2
2.4
2.6
Log10 P (mm)

body than acetone. The pressure dependence of methyl combination is found at substantially higher pressures than observed by Toby and Weiss (16) with azomethane as the third body, and this leads to the conclusion that dimethyl ether is also a less efficient third body than azomethane.

Values of log $k_5^{1/2}/k_4$ were interpolated from Figure 13 at a pressure corresponding to 100 mm pressure and are plotted in Figure 14 in the form of an Arrhenius plot. From this plot it is found that $1/2\ E_2 - E_4 = -10.5$ kcal. per mole. If the methyl radicals combine with no activation energy, the activation energy for the abstraction of hydrogen from dimethyl ether by methyl radicals is 10.5 kcal. per mole. Since the pressure dependence of the methyl radical combination is becoming evident at 100 mm pressure, there may be an apparent negative activation energy for the combination of methyl radicals. The negative activation energy may be about 2 kcal. at this pressure; hence the abstraction reaction will probably have an activation energy of about 9.5 kcal. per mole. In Chapter V the abstraction reaction is estimated to have an activation energy of 9.4 kcal. per mole from consideration of a different rate constant ratio. From the intercept of Figure 14, and using $A_5 = 2.2 \times 10^{13}$ cc mole^{-1} sec^{-1} for the combination of methyl radicals (6), the frequency factor for the abstraction reaction has been calculated to be $10^{11.82}$ cc mole^{-1} sec^{-1}, i.e., $A_4 = 6.6 \times 10^{11}$ cc mole^{-1} sec^{-1}.

Figure 14

An Arrhenius plot for the $k_5^{1/2}/k_4$ ratio at a pressure of 100 mm Hg.

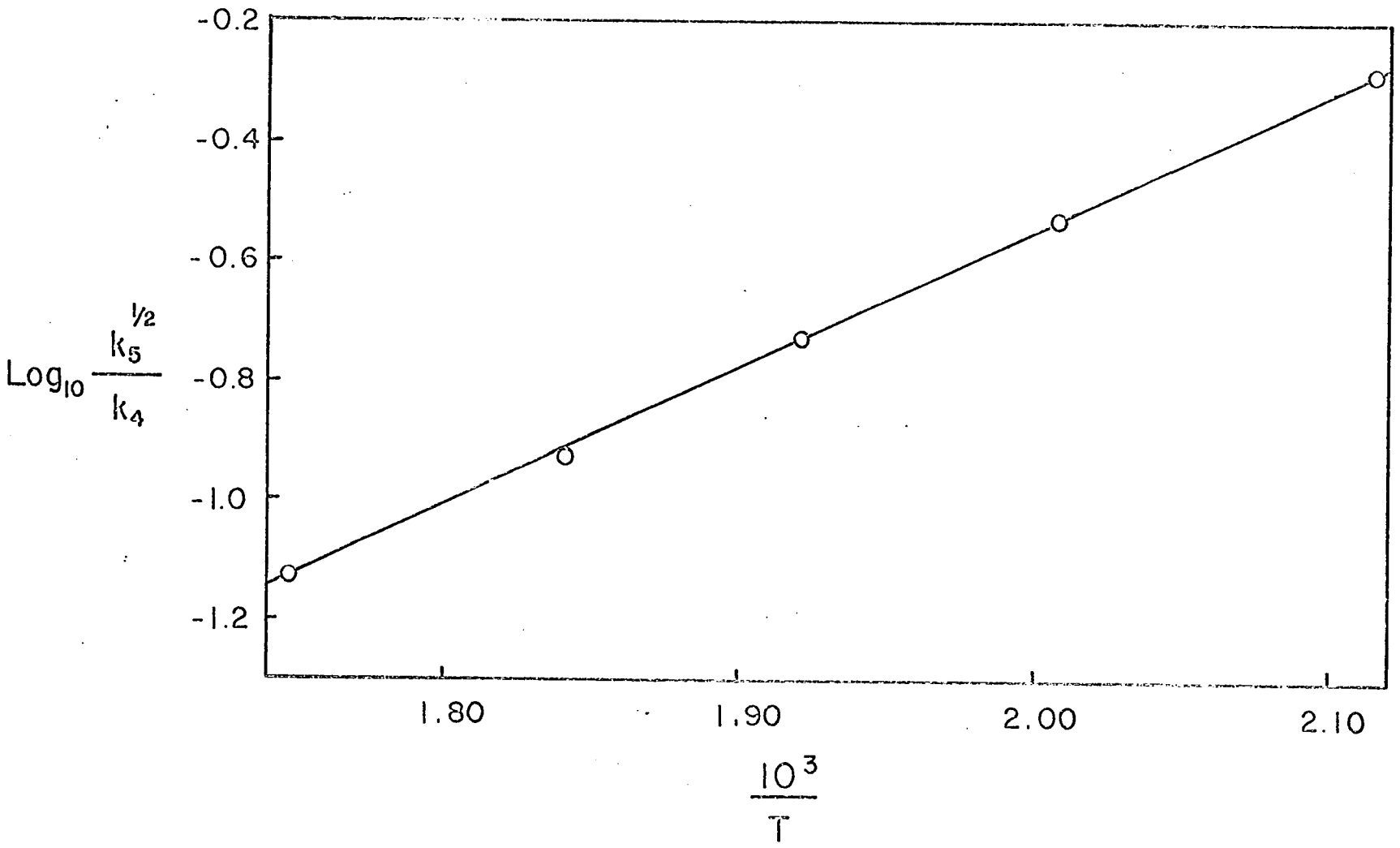
-0.2
-0.4
-0.6
-0.8
-1.0
-1.2
$\text{Log}_{10} \frac{k_5^{1/2}}{k_4}$
1.80
1.90
2.00
2.10
$\frac{10^3}{T}$

Kassel Integration

The pressure dependence of the combination of two species must be identical to the pressure dependence of the reverse unimolecular reaction. This means that as the combination reaction changes from second-order to third-order kinetics over a certain pressure range, so also must the unimolecular decomposition change from first-order to second-order kinetics over the same pressure range.

The reverse reaction of the combination of methyl radicals is the unimolecular decomposition of ethane, the kinetics of which have been thoroughly studied by Lin and Back (17). The rate constant for this reaction calculated for the first-order region is

$$k^{\infty} = 1.0 \times 10^{16} e^{-86000/RT} \text{ sec}^{-1}$$

With the use of this rate constant, and a collision diameter of 3.3A for ethane (as used by Lin and Back), Kassel integrations have been computed for various s values. By choosing the proper s value one may fit the pressure-dependence of the rate constants calculated for ethane decomposition to the observed pressure-dependence of the combination of methyl radicals. Figure 15 shows the pressure dependence of the rate constants calculated from the Kassel equation and fitted to the data on the combination of methyl radicals. The upper curve for each temperature is calculated for s = 9, while the lower curve is for s = 8. It is seen that an s value between 8 and 9 would more appropriately fit the experi-

Figure 15

Curves calculated from the Kassel equation for $k_5^{1/2}$ and fitted to the experimental data at five temperatures. For each temperature the upper curve was calculated with s = 9 and the lower curve was calculated with s = 8.

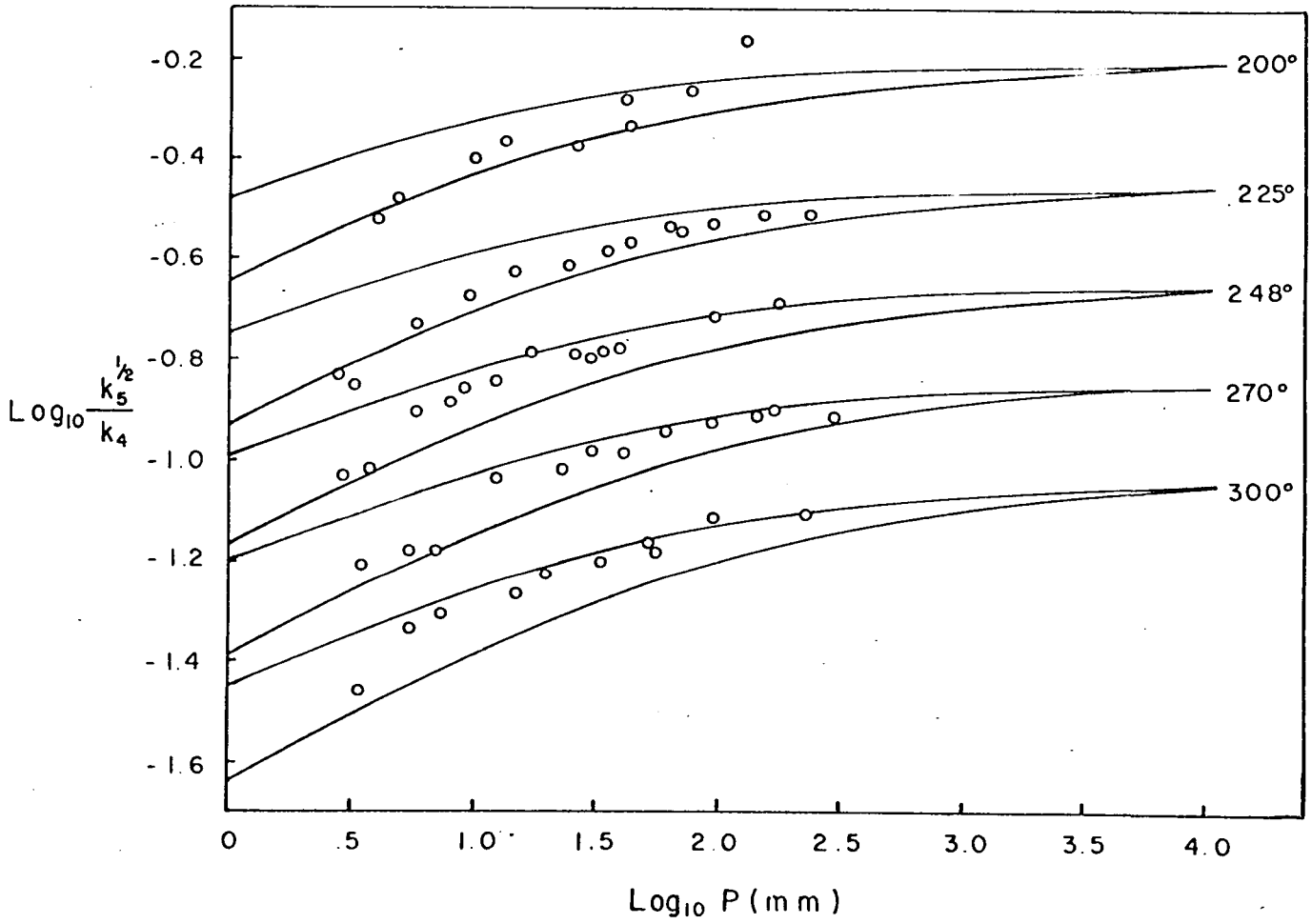
-0.2
-0.4
-0.6
-0.8
-1.0
-1.2
-1.4
-1.6
$\text{Log}_{10}\frac{k_5^{1/2}}{k_4}$
200°
225°
248°
270°
300°
0
.5
1.0
1.5
2.0
2.5
3.0
3.5
4.0
Log_{10} P (mm)

mental data. Thus 8 or 9 normal modes are contributing to the energization of ethane for its unimolecular decomposition. At higher temperatures Lin and Back concluded that 11 to 13 modes contribute to energization, on the basis of Kassel integrations carried out to fit the experimental data on the decomposition of ethane; they also note that there is evidence that the apparent s values are lower the lower the temperature. The present value of 8 or 9 is in agreement with the value s = 9 calculated by Gill and Laidler (18) and is close to the $\frac{3N-6}{2}$ (=9) value frequently found with the Kassel theory.

Effect of Carbon Dioxide

Several runs were carried out at low pressures of dimethyl ether, with added CO_2 as an inert gas. The rate constant for the combination of methyl radicals would be expected to increase under the influence of this additional third body. However, within the limits of experimental error the increase in the value of the rate constant was barely noticeable and certainly was not of the magnitude predicted from the increased pressure of CO_2. This observation agrees with the conclusions of Dodd and Steacie and of Toby and Weiss. The former authors concluded that CO_2 has an energy-transfer efficiency of only 0.03 of that of acetone. Toby and Weiss found the efficiency of CO_2 to be 0.06 relative to azomethane. It was concluded above that

dimethyl ether is a less efficient third body than either acetone or azomethane. From the relative positions of the fall-off curves observed for acetone and dimethyl ether as third bodies it may be estimated that acetone is 3 - 5 times as efficient as dimethyl ether. Carbon dioxide would still be a much less efficient third body than dimethyl ether. Only if the efficiency of carbon dioxide were greater than about 0.15 compared with dimethyl ether would the carbon dioxide have had a marked effect on the rate constant in the present experiments. Such a value is calculated if the efficiency of CO_2 is 0.03 compared with acetone and if dimethyl ether is 0.20 compared with acetone, as suggested above. Thus the efficiency of CO_2 relative to dimethyl ether is such that the effect of CO_2 on the rate constant would scarcely be detected in the present experiments.

Lin and Back (17) have observed that CO_2 is an efficient third body relative to ethane for the decomposition of ethane. At first this seems contradictory to the above conclusions. However, if ethane has a third body efficiency which is low and of the same magnitude as that of carbon dioxide, such a result would still be consistent with the present observations. Evidence that CO_2 has an efficiency similar to C_2H_6 is suggested from the work of Ayscough and Steacie (19). These authors studied the deactivation of vibrational states in electronically excited states produced in the photolysis of hexafluoroacetone.

For this process it was found that C_2F_6 and CO_2 had collision efficiencies of 0.36 and 0.31 respectively relative to the hexafluoroacetone. These values suggest that C_2H_6 and CO_2 should have nearly equal efficiencies for deactivation processes. The assignment of deactivation efficiencies found for one process to a second deactivating process must however be viewed with caution.

The fact that CO_2 had no noticeable effect on k_5, the rate constant for the combination of methyl radicals, but had a significant effect on k_3, the rate constant for the decomposition of the methoxymethyl radical (Chapter III), seems anomalous. A further reason for observing the effect of CO_2 on the methoxymethyl radical is the fact that the function plotted for k_3 was more sensitive to increases in the rate constant than the function plotted for k_5.

Homogeneity of Reaction

The use of 0°C to control the partial pressure of mercury in the reaction vessel has been shown to give rise to inhomogeneous reaction conditions associated with the concentration of Hg $^3P_1$ atoms. These effects have been considered in detail in Chapter II and III. Again, for the combination of methyl radicals the mercury concentration has a significant effect. The bulk of the work was conducted with the mercury concentration corresponding to the partial pressure of mercury at 0°C. Figure 16 compares results

Figure 16

The effect of mercury concentration on the rate-constant ratio $k_5^{1/2}/k_4$. The experimental points were obtained with a mercury concentration corresponding to the vapor pressure of mercury at -30°C. The solid curves are the same as shown in Figure 13 and were obtained for a mercury concentration corresponding to the vapor pressure of mercury at 0°C.

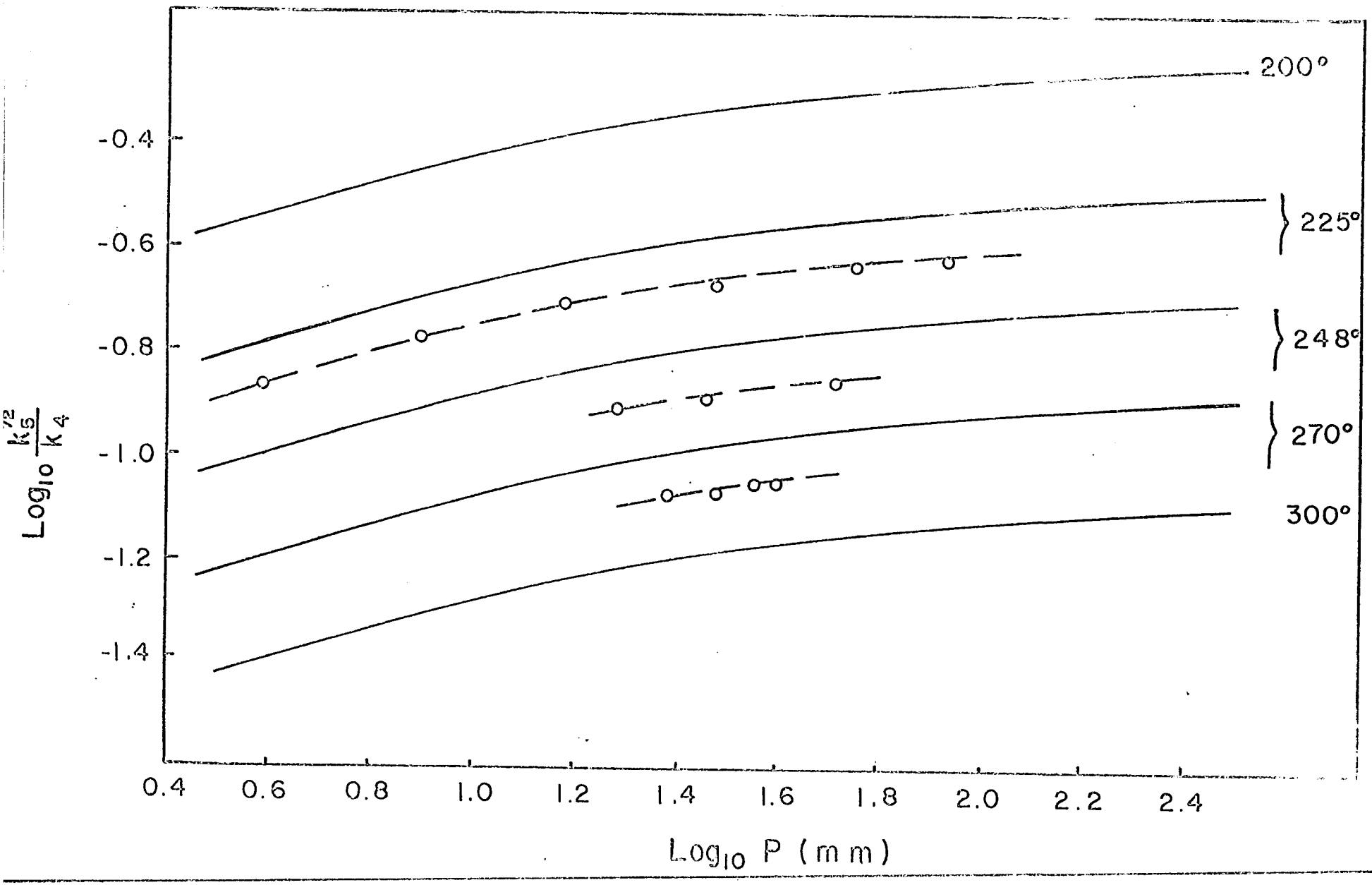
200°
225°
248°
270°
300°
-0.4
-0.6
-0.8
-1.0
-1.2
-1.4
0.4
0.6
0.8
1.0
1.2
1.4
1.6
1.8
2.0
2.2
2.4
$\log_{10} \frac{k'_5}{k_4}$
$\log_{10} P$ (mm)

obtained using -30°C to control the mercury concentration with the results obtained for 0°C. The solid lines are the curves obtained for 0°C as drawn through the experimental points shown in Figure 14. The experimental points and the dashed lines are the values found for -30°C. The rate constant ratio $k_5^{1/2}/k_4$ has decreased by 0.08 log units. The data at 225°C show that the shape of the fall-off curve has not changed, thus not invalidating conclusions about the pressure dependence of k_5. It is also noted that each curve has been shifted vertically by the same number of log units; hence the activation energy for $1/2\ E_2 - E_4$ is not changed. However, the A factor for the abstraction reaction must be corrected by $10^{0.08}$ giving $A_4 = 10^{11.90}$ cc $mole^{-1}$ sec^{-1} or $A_4 = 8.0 \times 10^{11}$ cc $mole^{-1}$ sec^{-1}.

CHAPTER V

THE COMBINATION OF METHYL RADICALS WITH METHOXYMETHYL RADICALS

INTRODUCTION

For the mercury-photosensitized decomposition of dimethyl ether the combination of methyl radicals with methoxymethyl radicals has been proposed as a termination process by Marcus, Darwent and Steacie (1) and by Pottie, Harrison and Lossing (2). The latter authors observed methyl ethyl ether in the products analysed by a mass-spectrometric technique. This same termination step has been proposed for the thermal decomposition of dimethyl ether (4,5,20), and methyl ethyl ether has been observed in the products by Anderson and Benson (21). Details of the kinetics of methyl ethyl ether formation by this radical combination have not been reported previously.

In the present study of the mercury-photosensitized decomposition of dimethyl ether, the formation of methyl ethyl ether has been examined and certain aspects of the kinetics of the combination reaction have been elucidated.

EXPERIMENTAL

The details of the apparatus and technique used in the study of the mercury-photosensitized decomposition

of dimethyl ether have been outlined in Chapter II.

RESULTS AND DISCUSSION

The scheme of reactions which explain the mercury-photosensitized decomposition of dimethyl ether has been given in Chapter II. The same numbering of reactions [1]-[7] is used in the following discussion.

This chapter deals with the kinetics of reaction [6], the combination of methyl and methoxymethyl radicals. With the experimental rates of formation of methane, 1,2-dimethoxyethane, ethane and methyl ethyl ether, one can examine the rate constant k_6 in two ways.

The rates of reactions [2], [4] and [6] are as follows:

[8] $$v_2 = k_2[CH_2OCH_3]^2$$

[9] $$v_4 = k_4[CH_3][CH_3OCH_3]$$

[10] $$v_6 = k_6[CH_3][CH_2OCH_3]$$

From the above relationships it follows that

[11] $$\frac{k_6}{k_4 k_2^{1/2}} = \frac{v_6[CH_3OCH_3]}{v_4 v_2^{1/2}} = \frac{v_{MEE}[CH_3OCH_3]}{v_{CH_4}(v_{dimer})^{1/2}}$$

Thus from the measured rates of formation of methyl ethyl ether (MEE), methane and 1,2-dimethoxyethane (dimer), the rate constant ratio $k_6/k_4k_2^{1/2}$ may be evaluated.

The second rate-constant ratio is obtained by considering reactions [3], [4], and [6]:

[12] $$v_3 = k_3[CH_2OCH_3]$$

[13] $$v_4 = k_4[CH_3][CH_3OCH_3]$$

[14] $$v_6 = k_6[CH_3][CH_2OCH_3]$$

From the above it follows that:

[15] $$\frac{k_3k_4}{k_6} = \frac{v_3v_4}{[CH_3OCH_3]v_6}$$

As discussed in Chapters II and III consideration of the steady-state concentration of methyl radicals yields

[16] $$v_3 = v_{CH_4} + 2v_{C_2H_6} + v_{MEE}$$

Relationship [15] may now be written as

[17] $$\frac{k_3k_4}{k_6} = \frac{(v_{CH_4} + 2v_{C_2H_6} + v_{MEE})(v_{CH_4})}{[CH_3OCH_3]v_{MEE}}$$

Thus from the measured rates of formation of methane, ethane and methyl ethyl ether, the rate constant ratio k_3k_4/k_6 may be evaluated.

The combination of methyl radicals with methoxymethyl radicals has been found to exhibit a pressure dependence. Figure 17 shows the variation of $k_6/k_4k_2^{1/2}$ with pressure in a log-log plot. At pressures below about 15 mm the rate-constant ratio $k_6/k_4k_2^{1/2}$ decreases. The rate constants k_4 and k_2 should not be influenced by pressures in this range; the former is for the abstraction reaction, while the latter is for the formation of 1,2-dimethoxyethane and should have a pressure dependence only at very low pressures. The experimental points are somewhat scattered but the decrease in the rate constant at lower pressures is substantial and pressure dependence quite marked.

Figure 17

A log-log plot of the pressure dependence of $k_6/k_4k_2^{1/2}$ at 200, 248 and 270°C.

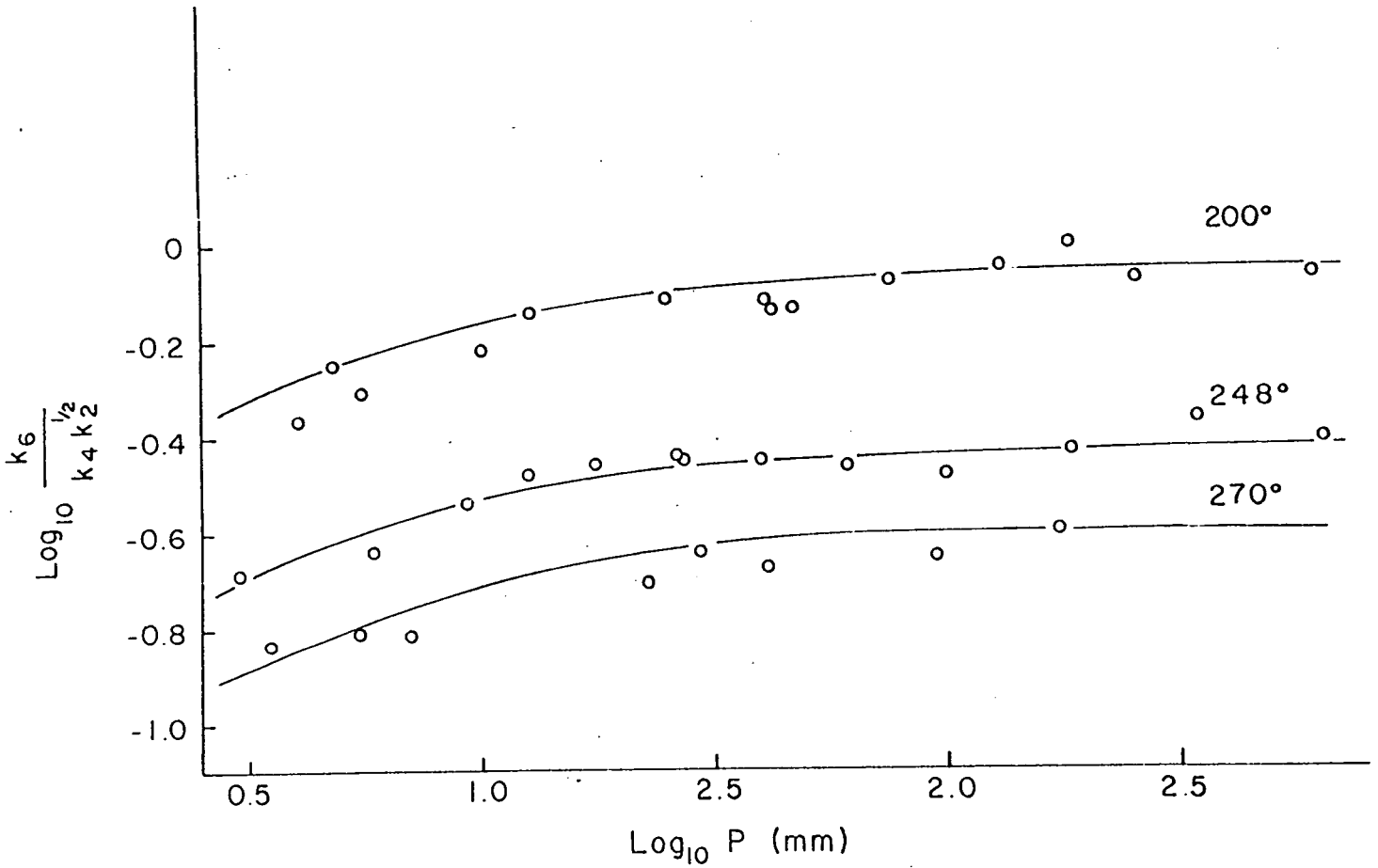
200°
248°
270°
0
-0.2
-0.4
-0.6
-0.8
-1.0
0.5
1.0
2.5
2.0
2.5
$\log_{10} \frac{k_6}{k_4 k_2^{1/2}}$
$\log_{10}$ P (mm)

Values of log $k_6/k_4k_2^{1/2}$ were interpolated from Figure 17 at a pressure corresponding to 100 mm and an Arrhenius plot was made, as shown in Figure 18. On the assumption that reactions [2] and [6] both have zero activation energy and that both these reactions have the same frequency factor as the combination of methyl radicals (2.2×10^{13} sec^{-1} as given by Shepp (6)), the activation energy E_4 is calculated to be 9.2 kcal. per mole and the frequency factor A_4 is $10^{10.76}$ cc $mole^{-1}$ sec^{-1}. Thus the rate constant for the abstraction reaction is given by

[18] $$k_4 = 5.8 \times 10^{10}\ e^{-9,200/RT}\ cc\ mole^{-1}\ sec^{-1}$$

Both Arrhenius parameters are lower than the values quoted in Chapter IV. The scatter in the experimental points in Figure 17, with values at only three temperatures, leaves some doubt about the values of these Arrhenius parameters.

The pressure dependence of the rate constant ratio k_3k_4/k_6 has been considered. Figure 19 shows a plot of log k_3k_4/k_6 against the logarithm of the pressure. The rate constant for the abstraction reaction, k_4, should have no pressure dependence. On the other hand k_3, the rate constant for the decomposition of the methoxymethyl radical, has been shown in Chapter III to be pressure dependent, and k_6, the rate constant for the combination of methyl radicals with methoxymethyl radicals, has been shown to be pressure dependent in the above discussion. The rate-constant ratio k_3k_4/k_6 exhibits an unusual pressure depen-

Figure 18

An Arrhenius plot for the rate-constant ratio $k_6/k_4k_2^{1/2}$ at a pressure of 100 mm.

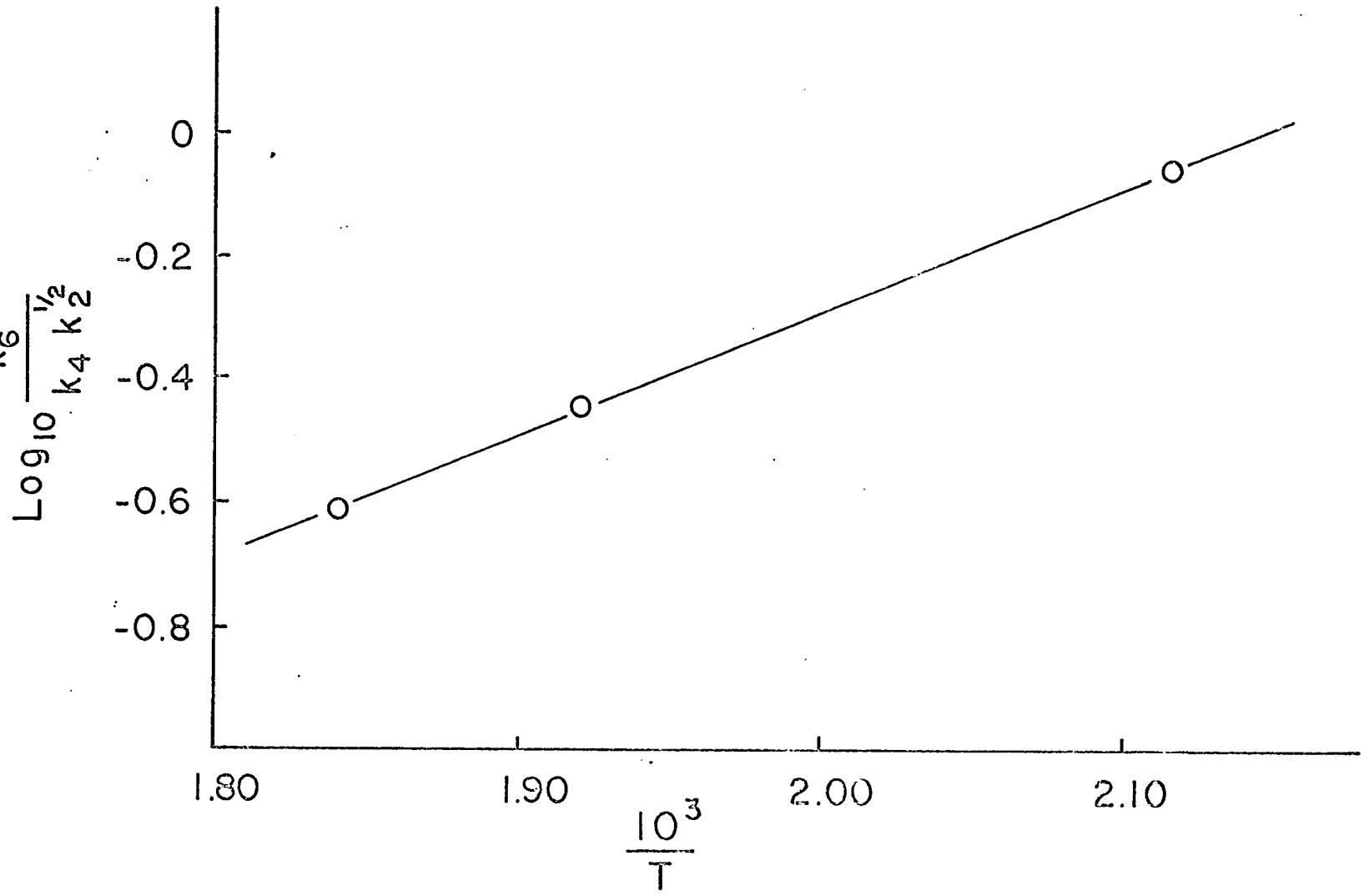
0
-0.2
-0.4
-0.6
-0.8
$\log_{10} \frac{k_6}{k_4 k_2^{1/2}}$
1.80
1.90
2.00
2.10
$\frac{10^3}{T}$

Figure 19

The pressure dependence of k_3k_4/k_6, shown in a log-log plot, for five temperatures from 200 to 300°C.

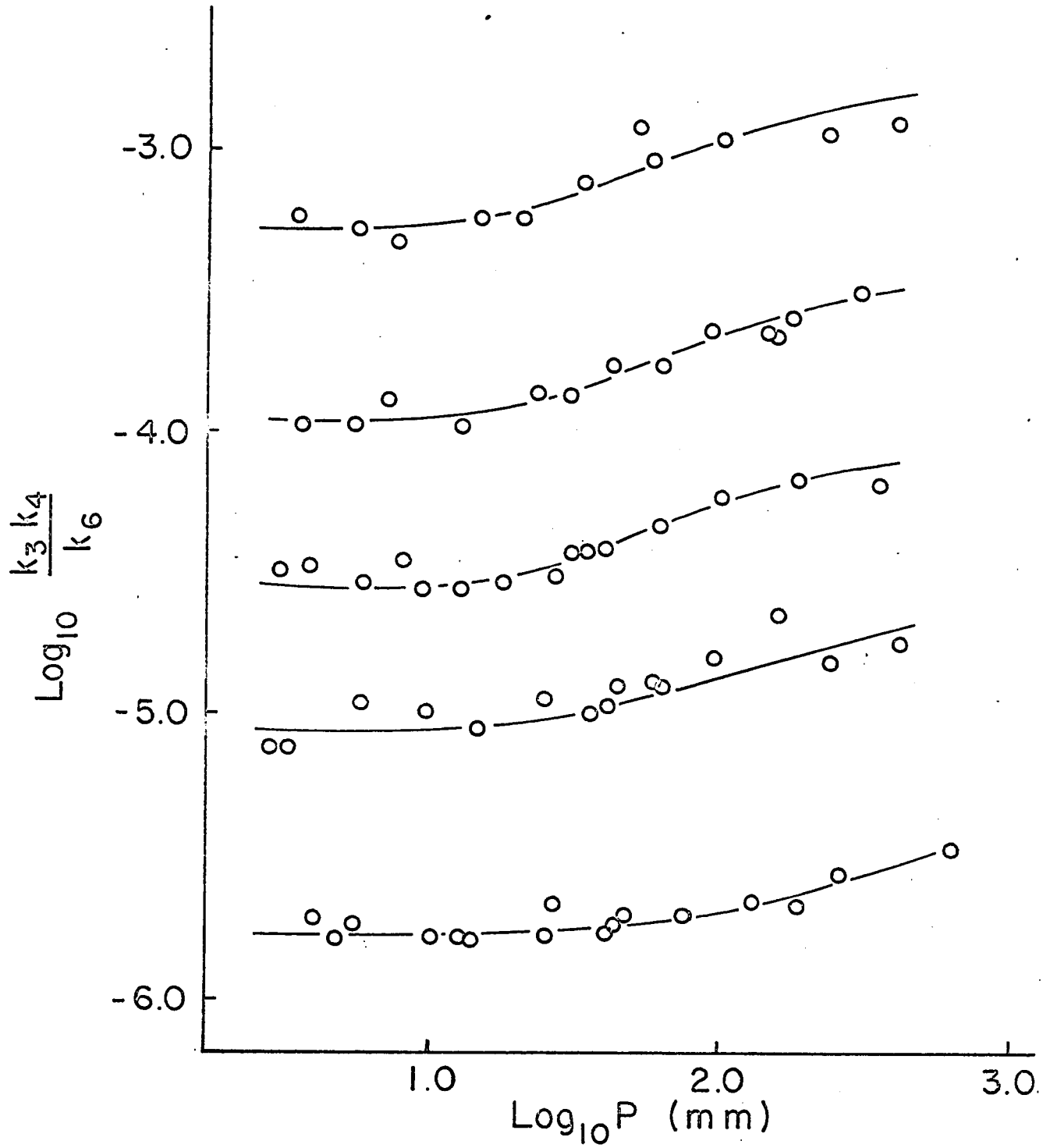
-3.0
-4.0
-5.0
-6.0
$\log_{10} \frac{k_3 k_4}{k_6}$
1.0
2.0
3.0
$\log_{10} P$ (mm)

dence. For decreasing values of pressure, the value of this ratio decreases, but as even lower pressures are reached the value levels off to a constant, as seen in Figure 19. This is explained by the pressure dependence of the separate rate constants k_3 and k_6. The rate constant k_3 has been found to be pressure dependent up to quite high pressures, while k_6 is pressure dependent only at lower pressures. As the values of pressure decrease the pressure dependence of k_3 causes the ratio k_3k_4/k_6 to decrease, but as lower pressures are reached the pressure dependence of k_6 in the denominator of the ratio compensates to yield a constant value of the ratio. The effect observed in Figure 19 is good supporting evidence for the pressure dependence of both k_3 and k_6.

Values of log k_3k_4/k_6 interpolated from Figure 19 at a pressure corresponding to 100 mm are shown in an Arrhenius plot in Figure 20. With the assumption that $E_6=0$, the slope of the Arrhenius plot gives $E_3 + E_4 = 34.2$ kcal. per mole. In Chapter III E_3 was evaluated as 24.8 kcal. per mole at the same pressure. From the difference one obtains $E_4 = 9.4$ kcal/mole. Intercepts evaluated from the same Arrhenius plots yield $A_4 = 10^{11.06}$, under the assumption that $A_6 = A_5 = 2.2 \times 10^{13}$ cc mole^{-1} sec^{-1}; hence $k_4 = 1.1 \times 10^{11}\ e^{-9,400/RT}$ cc mole^{-1} sec^{-1}. This is the third method used to evaluate k_4. This value of E_4 is probably the most reliable since E_4 was evaluated independently at this

Figure 20

An Arrhenius plot for the rate-constant ratio k_3k_4/k_5 at a pressure of 100 mm.

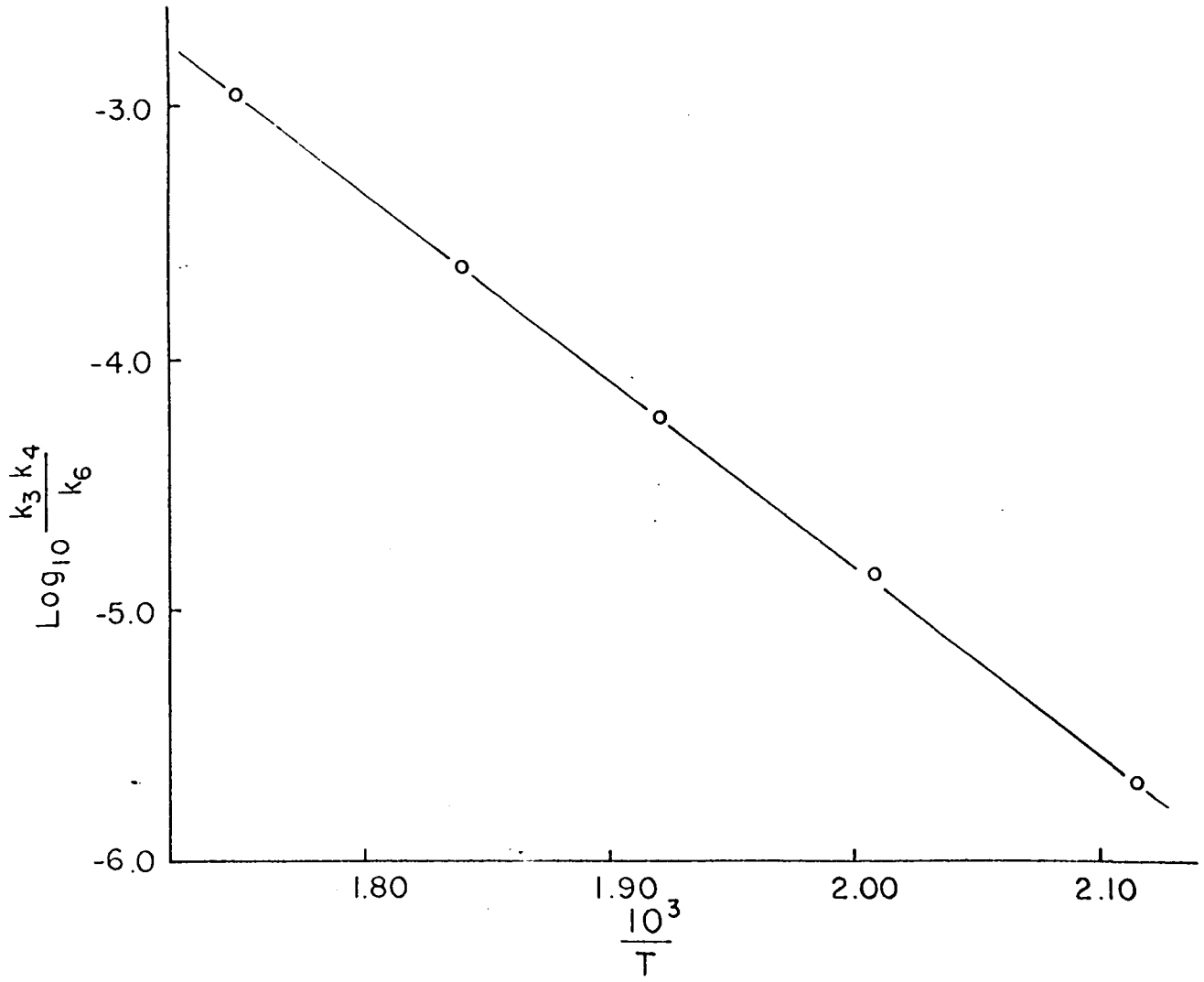
-3.0
-4.0
-5.0
-6.0
$\log_{10} \frac{k_3 k_4}{k_6}$
1.80
1.90
2.00
2.10
$\frac{10^3}{T}$

pressure and since E_6 is almost certainly not negative at this pressure. The value of A_4 could be somewhat low since the assumption that $A_6 = 2.2 \times 10^{13}$ cc mole^{-1} sec^{-1} (Shepp's value for methyl radical combination) may not hold exactly. A steric factor which reduced A_6 would be reflected as an increase in A_4. The value of E_4 agrees well with 9.5 kcal. per mole found by Trotman-Dickenson and Steacie (7) from the photolysis of acetone in the presence of dimethyl ether.

Experiments using added CO_2 to test the pressure dependence of k_6 were inconclusive. Tests were made of the non-homogeneity of reaction conditions resulting from the use of 0°C to control the mercury vapor pressure in the reaction vessel; these were done with the mercury at -30°C. The results showed scatter but the values of $k_6/k_4k_2^{1/2}$ were not substantially different from those obtained under the less homogeneous conditions. This result may have arisen fortuitously owing to compensating effects on k_6 in the numerator and $k_2^{1/2}$ in the denominator.

Thermochemistry of Methyl Ethyl Ether Decomposition

A calculation of the bond dissociation energy for the C-C bond in methyl ethyl ether can be made from thermochemical data. The following heats of formation have been used: $\Delta H_f^\circ(CH_3OCH_2CH_3) = -51.73$ (8), $\Delta H_f^\circ(CH_2OCH_3) = -5.56$ (22) and $\Delta H_f^\circ(CH_3) = 32.0$ (9), all in kcal. per mole.

The calculated heat of reaction in going from methyl ethyl ether to a methyl radical and a methoxymethyl

radical is -78.17 kcal. per mole. Under the assumption that a methyl radical can combine with a methoxymethyl radical with zero activation energy, the endothermicity of the above reaction will be the activation energy for the decomposition of methyl ethyl ether through a C-C bond rupture, and is also $D(CH_3OCH_2-CH_3)$.

Application of the Kassel Equation

The pressure dependence of the combination of methyl radicals with methoxymethyl radicals must be the same as the pressure dependence of the unimolecular decomposition of methyl ethyl ether occurring at the C-C bond. The decomposition of methyl ethyl ether by a C-C split may be hypothetical since pyrolysis might be expected to occur through a C-O split as found for both dimethyl and diethyl ethers. The pressure dependence of the decomposition through the C-C split is interesting, however, since from this pressure dependence one can make an estimate of the number of normal modes contributing energy to this decomposition; this estimate should be of the same order as the number of modes which contribute to a C-O split since it is presumed that those modes which can exchange energy to the C-C bond would probably also be effective in exchanging energy to the C-O bond.

Kassel integrations have been carried out on an IBM 1620-II computor, for the unimolecular decomposition of methyl ethyl ether. For the calculations the high-

pressure first-order rate constant for the decomposition of methyl ethyl ether has been taken as

$$k_{-6}^{\infty} = 4.8 \times 10^{15}\ e^{-78,200/RT}\ sec^{-1}$$

This activation energy was obtained from the calculated $D(CH_3OCH_2-CH_3) = 78.2$ kcal. per mole, as already discussed. The frequency factor was obtained from the geometric mean of the frequency factors for the unimolecular decomposition of ethane and for the unimolecular decomposition of 1,2-dimethoxyethane. These frequency factors are 1.0×10^{16} sec^{-1} (22) and 2.3×10^{15} sec^{-1} (23) respectively.

The pressure dependence observed experimentally was for methyl ethyl ether formation rather than decomposition. The process involving energy exchange was the stabilization of the methyl ethyl ether through collision with dimethyl ether. For the Kassel integrations a collision diameter of 5.0 A has been assumed for the collision involving a molecule of dimethyl ether and a molecule of methyl ethyl ether, and $\frac{2M_A M_B}{M_A + M_B}$ was taken as 52.157.

Figure 21 shows the fall-off curves calculated from the Kassel equation and fitted to the experimental pressure dependence. The curves shown were obtained for s = 10 and provided the best fit.

The value s = 10, although higher than has been observed for many unimolecular decompositions, seems to be rather low for a molecule as large as methyl ethyl ether. For this molecule containing 12 atoms the rough formula

Figure 21

The theoretical pressure dependence of k_6 calculated from the Kassel equation and fitted to the pressure dependence of the $k_6/k_4k_2^{1/2}$ ratio. The Kassel integrations for k_6 were computed with s = 10.

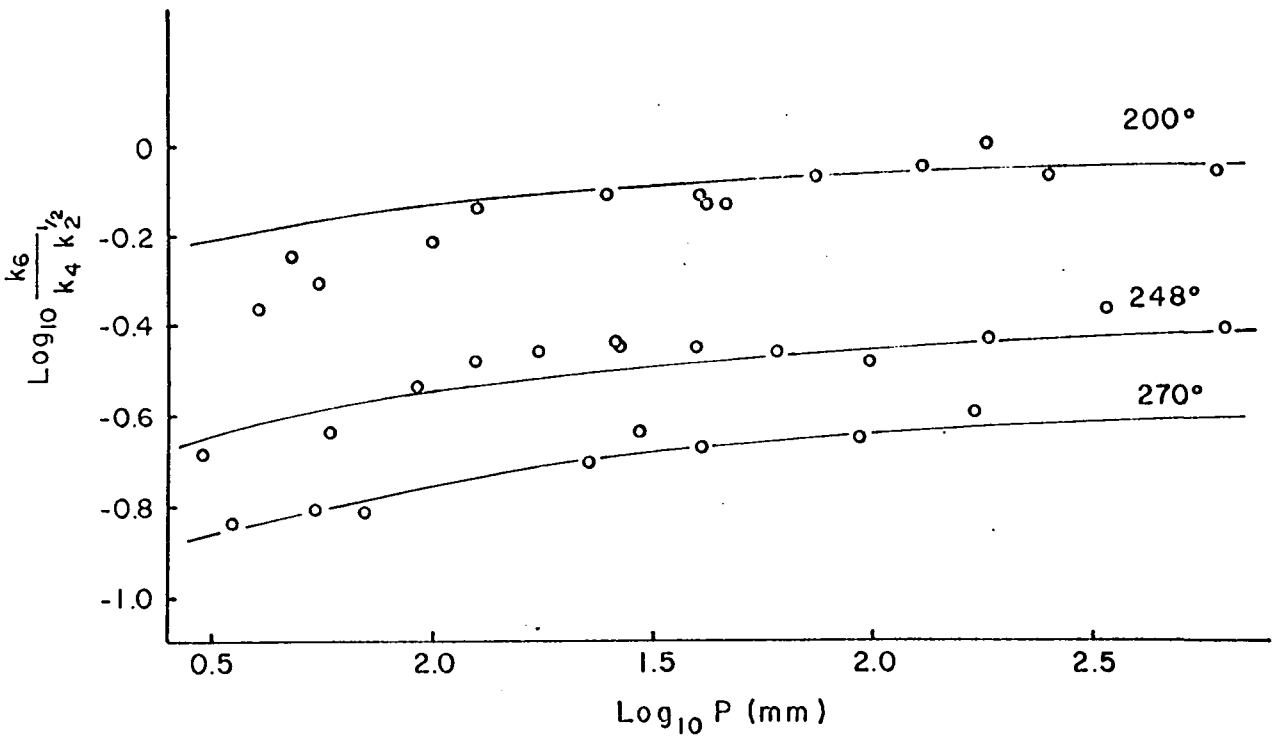
200°
248°
270°
0
-0.2
-0.4
-0.6
-0.8
-1.0
0.5
2.0
1.5
2.0
2.5
$\log_{10} \frac{k_6}{k_4 k_2^{1/2}}$
$\log_{10} P$ (mm)

$s = \frac{3N-6}{2}$ would suggest an s value of 15. The low s value observed may arise as a result of the large number of C-H stretching modes which may not contribute to energization because of the high zero-point energies in these modes.

Pressure dependence for the unimolecular decomposition of a species as large as methyl ethyl ether has been observed elsewhere. Both Hershenson and Benson (24) and Mulcahy and Williams (25) have observed that the decomposition of t-butoxy radical, to give acetone and a methyl radical, is pressure dependent. Although no Kassel integrations have been carried out for this decomposition, it would be expected that the s value obtained would be low compared with the large number of modes in this species containing 14 atoms.

CHAPTER VI

THERMOCHEMISTRY OF THE METHOXYMETHYL RADICAL

INTRODUCTION

There is little direct information available on the thermochemistry of the methoxymethyl radical, CH_3OCH_2. Benson (26) assumed a value of 94 kcal. per mole for $D(CH_3OCH_2-H)$, which leads to $\Delta H_f^o = -3$ kcal. per mole for the radical CH_3OCH_2. More recently Martin, Lampe and Taft (27) have obtained $\Delta H_f^o = -14 \pm 3$ kcal. per mole from appearance potential measurements; this value leads to $D(CH_3OCH_2-H) = 82 \pm 3$ kcal. per mole. These values are very different from those favoured by Benson, whose values are supported by the results of the present work.

The procedure in the present work was to measure the activation energy for the decomposition of 1,2-dimethoxyethane and to confirm that there are no chains and that rupture occurs at the C-C bond. The result can therefore be identified with the C-C bond dissociation energy. Together with a very reliable value for the heat of formation of 1,2-dimethoxyethane obtained at our request by S. Marantz and G. T. Armstrong (28) at the National Bureau of Standards, this dissociation energy leads to a value for the heat of formation of the radical.

A second approach involved a similar study using chloromethyl methyl ether, CH_3OCH_2Cl, which undergoes dissociation at the C-Cl bond. Unfortunately there is no reliable value for the heat of formation of this compound, and there are formidable experimental difficulties with regard to this. Our procedure was to obtain some information from appearance-potential data, and the results provide some useful confirmation for the results obtained using 1,2-dimethoxyethane.

EXPERIMENTAL

The pyrolyses of 1,2-dimethoxyethane and chloromethyl methyl ether were carried out in a static system having a quartz reaction vessel of volume 166 cc. The apparatus used is the same as described in detail in Chapter II. No modifications of the apparatus were made for the study of these thermal decompositions.

The materials used were of the following standards. Chloromethyl methyl ether from the Aldrich Chemical Company with $n_D^{20} = 1.3979$ was further purified by distillation on the vacuum line. 1,2-Dimethoxyethane supplied by the Aldrich Chemical Company, $n_D^{20} = 1.3772$, was dried with lithium aluminium hydride and redistilled; a centre fraction had a boiling point of 83.8 - 84.0°C. Phillips Research Grade propylene quoted to have purity of 99.9 mole per cent was used after degassing in the vacuum line. The toluene used was Fisher Certified Reagent grade.

For the pyrolysis of 1,2-dimethoxyethane in the presence of toluene about 10% 1,2-dimethoxyethane and 90% toluene was used. Since the total pressure was low ($\leq$ 20 mm) it was not possible to measure the pressures of 1,2-dimethoxyethane manometrically, and the following technique was used to obtain a sample of the mixture. Appropriate quantities of 1,2-dimethoxyethane and toluene were accurately weighed into a small sample bulb equipped with a ground-glass joint. The entire sample was then introduced into the vacuum system and twice degassed briefly to remove dissolved gases. The sample was allowed to equilibriate at room temperature and portions of the sample were expanded to the reaction vessel; the total pressure was read on a mercury manometer. From the weights of toluene and 1,2-dimethoxyethane, the partial pressure of 1,2-dimethoxyethane was calculated. At the end of the reaction time reactant and products were trapped out with liquid nitrogen. The noncondensable gases were then collected with Toepler pump and analyzed by vapor-phase chromatography. Methane was determined quantitatively on a twelve-foot silica-gel column (100-200 mesh).

For the thermal decomposition of chloromethyl methyl ether in the presence of toluene the sample of reactants was prepared in the manifold of the apparatus. The ether was introduced into the manifold and the pressure recorded; with the ether trapped out, toluene was admitted

to the manifold, and after the toluene and ether had equilibrated to room temperature, the total pressure was noted. After time had been allowed for mixing, a sample from the manifold was expanded into the reaction vessel. Products of the reaction were collected and analyzed in the same manner as given above for 1,2-dimethoxymethane. The measurement of the pressure of toluene and chloromethyl methyl ether in the manifold was not as accurate as one would wish since the total pressure involved was not greater than about 25 mm. In order to improve on the measurements of pressure of reactant, propylene was used in the place of toluene. For the thermal decomposition of chloromethyl methyl ether in the presence of propylene it was possible to measure the pressures of ether and propylene plus ether with much greater precision, with a high ratio of propylene to ether. From a quantity of propylene plus ether in the manifold a sample was expanded to the reaction vessel. Methane was collected and analyzed in the same manner as for the pyrolysis of 1,2-dimethoxyethane.

Blank runs were conducted with toluene and propylene separately. A twenty-minute run for toluene at 490°C revealed that no methane was produced; this shows that the toluene contained no impurities which could lead to extraneous production of methane. A twenty-minute run with propylene at 390°C showed a small peak for methane, probably arising from a slow pyrolysis of propylene at this tempera-

ture. The rate of methane formation was only a few per cent of the rate of methane formation from chloromethyl methyl ether.

RESULTS

Decomposition of 1,2-dimethoxyethane

The pyrolysis of 1,2-dimethoxyethane in the presence of toluene was studied in a static system at temperatures from 465° to 510°C. The function of the toluene was to scavenge methyl radicals with the formation of methane, the rate of formation of which was measured.

The C-C bond in the molecule is undoubtedly much weaker than a C-O bond, especially since the CH_3O groups will have the effect of lowering the C-C bond strength. It has therefore been assumed that the initial step in the pyrolysis is the dissociation into two CH_3OCH_2 radicals. All of the results support this conclusion. For example, the only products other than dibenzyl are methane, carbon monoxide and hydrogen, the latter two substances coming from the decomposition of the formaldehyde. The splitting of C-O bonds would inevitably lead to the formation of other products which were not observed.

The reaction scheme has therefore been taken to be

[1] $$CH_3OCH_2CH_2OCH_3 \longrightarrow 2\ CH_3OCH_2$$

[2] $$CH_3OCH_2 \longrightarrow CH_3 + CH_2O$$

[3] $$CH_3 + C_6H_5CH_3 \longrightarrow CH_4 + C_6H_5CH_2$$

[4] $$2\ C_6H_5CH_2 \longrightarrow C_6H_5CH_2CH_2C_6H_5$$

The CH_3OCH_2 radicals are expected to decompose rapidly by reaction [2], the rate constant for which is (29)

$$k = 2.0 \times 10^{13}\ e^{-25,500/RT}\ sec^{-1}$$

That this is so is confirmed by the fact that only minute traces of dimethyl ether are found in the system; this would be formed from the abstraction of H from toluene if CH_3OCH_2 radicals were present at appreciable concentrations. It follows that the rate of formation of methane is a measure of the rate of splitting of the C-C bond.

Figure 22 shows a double logarithmic plot of the rate of methane formation against the concentration of 1,2-dimethoxyethane. The line drawn is of unit slope; the order is clearly close to unity, in agreement with the reaction scheme. The rate of methane production is twice that of the decomposition of 1,2-dimethoxyethane; thus

$$v_{CH_4} = 2v_1 = 2\ k_1[CH_3OCH_2CH_2OCH_3]$$

The quantity $v_{CH_4}/[CH_3OCH_2CH_2OCH_3]$ has been evaluated for a series of runs at various temperatures and the results are shown in Table III. An Arrhenius plot of log $(v_{CH_4}/[CH_3OCH_2CH_2OCH_3])$ is shown in Figure 23. Use of the method of least squares led to $k_1 = 2.3 \times 10^{15}\ e^{-71,300/RT}\ sec^{-1}$.

The standard deviation for log A is ± 0.45, and that for E is $\pm 1,600$ kcal. per mole.

Figure 22

Order of reaction of methane formation with respect to 1,2-dimethoxyethane concentration, for the pyrolysis of 1,2-dimethoxyethane at 490°C in the presence of toluene.

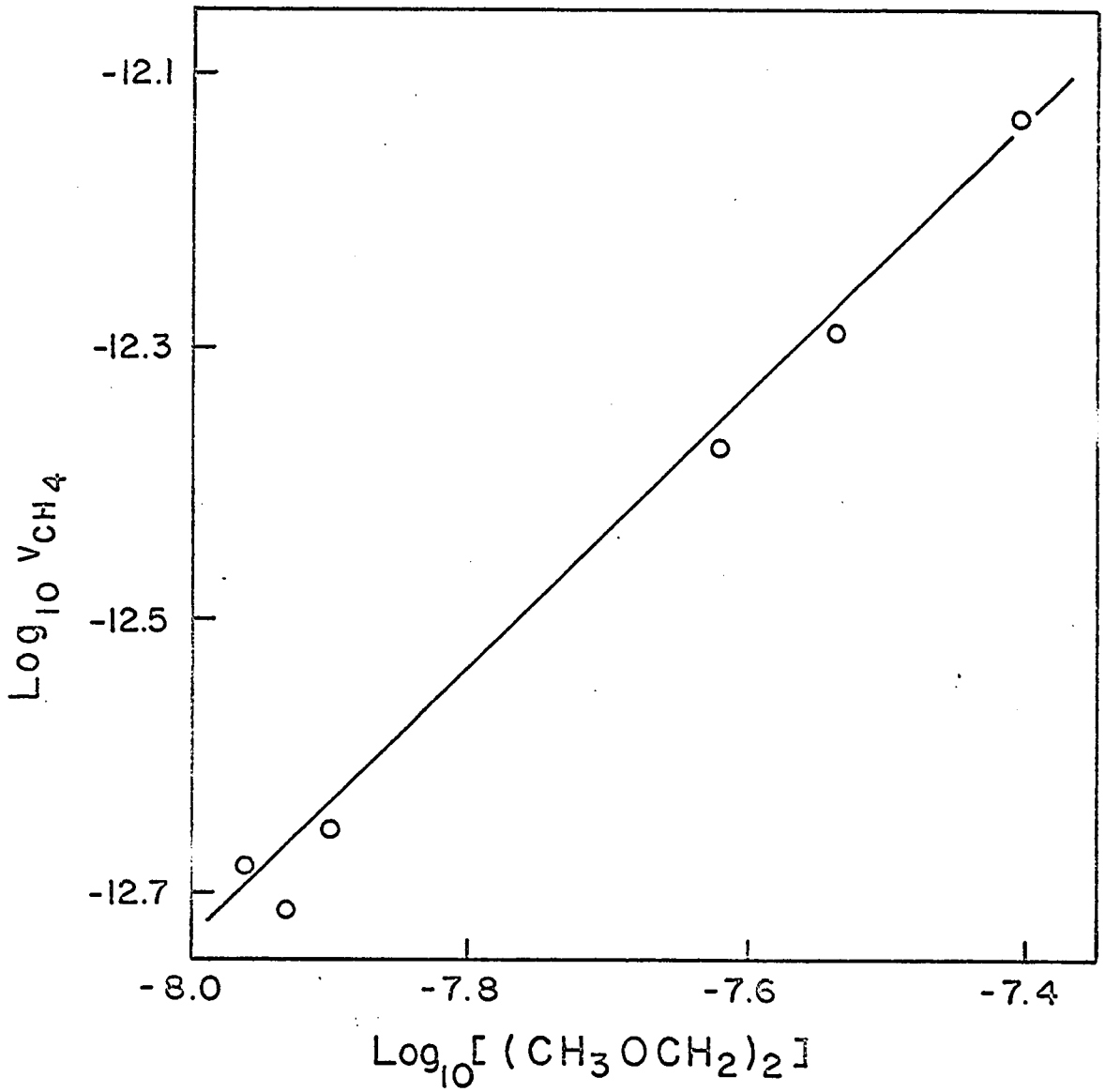
-12.1
-12.3
-12.5
-12.7
$Log_{10} v_{CH_4}$
-8.0
-7.8
-7.6
-7.4
$Log_{10}[(CH_3OCH_2)_2]$

TABLE III

Data for the pyrolysis of 1,2-Dimethoxyethane in the presence of Toluene

Temperature °C	Pressure of Toluene $(CH_3OCH_2)_2$ mm	Pressure of $(CH_3OCH_2)_2$ mm	Reaction Time sec	v_{CH_4} moles cc^{-1} $sec^{-1} \times 10^{12}$	$\frac{v_{CH_4}}{[(CH_3OCH_2)_2]}$ $sec^{-1} \times 10^{5}$
470	7.0	0.501	600	0.04997	0.4626
490	7.8	0.558	600	0.1936	1.651
480	4.8	0.343	600	0.06958	0.9521
500	4.5	0.322	300	0.2189	3.279
470	20.4	1.823	900	0.2066	0.5252
480	17.4	1.555	600	0.2833	0.8559
490	6.7	0.599	600	0.2220	1.765
500	4.7	0.420	480	0.3249	3.730
510	3.8	0.340	300	0.4301	6.186
465	19.8	1.943	1200	0.1683	0.3986
475	15.4	1.511	900	0.2252	0.6951
485	11.9	1.168	720	0.3073	1.244
495	9.6	0.942	480	0.4665	2.372
505	7.2	0.707	300	0.5719	3.928
490	19.1	1.871	600	0.7388	1.879
490	14.1	1.381	600	0.5130	1.767
490	11.6	1.136	600	0.4232	1.772
490	5.3	0.519	600	0.2087	1.913

Figure 23

An Arrhenius plot for the thermal decomposition of 1,2-dimethoxyethane.

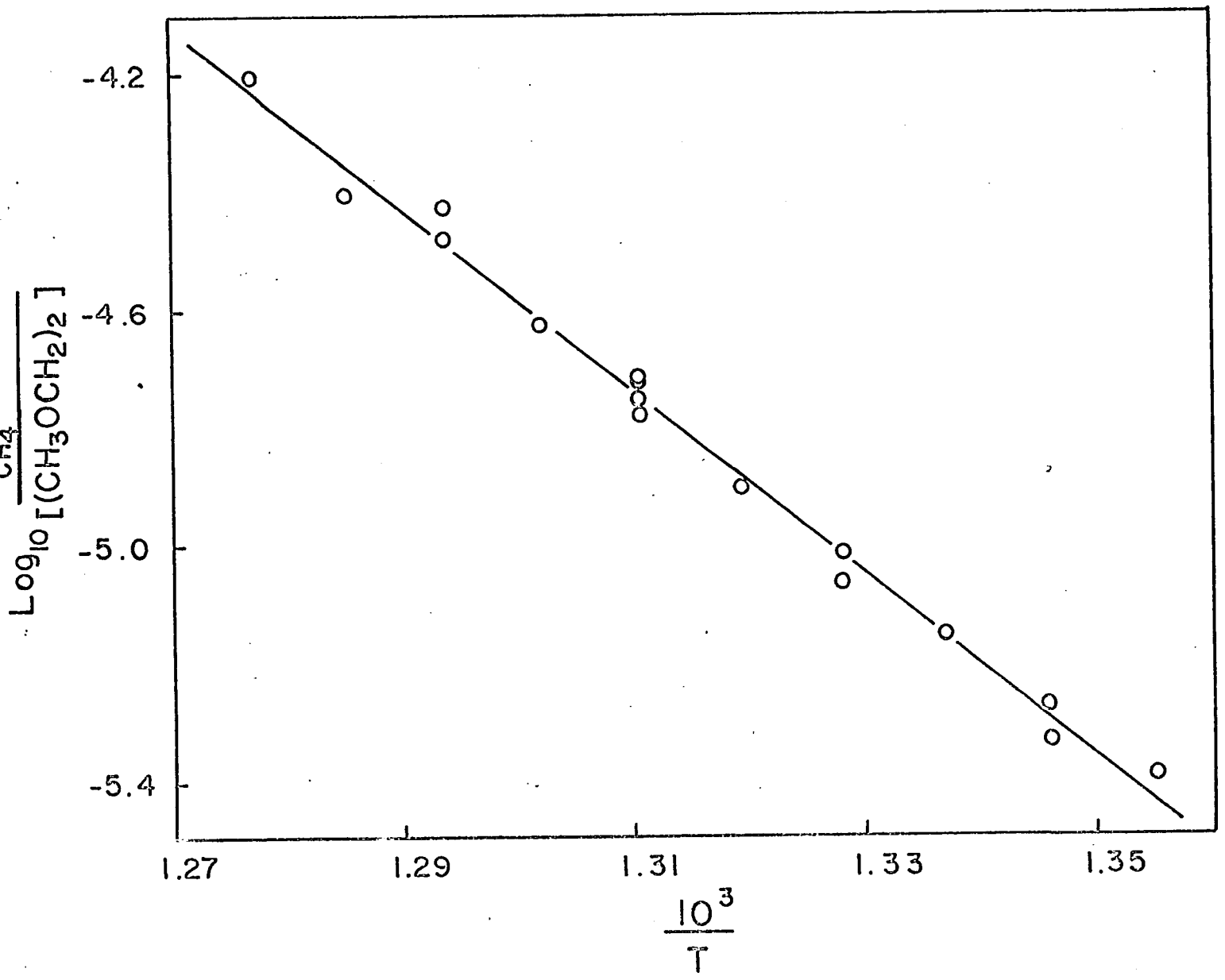
-4.2
-4.6
-5.0
-5.4
$\log_{10} \frac{v_{CH_4}}{[(CH_3OCH_2)_2]}$
1.27
1.29
1.31
1.33
1.35
$\frac{10^3}{T}$

Marantz and Armstrong (28) have measured the heat of combustion of 1,2-dimethoxyethane, and their results lead to -90.02 ± 0.05 kcal. per mole for the heat of formation of the liquid. The heat of vaporization has been calculated from vapor-pressure data of Kobe, Ravicz and Vohra (30); Figure 24 shows a plot of log P vs. 1/T, and the results lead to ΔH_v = 7.60 kcal. per mole. The heat of formation of the vapor is therefore -82.4 kcal. per mole.

On the assumption that the methoxymethyl radicals combine with zero activation energy the activation energy of 71.3 kcal. per mole is the dissociation energy $D(CH_3OCH_2 - CH_2OCH_3)$. These results lead to

$$\Delta H_f^0 (CH_3OCH_2) = -5.6 \pm 0.8 \text{ kcal. per mole,}$$

for the standard heat of formation of the radical. The heat of formation of dimethyl ether was recently found by Pilcher, Pell and Coleman (8) to be -44.0 ± 0.1. These values lead to $D(CH_3OCH_2 - H)$ = 90.5 ± 0.9 kcal. per mole for the heat of dissociation of the C-H bond in dimethyl ether.

Decomposition of Chloromethyl Methyl Ether

The pyrolysis of CH_3OCH_2Cl was studied in the presence of toluene and also of propylene, both of which are effective scavengers for methyl radicals. In each study the rate of methane production was measured at temperatures from 360° to 400°C.

Figure 24

A plot of the vapor pressure of 1,2-dimethoxyethane against the reciprocal of the temperature. The data were obtained from (30).

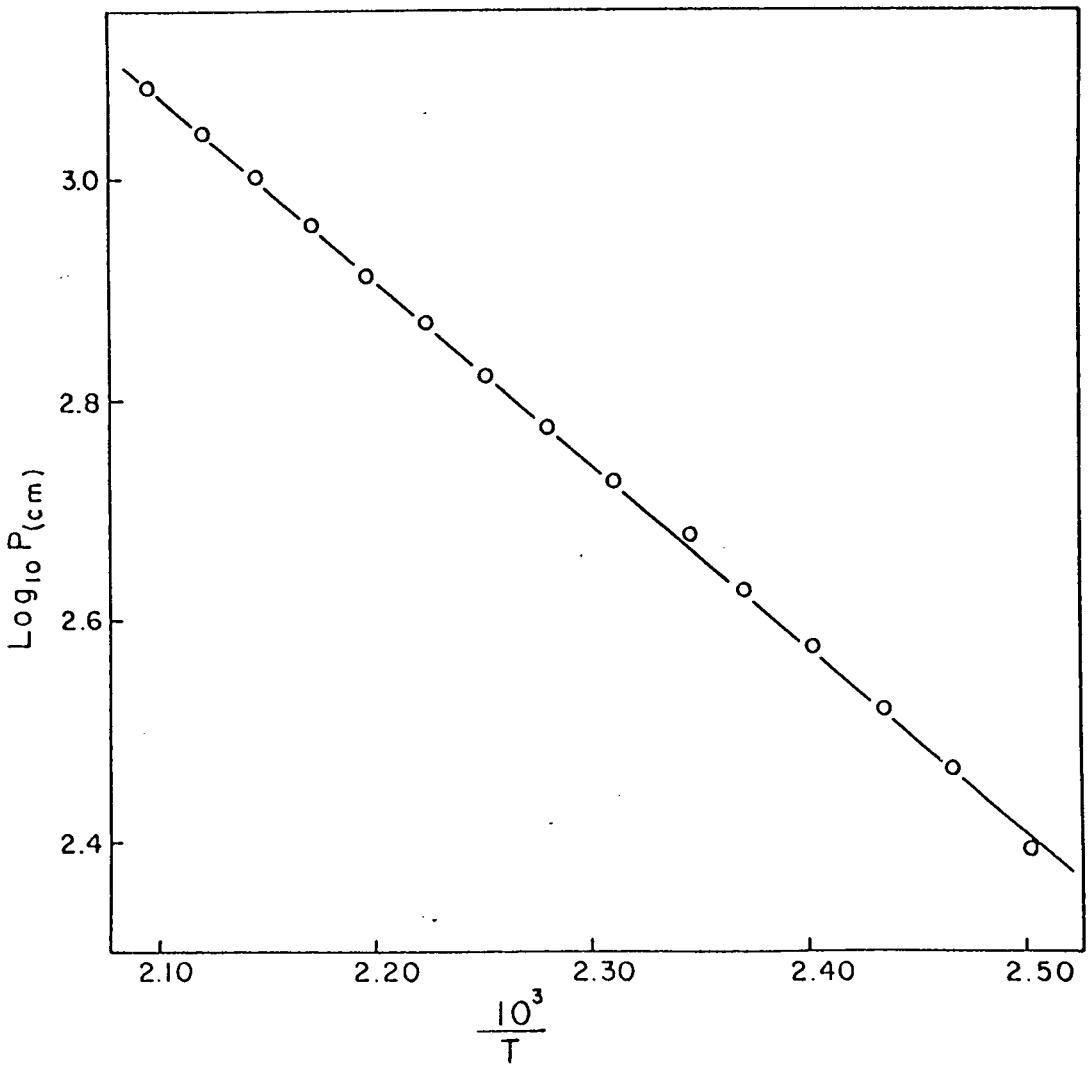
3.0
2.8
2.6
2.4
$\text{Log}_{10} P_{(cm)}$
2.10
2.20
2.30
2.40
2.50
$\frac{10^3}{T}$

The following appears to be the reaction scheme in the presence of propylene:

[5] $CH_3OCH_2Cl \longrightarrow CH_3OCH_2 + Cl$

[2] $CH_3OCH_2 \longrightarrow CH_3 + CH_2O$

[6] $CH_3 + CH_3 - CH = CH_2 \longrightarrow CH_4 + CH_2 - CH = CH_2$

followed by termination processes. The C-Cl bond is considerably weaker than the C-H bond, and the decomposition of CH_3OCH_2 is fast; the rate of methane formation is therefore the rate of the C-Cl bond split.

Results for the decomposition of chloromethyl methyl ether in the presence of propylene are shown in Table IV. Figure 25 shows a plot of log v_{CH_4} against log $[CH_3OCH_2Cl]$, and the order is unity. The logarithm of the ratio of v_{CH_4} to $[CH_3OCH_2Cl]$, which is k_5, is plotted against 1/T in Figure 26, and the rate expression is found to be

$$k_5 = 3.8 \times 10^{18} e^{-69,900/RT} \text{ sec}^{-1}$$

In the presence of toluene the mechanism is similarly

[5] $CH_3OCH_2Cl \longrightarrow CH_3OCH_2 + Cl$

[2] $CH_3OCH_2 \longrightarrow CH_3 + CH_2O$

followed by reactions [3] and [4]. Results are shown in Table V, and Figure 26 shows an Arrhenius plot which leads to

$$k_5 = 4.3 \times 10^{18} e^{-69,300/RT} \text{ sec}^{-1}$$

TABLE IV

Data for the pyrolysis of Chloromethyl Methyl Ether in the presence of Propylene

Temperature	Pressure of Propylene + CH_3OCH_2Cl	Pressure of CH_3OCH_2Cl	Reaction Time	v_{CH_4}	$\frac{v_{CH_4}}{[CH_3OCH_2Cl]}$
°C	mm	mm	sec	moles cc^{-1} sec^{-1} x 10^{12}	sec^{-1} x 10^6
400	460.5	4.96	127	9.189	77.77
370	428.7	6.30	420	0.9740	6.198
390	251.5	3.70	240	3.302	36.92
360	404.0	5.86	720	0.4522	3.045
380	362.5	6.88	300	2.370	14.02
380	238.5	4.53	300	1.714	15.42
380	163.7	3.11	300	1.154	15.12
360	163.5	7.77	600	0.5604	2.849
370	87.5	4.16	600	0.6370	6.147
380	58.0	2.75	600	0.9564	14.14
390	40.6	1.93	600	1.713	36.73

Figure 25

Order of reaction of methane formation with respect to chloromethyl methyl ether concentration, for the pyrolysis of chloromethyl methyl ether at 380°C in the presence of propylene.

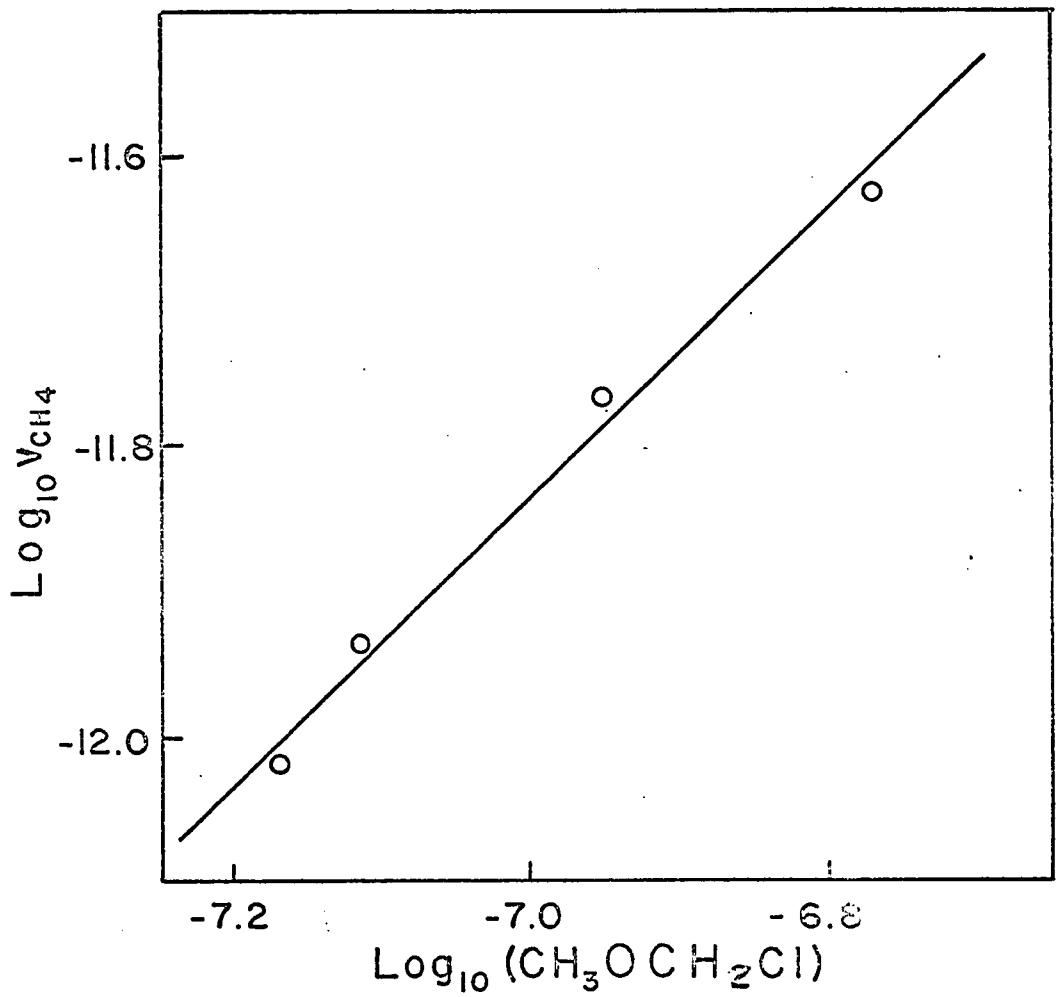
-11.6
-11.8
-12.0
Log10 VCH4
-7.2
-7.0
-6.8
Log10 (CH3OCH2Cl)

Figure 24

Arrhenius plots for the thermal decomposition of chloromethyl methyl ether.

○: CH_3OCH_2Cl + toluene.

●: CH_3OCH_2Cl + propylene.

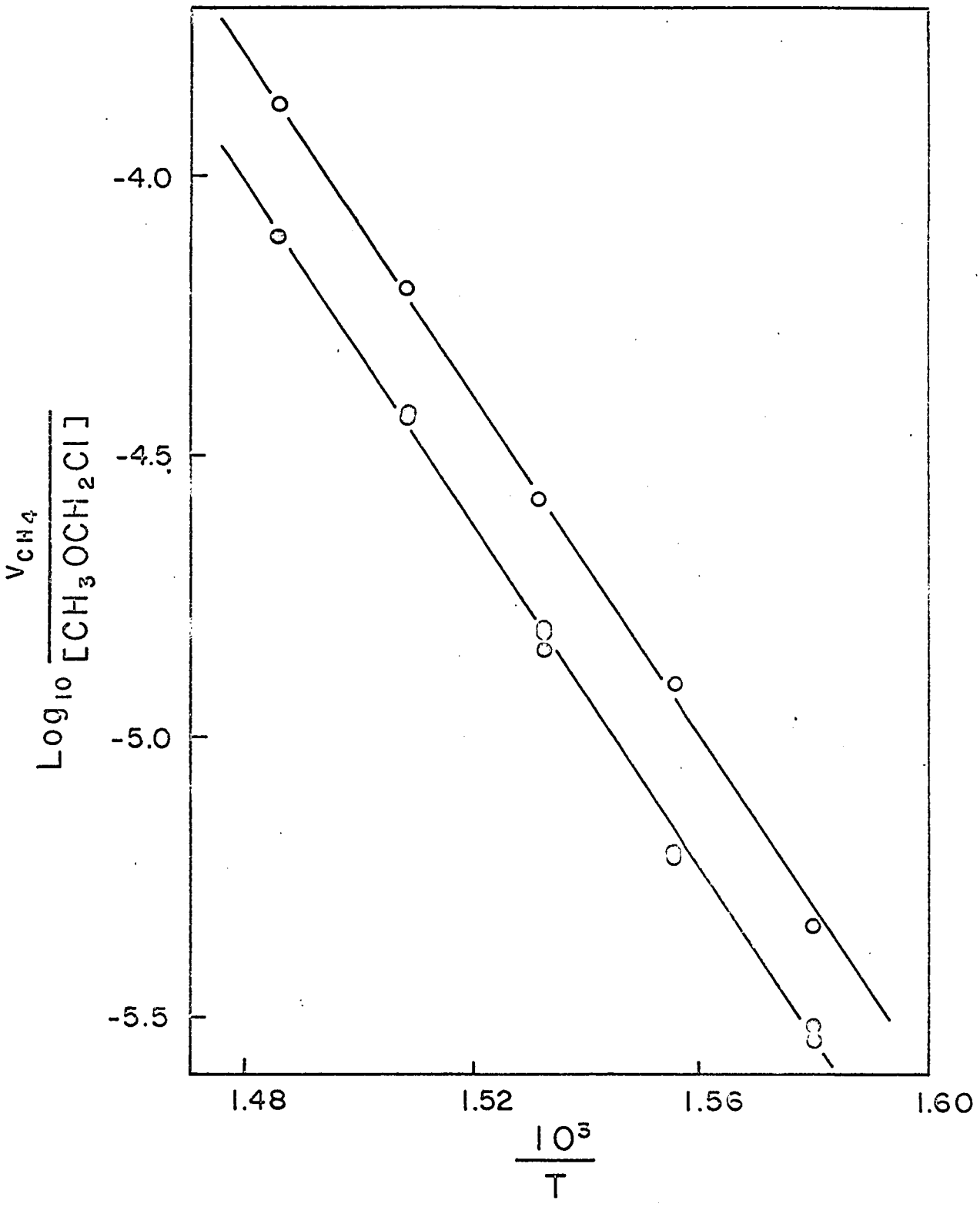
-4.0
-4.5
-5.0
-5.5
1.48
1.52
1.56
1.60
$\log_{10} \frac{v_{CH_4}}{[CH_3OCH_2Cl]}$
$\frac{10^3}{T}$

TABLE V

Data for the thermal decomposition of Chloromethyl Methyl Ether in the presence of Toluene

Temperature °C	Pressure of Toluene + $(CH_3OCH_2)Cl$ mm	Pressure of $(CH_3OCH_2)Cl$ mm	Time of Reaction sec	v_{CH_4} moles cc^{-1} $sec^{-1} \times 10^{12}$	$\frac{v_{CH_4}}{[CH_3OCH_2Cl]}$ $sec^{-1} \times 10^{6}$
380	13.0	5.18	240	3.348	26.33
370	14.0	6.53	300	2.012	12.37
390	9.5	3.88	120	5.879	62.62
360	12.4	4.46	600	0.5187	4.586
400	8.0	2.76	120	8.760	133.0

It is to be seen from Figure 26 that the rate constant in the presence of propylene is significantly below that in the presence of toluene, although the activation energies are very close. This discrepancy probably arises from some loss of methyl radicals by addition to propylene,

[7] $CH_3 + CH_3 - CH = CH_2 \longrightarrow$ butyl radicals.

The butyl radicals may revert to $CH_3 + CH_2 - CH = CH_2$ but may decompose or abstract from propylene.

Miyoshi and Brinton (31) found the activation energies for the addition and abstraction reactions of methyl radicals with propylene to be 8.8 and 8.2 kcal. per mole respectively. Over the temperature range of the present study the ratio of the two rates would change by only 2.5 per cent, and this may explain why there is not much difference between the activation energies for the pyrolyses in the presence of toluene and propylene. In the subsequent calculations an average value of 69.6 kcal. per mole has been taken for the activation energy, which is assumed to be the dissociation energy $D(CH_3OCH_2-Cl)$.

No heat of formation for chloromethyl methyl ether is given in the literature, and its measurement presents some difficulties. As an alternative procedure, we have determined the appearance potentials of mass 45 ($CH_3OCH_2^+$) for both CH_3OCH_3 and CH_3OCH_2Cl. If there is no excess energy in either of the species produced the following

relationships hold between the appearance potentials A and the ionization potentials I:

$$A_{R^+}(CH_3OCH_3) = I_{R^+} + D(CH_3OCH_2\text{-}H)$$

$$A_{R^+}(CH_3OCH_2Cl) = I_{R^+} + D(CH_3OCH_2\text{-}Cl)$$

whence

$$A_{R^+}(CH_3OCH_3) - A_{R^+}(CH_3OCH_2Cl) = D(CH_3OCH_2\text{-}H) - D(CH_3OCH_2\text{-}Cl)$$

This relationship will still hold if there are excess energies in the R^+ ions provided they are the same in the two cases.

The appearance potentials were measured for the two ethers using the procedure of Warren (32), with xenon used as the standard for each determination. The ion currents of mass 45 ($CH_3OCH_2^+$) and of mass 129 (Xe^+) were measured as a function of voltage for each of the ethers, with xenon present in the sample. The plots of ion current against voltage are shown in Figures 27 and 28. In Warren's procedure the slopes of the linear portions of the plots are made equal by multiplying all ion currents of either the unknown or the calibrant by an appropriate factor; Figures 29 and 30 show the plots, at low ion current, after this was done. The final step is to extrapolate to zero ion current the voltage difference between calibrant and unknown. These differences, taken from Figures 29 and 30, are plotted against ion current in Figure 31. Extrapolation to zero ion current gives the difference between the appearance potentials of the unknown and the calibrant.

Figure 27

A plot of ion current against voltage for mass 45 and mass 129, obtained from a mixture of xenon and dimethyl ether.

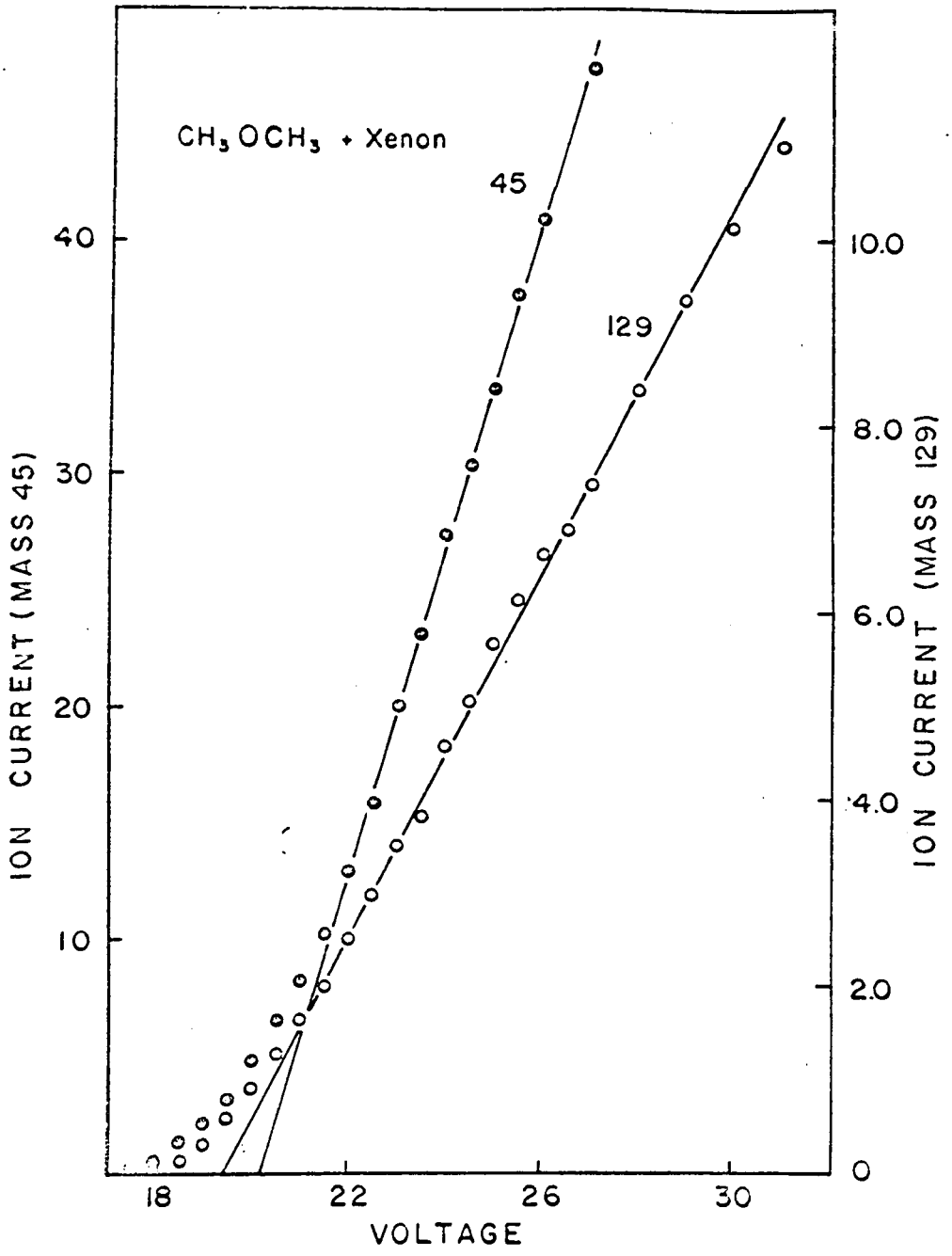
CH3OCH3 + Xenon
45
129
ION CURRENT (MASS 45)
ION CURRENT (MASS 129)
VOLTAGE
40
30
20
10
10.0
8.0
6.0
4.0
2.0
0
18
22
26
30

Figure 28

A plot of ion current against voltage for mass 45 and mass 129, obtained from a mixture of xenon and chloromethyl methyl ether.

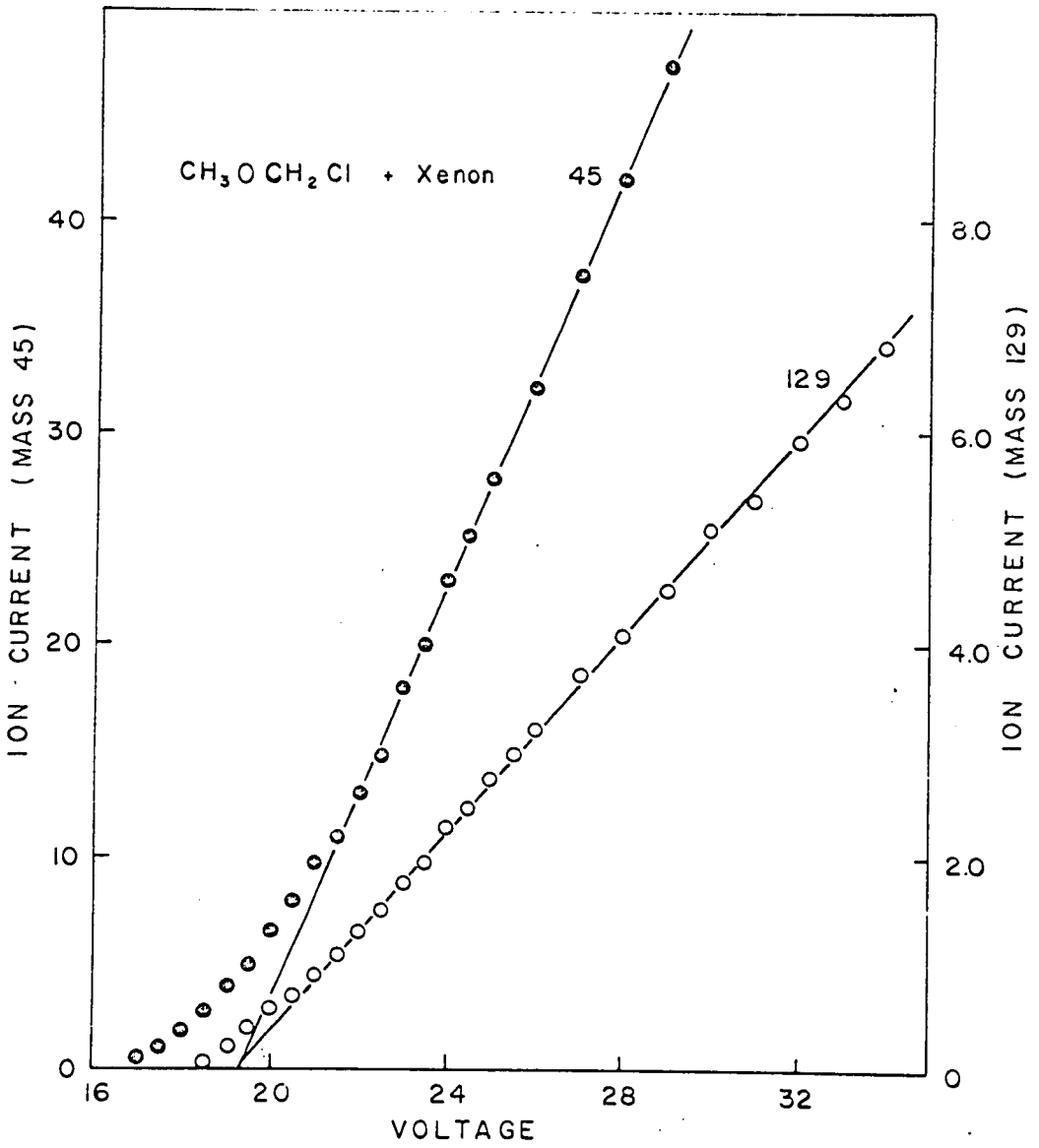
CH_3OCH_2Cl + Xenon
45
129
ION CURRENT (MASS 45)
ION CURRENT (MASS 129)
VOLTAGE
0
10
20
30
40
2.0
4.0
6.0
8.0
16
20
24
28
32

Figure 29

A plot of ion current against voltage for mass 45 and mass 129, in the low ion current region. The data are for a xenon-dimethyl ether mixture.

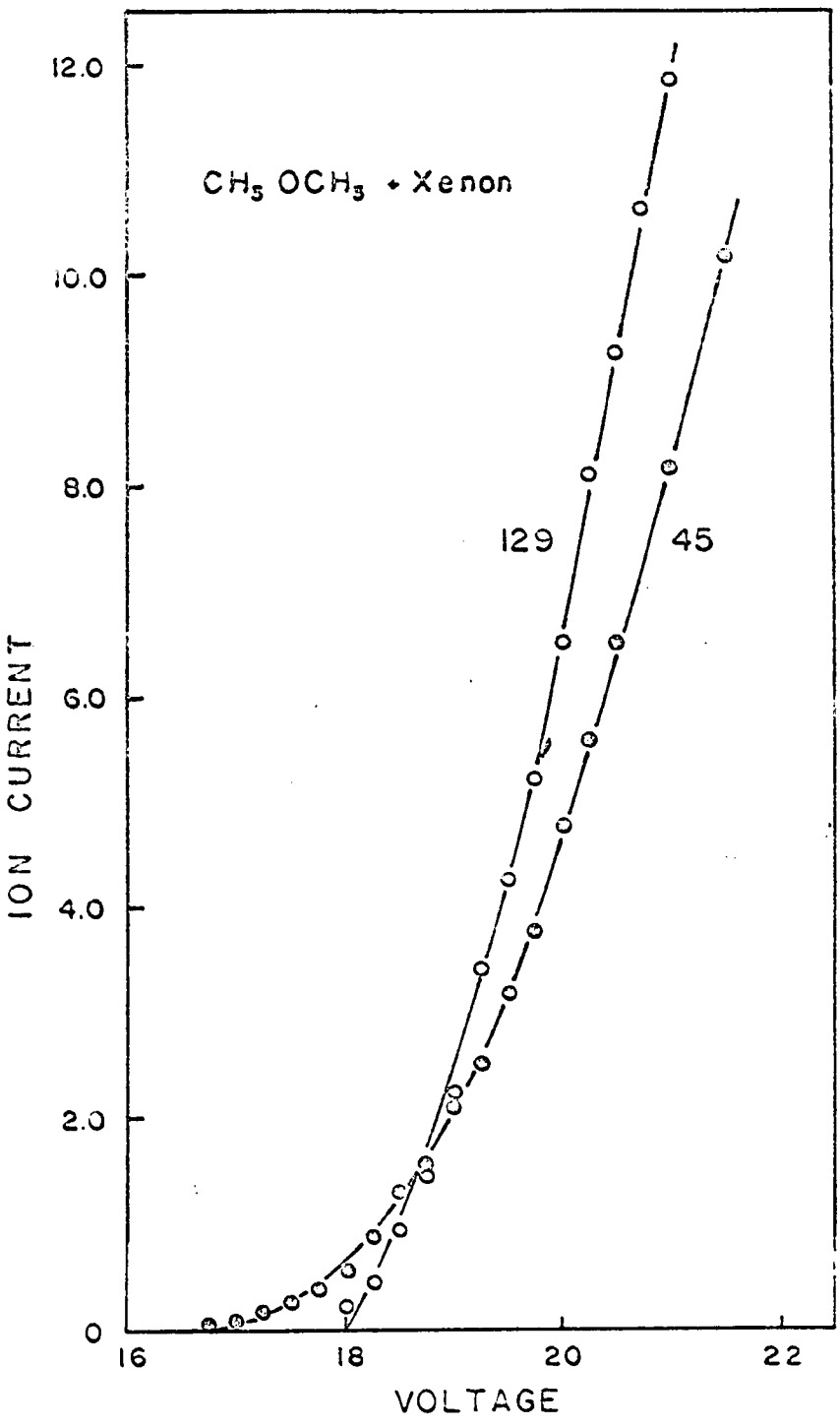
12.0
10.0
8.0
6.0
4.0
2.0
0
ION CURRENT
CH5 OCH3 + Xenon
129
45
16
18
20
22
VOLTAGE

Figure 30

A plot of ion current against voltage for mass 45 and mass 129, in the low ion current region. The data are for a xenon-chloromethyl methyl ether mixture.

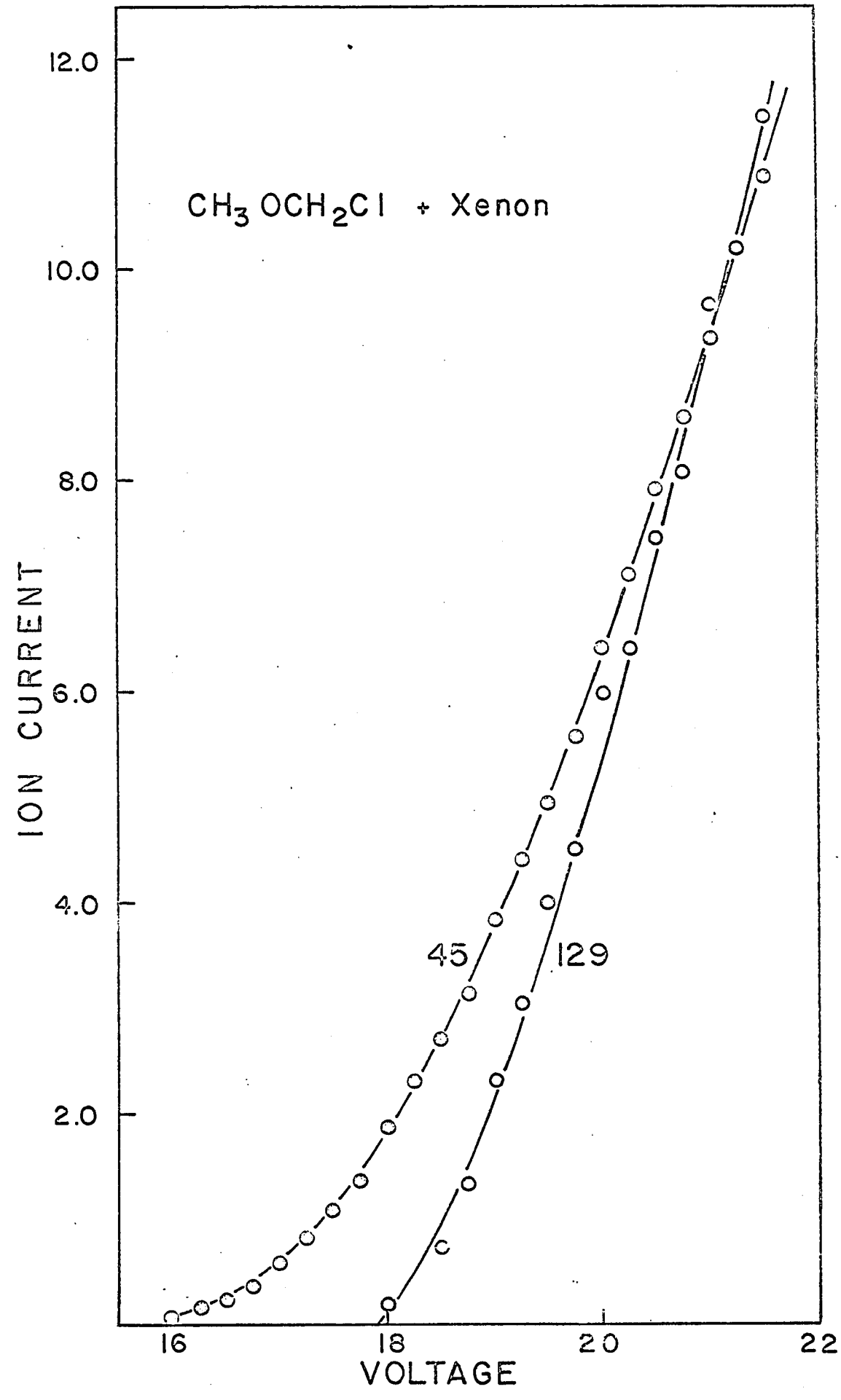
12.0
10.0
8.0
6.0
4.0
2.0
ION CURRENT
CH_3OCH_2Cl + Xenon
45
129
16
18
20
22
VOLTAGE

Figure 31

Voltage differences between mass 129 and mass 45 as a function of ion current. The intercept at zero ion current gives the appearance potential of mass 45 relative to the ionization potential of xenon.

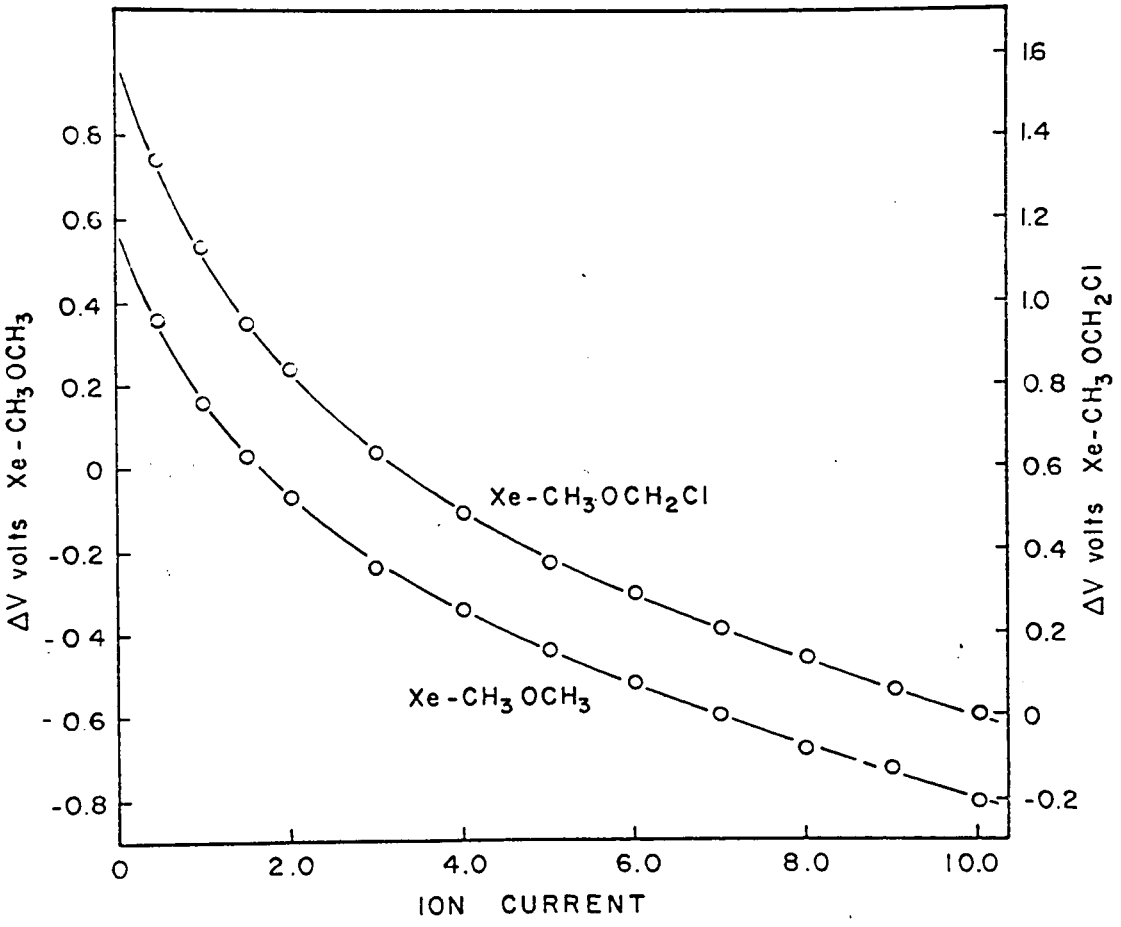
ΔV volts Xe - CH3OCH3
ΔV volts Xe - CH3OCH2Cl
0.8
0.6
0.4
0.2
0
-0.2
-0.4
-0.6
-0.8
1.6
1.4
1.2
1.0
0.8
0.6
0.4
0.2
0
-0.2
Xe - CH3OCH2Cl
Xe - CH3OCH3
0
2.0
4.0
6.0
8.0
10.0
ION CURRENT

In order to obtain a reliable extrapolation a second plot of differences was made, and is shown in Figure 32; this plot extrapolates well to give $\Delta(\Delta V)$ = 1.01 eV (23.3 kcal. per mole). Therefore

$D(CH_3OCH_2\text{-}H) - D(CH_3OCH_2\text{-}Cl) = 23.3$ kcal. per mole.

With the value of 69.6 for $D(CH_3OCH_2\text{-}Cl)$ this leads to

$D(CH_3OCH_2\text{-}H) = 92.9$ kcal. per mole.

This provides useful support for the value of 90.5 obtained from the pyrolysis of 1,2-dimethoxyethane. The lower value is, however, to be considered more reliable because of the difficulties associated with the appearance-potential method.

The absolute appearance potentials can be calculated by using the value of 12.13 eV for xenon (33,34); the results are

$$A_R{}^+(CH_3OCH_3) = 11.51 \text{ eV}$$

$$A_R{}^+(CH_3OCH_2Cl) = 10.50 \text{ eV}$$

The first value compares satisfactorily with the values of 11.65 eV given by Lossing (35), and 11.42 eV given by Martin, Lampe and Taft (27). No previous values are available for CH_3OCH_2Cl.

DISCUSSION

The present work leads to the following thermochemical values, based on the results with 1,2-dimethoxyethane:

Figure 32

The voltage difference between the curves of Figure 31, plotted as a function of ion current. The extrapolation to zero ion current gives the voltage difference in the appearance potentials of mass 45 obtained from dimethyl ether and chloromethyl methyl ether.

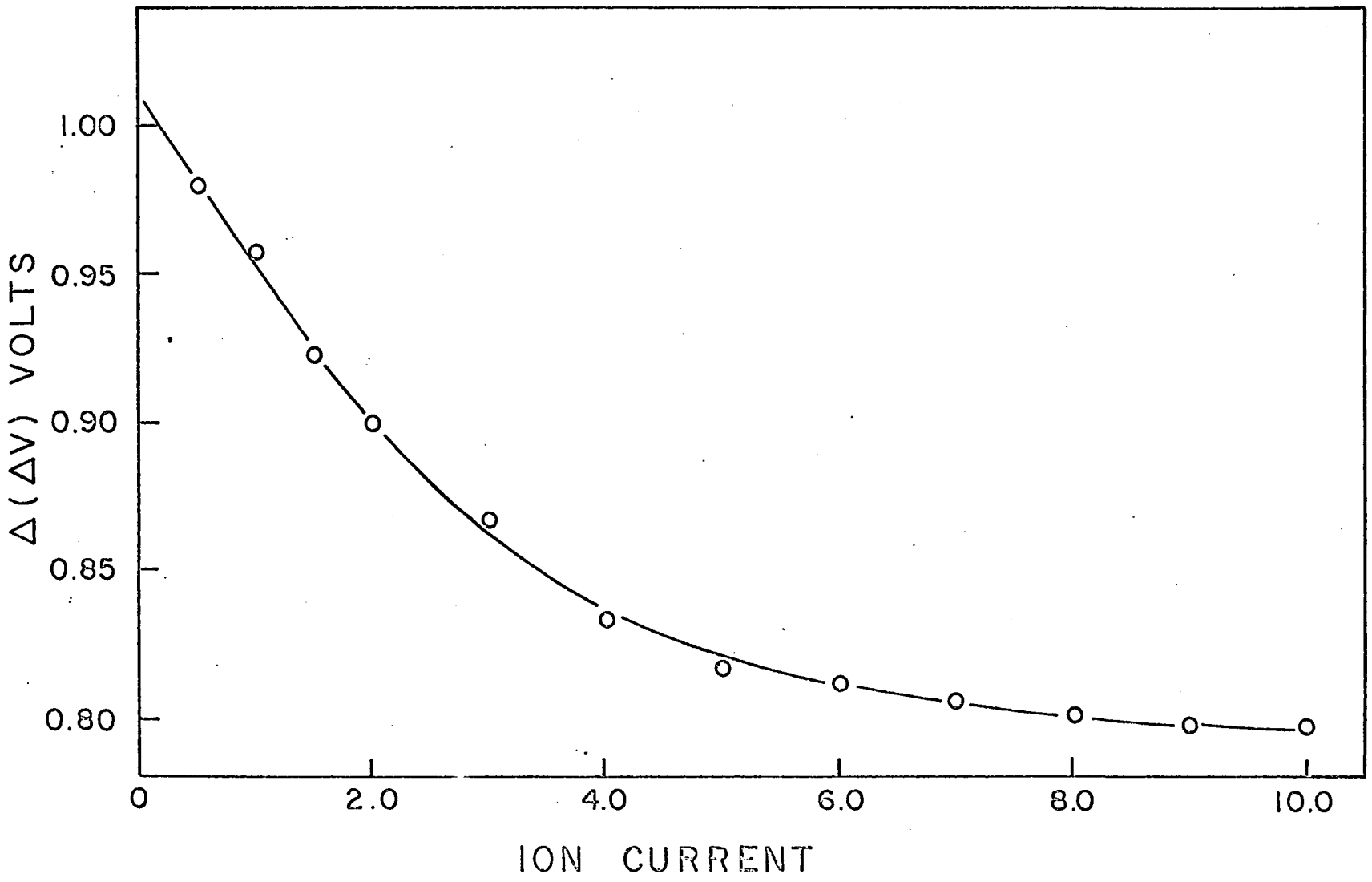
1.00
0.95
0.90
0.85
0.80
Δ(ΔV) VOLTS
0
2.0
4.0
6.0
8.0
10.0
ION CURRENT

$\Delta H_f^0(CH_3OCH_2)$ = -3.6 ± 0.8 kcal. per mole

$D(CH_3OCH_2-H)$ = 90.5 ± 0.9 kcal. per mole

The former value is substantially different from that given by Martin, Lampe and Taft (27), and lies outside the limits of error stated by them. Their value leads to a value of 54 kcal. per mole for $D(CH_3OCH_2-CH_2OCH_3)$; this is much too low a value for a compound which is reasonably stable up to about 460°C, and which according to our work decomposes with an activation energy of 71.3 kcal. per mole.

On the other hand our thermochemical values compare favorably with those estimated by Benson (26): he suggested 94 kcal. for $D(CH_3OCH_2-H)$.

Other thermochemical values may be calculated from our results. The heats of formation of methyl ethyl ether and n-propyl methyl ether have been given as -51.7 and -56.8 kcal. per mole respectively (8). With the values $\Delta H_f^0(CH_3)$ = 32.0 kcal. per mole (9) and $\Delta H_f^0(C_2H_5)$ = 26.2 kcal. per mole (36) the following values are calculated:

$D(CH_3OCH_2-CH_3)$ = 78.1 kcal. per mole

$D(CH_3OCH_2-CH_2CH_3)$ = 77.4 kcal. per mole

It is of interest that these values lie half way between the value of 85.0 kcal. per mole for ethane (17) and 71.3 for 1,2-dimethoxyethane; it appears that each methoxy group lowers a neighboring C-C bond dissociation energy by about 7 kcal.

CHAPTER VII

THE THERMAL DECOMPOSITION OF THE ETHYL RADICAL

INTRODUCTION

The thermal decomposition of the ethyl radical to give an ethylene molecule and a hydrogen atom presents an interesting kinetic problem in itself, and its understanding is of importance in connection with a number of complex reaction mechanisms. During recent years there has been some doubt about the kinetic order of the reaction and about the values of the kinetic parameters. Work on the pyrolysis of ethane (22) and butane (37), in particular, has provided indirect but convincing evidence that the decomposition of the radical is a unimolecular reaction which is in its pressure-dependent region at the pressures commonly used in pyrolysis experiments.

The present investigation was conducted in order to obtain further and somewhat more direct information regarding the pressure dependence of the decomposition of the ethyl radical; a greater range of pressure has been used and the results have led to values for the limiting high-pressure and low-pressure Arrhenius parameters. The ethyl radicals were generated by the mercury-photosensitized decomposition of ethane.

Bywater and Steacie (38) have investigated the mercury-photosensitized decomposition of ethane at a pressure of 400 mm. From quantum-yield studies these authors concluded that for temperatures above 400°C there was a chain reaction, and they proposed the following mechanism:

[1] $Hg(^3P_1) + C_2H_6 \longrightarrow C_2H_5 + H + Hg(^1S_0)$

[2] $H + C_2H_6 \longrightarrow H_2 + C_2H_5$

[3a] $2\ C_2H_5 \longrightarrow C_4H_{10}$

[3b] $\longrightarrow C_2H_4 + C_2H_6$

[4] $C_2H_5 \longrightarrow C_2H_4 + H$

Bywater and Steacie concluded that the activation energy for reaction [4] was 39.5 kcal. per mole. In a study of the pyrolysis of butane Purnell and Quinn observed activation energies of 35.3 and 32.8 kcal. per mole for pressures of 100 and 12.5 mm respectively. Recently, Lin and Back (17), in a study of the pyrolysis of ethane, have examined the decomposition of the ethyl radical over a 10-fold range of pressure. By applying Powell's method they have evaluated the limiting high-pressure and low-pressure rate constants:

$$k^{\infty} = 3.8 \times 10^{13}\ e^{-38000/RT}\ sec^{-1}$$

$$k^{0} = 1.8 \times 10^{18}\ e^{-32400/RT}\ cc\ mole^{-1}\ sec^{-1}.$$

In the photolysis of propionaldehyde Kerr and Trotman-Dickenson (39) observed a rate constant expressed by:

$$k = 10^{11.2}\ e^{-31000/RT}\ sec^{-1}$$

but concluded that this activation energy was too low to describe the high-pressure rate constant. The low Arrhenius parameters may have resulted from a pressure dependence of the rate constant since their experiments were conducted at a pressure of about 30 mm.

EXPERIMENTAL

Reagents

Phillips Research Grade ethane stated to be 99.99 mole percent pure was used. It was further purified by trap-to-trap distillation and finally degassed in the storage vessel at -160°C. The only impurities detected by gas chromatography were traces of air and ethylene, neither of which were present in sufficient quantities to affect the measured rates of reaction.

Apparatus and Procedure

The mercury-photosensitized decomposition of ethane was studied in a static system with a quartz reaction vessel of volume 166 cc. The mercury lamp was a low-pressure lamp operated at room temperature and at a constant current of 9.0 ma. Details of the apparatus have been described in Chapter II.

Prior to each experiment the system was evacuated to a pressure of 2×10^{-5} mm or less. The mercury saturator trap in the lead to the reaction vessel was immersed in liquid nitrogen for a minimum time of 45 minutes, and then

in a bath at -30°C immediately before the reaction was conducted. A sample of ethane was introduced to the reaction vessel from the manifold and trapped with liquid nitrogen in a U-tube in the lead to the reaction vessel. After the reaction vessel was isolated by the closing of a mercury cut-off, the ethane was allowed to expand, passing through the mercury saturator trap and into the reaction vessel. The mercury lamp was switched on at least 20 minutes before use; reaction was started with the removal of a shutter and was stopped by switching off the lamp.

For pressures of less than 40 mm of ethane, products were separated into two fractions: non-condensable and condensable in a solid nitrogen trap. The non-condensable fraction, which was found to contain only hydrogen, was measured in a gas burette. The condensable fraction was collected with a Toepler pump and chromatographic analysis was conducted by sweeping the sample from a U-tube on the top of the Toepler pump. For pressures greater than 40 mm., an additional trap at -160°C (isopentane slush) was used. Ethane was distilled from the -160° trap until the quantity of reactant was reduced to a level that could be collected with the Toepler pump.

The condensable products were analyzed by gas chromatography on a 30-foot column of squalane on 60-80 mesh Chromosorb P (30% load) with helium as the carrier gas. For the lower pressure runs it was possible

quantitatively to determine ethylene, which was eluted before ethane, but for higher pressures of ethane, the ethylene peak was distorted by the huge ethane peak. Butane was retained much longer than ethane and was readily determined.

RESULTS AND INTERPRETATION

The mercury-photosensitized decomposition of ethane was studied at temperatures of 400, 430, 470 and 500°C. At each temperature the reactions were examined at pressures from 4 to 650 mm of ethane.

The products of reaction are hydrogen, butane and ethylene. For many runs it was possible to analyze the quantities of all three products. However, the difficulty involved in the separation of ethylene from large quantities of ethane, by gas chromatography, restricted the analysis of ethylene to runs for which the pressure in the reaction vessel was less than 40 mm. A search for other products, in particular acetylene or mercury alkyls, revealed no further products of reaction.

A single run was carried out at each pressure and temperature. The degree of conversion varied with the pressure of reactant used. For pressures in the middle of the range studied, the conversion was about 0.3%. At the highest pressures used, conversion was as low as 0.02% while for the lowest pressures, conversion reached a maximum of 2-3%. To obtain exactly identical conditions for a

series of runs at a particular pressure and temperature, it is necessary to have not only identical pressures and temperatures, but also identical light intensity and mercury concentration in the reaction vessel. The last of these conditions is the most difficult to reproduce when one is in the region of low mercury concentration where complete absorption of the light is not occurring. This is further discussed later in this chapter. A time-course study has been made at 470°C at a pressure of 32 mm. The results are shown in Table VI and show that the rates of product formation vary, but not in a regular pattern related to reaction time. Furthermore the $k_4/k_{3a}^{1/2}$ ratio, which is being examined in this work, has not been significantly altered in any trend with reaction time. The author attributes the variation in reaction rates to differences in mercury concentration in the reaction vessel and the resulting different rates of initiation associated with the mercury concentration.

Further justification for the assumption of initial conditions is obtained from the work of Dywater and Steacie (38) where deviation from initial rate was observed at reaction times greater than five minutes and only at 500°C. At the same temperature shorter reaction times were generally used in the present work, and conversions were significantly lower since a lower concentration of mercury was used.

TABLE VI

Time Course Study at 470°C

Run #	Reaction Time sec	Pressure mm	v_{H_2} [a]	$v_{C_4H_{10}}$ [a]	$\frac{v_{H_2}-1.117\ v_{C_4H_{10}}}{(v_{C_4H_{10}})^{1/2}}$ [b]	$\text{Log}\frac{v_{H_2}-1.117\ v_{C_4H_{10}}}{(v_{C_4H_{10}})^{1/2}}$
53	900	31.9	10.66	1.050	9.255	-5.034
54	600	32.9	11.38	1.135	9.965	-5.002
55	300	32.6	10.94	0.908	10.42	-4.982
56	150	32.3	12.33	1.245	9.800	-5.009
57	300	32.6	11.52	1.022	10.27	-4.988
58	1200	33.8	10.86	0.981	9.862	-5.006

[a] Rates are given in moles cc^{-1} sec^{-1} x 10^{12}

[b] $Moles^{1/2}$ $cc^{-1/2}$ $sec^{-1/2}$ x 10^{6}

The mechanism given by equations [1] to [4] has been used as a basis for interpreting the results. From this scheme the rate of decomposition of the ethyl radical is given by:

[5] $$v_4 = k_4[C_2H_5]$$

where k_4 is a defined first-order rate coefficient. Also

[6] $$v_{3a} = k_{3a}[C_2H_5]^2$$

From these equations one obtains:

[7] $$\frac{v_4}{v_{3a}^{1/2}} = \frac{k_4}{k_{3a}^{1/2}}$$

It is this ratio of rate constants which has been examined in detail.

The rate of reaction [3a] is obtained directly from the measurement of butane. The rate of reaction [4] is obtained from consideration of the steady-state condition which gives

[8] $$v_4 = v_2 = v_{3a} = v_{3b}$$

The sum of $v_{3a} + v_{3b}$ represents the total consumption of ethyl radicals by combination and disproportionation. The disproportionation/combination ratio, d/c, has been measured by various authors and found to be independent of temperature and pressure. For the calculations of this chapter the value of d/c = 0.117 ± 0.006 given by Roquitte and Futrell (40) has been used. For d/c = 0.117, the sum of $v_{3a} + v_{3b}$ is given by 1.117 v_{3a}. Thus from equation [9],

[9] $$v_4 = v_{H_2} = 1.117\, v_{C_4H_{10}}$$

In experiments where ethylene was measured, a useful check on the value of v_4 was provided by the relationship:

[10] $$v_4 = v_{C_2H_4} - 0.117\, v_{C_4H_{10}}$$

For the calculation of the results reported in this chapter, the value of v_4 from [9] was used, since this relationship could be used over the entire pressure range studied, while the latter method could be used only when the measurement of ethylene was possible.

The choice of d/c ratio does not significantly affect the calculated $v_4/v_{3a}^{1/2}$ ratios. The use of d/c = 0.15 instead of 0.117 decreases the ratio by about 0.1% at 500° while at 400° the decrease is in the order of 1-3%.

The experimental data and calculations are shown in Table VII. The mass balance equation

[11] $$v_{C_2H_4} + v_{C_4H_{10}} = v_{H_2}$$

follows at once from equation [8]. Table VII includes the ratio moles C_2H_4 + C_4H_{10}/moles H_2 for those runs where the measurement of ethylene was possible. The fact that this ratio is always close to 1.0 gives support to the reaction scheme given in equations [1] to [4].

The rate constant ratio $k_4/k_{3a}^{1/2}$ was evaluated at 400, 430, 470 and 500°C over a wide range of pressures. Figure 33 shows a plot of log $k_4/k_{3a}^{1/2}$ against the logarithm of pressure. The rate constant k_{3a} for the combination of

TABLE VII

Rates of Formation of Products for Typical Runs

Run #	Temp. °C	Time of Run sec	Pressure mm	v_{H_2}*	$v_{C_2H_4}$*	$v_{C_4H_{10}}$*	$\frac{v_{C_2H_4}+v_{C_4H_{10}}}{v_{H_2}}$	$\log_{10}\frac{v_{H_2}-1.117v_{C_4H_{10}}}{(v_{C_4H_{10}})^{1/2}}$
46	500	180	71.2	41.36		1.175		-4.432
47	500	180	41.7	26.53		0.7687		-4.534
74	500	300	11.7	10.71	9.719	0.4831	0.95	-4.835
75	500	600	6.1	5.547	5.073	0.2504	0.96	-4.978
77	500	300	208.9	68.41		1.272		-4.226
78	500	300	615.5	109.5		1.629		-4.074
79	500	300	357.7	105.3		2.025		-4.140
21	470	300	40.4	13.40		1.286		-4.977
26	470	300	98.8	22.50		1.819		-4.819
30	470	240	462.7	41.23		1.538		-4.497
70	470	600	17.2	6.707	5.962	0.7656	1.00	-5.175

Table VII(continued)

Run #	Temp. °C	Time of Run sec	Pressure mm	v_{H_2}*	$v_{C_2H_4}$*	$v_{C_4H_{10}}$*	$\frac{v_{C_2H_4}+v_{C_4H_{10}}}{v_{H_2}}$	$\log_{10}\frac{v_{H_2}-1.117v_{C_4H_{10}}}{(v_{C_4H_{10}})^{1/2}}$
71	470	600	11.1	5.169	4.201	0.5817	0.93	-5.227
72	470	300	27.7	9.763	9.126	0.9351	1.03	-5.045
80	470	300	398.3	34.83		1.321		-4.537
105	470	600	4.0	1.342	1.130	0.1285	0.94	-5.476
14	430	600	68.8	6.261		1.837		-5.508
15	430	600	176.3	9.030		2.133		-5.342
17	430	600	498.2	12.08		2.402		-5.217
19	430	900	29.8	4.251		1.369		-5.633
84	430	1200	13.3	2.353	1.448	0.771	0.94	-5.770
87	430	1200	7.1	0.8343	0.5321	0.1994	0.88	-5.864
88	430	1800	4.4	0.7346	0.4152	0.2245	0.87	-5.991
89	400	1200	38.9	2.068	1.111	0.9063	0.98	-5.955
90	400	1200	22.9	1.190	0.6093	0.5518	0.98	-6.112

Table VII(continued)

Run #	Temp. °C	Time of Run sec	Pressure mm	v_{H_2}*	$v_{C_2H_4}$*	$v_{C_4H_{10}}$*	$\frac{v_{C_2H_4} \cdot v_{C_4H_{10}}}{v_{H_2}}$	$\log_{10} \frac{v_{H_2} - 1.117 v_{C_4H_{10}}}{(v_{C_4H_{10}})^{1/2}}$
91	400	1200	13.9	1.243	0.5159	0.6714	0.96	-6.221
94	400	600	640.9	4.723		1.343		-5.556
95	400	1200	394.2	3.763		1.179		-5.647
96	400	1200	128.3	2.888		1.122		-5.812
101	400	1800	35.7	2.245	1.137	1.132	1.01	-6.036
102	400	600	14.9	0.9861	0.4728	0.4464	0.93	-6.137
103	400	600	38.7	1.892	1.061	0.8110	0.99	-5.961

* Rates are given in moles cc^{-1} sec^{-1} x 10^{12}

Figure 33

A double logarithm plot of pressure against the rate-constant ratio $k_4/k_{3a}^{1/2}$, showing the pressure dependence of k_4 at four temperatures.

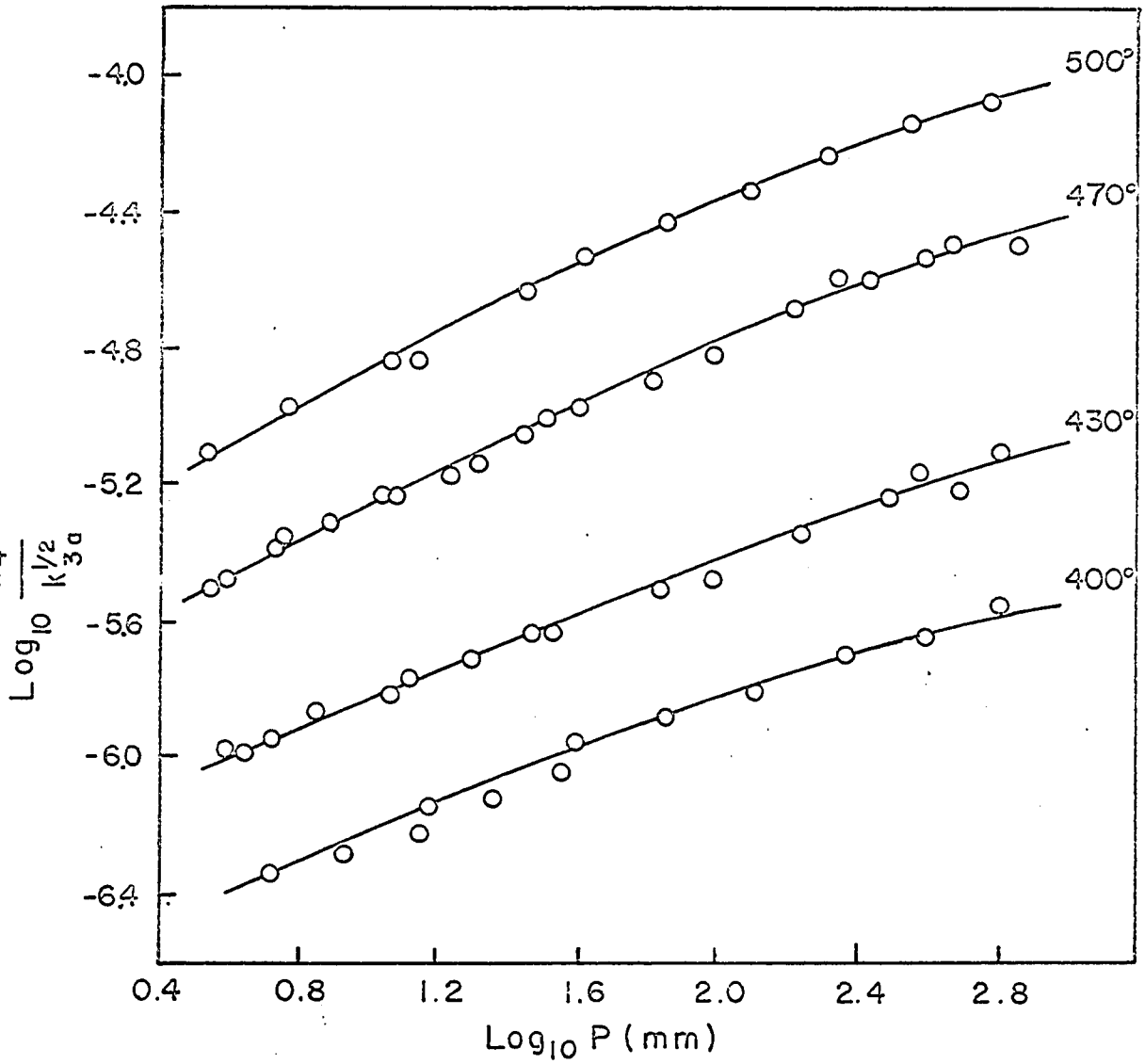
-4.0
-4.4
-4.8
-5.2
-5.6
-6.0
-6.4
$\log_{10} \frac{k_4}{k_{3a}^{1/2}}$
500°
470°
430°
400°
0.4
0.8
1.2
1.6
2.0
2.4
2.8
$\log_{10} P$ (mm)

ethyl radicals should be pressure independent, so that the lower values of $k_4/k_{3a}^{1/2}$ for lower pressures can be attributed to the pressure dependence of the decomposition of the ethyl radical. The slopes of these fall-off curves range from about 0.40 at 600 mm to about 0.60 at 5 mm; thus, the order of reaction for the decomposition of the ethyl radical ranges from 1.4 for the highest pressures studied to 1.6 at the lowest pressures studied. It should be noted that the decomposition of the ethyl radical is pressure-dependent over the entire range of pressures most frequently encountered in gas-phase reactions. The order of the reaction is in good agreement with the value 1.55 suggested by Quinn (41),(37) and with the values 1.38 to 1.59 obtained by Lin and Back (22).

Values of log $k_4/k_{3a}^{1/2}$ were interpolated from Figure 33 at log P = 2.80 (630 mm pressure) and plotted against the reciprocal of temperature as shown in Figure 34. With the assumption that ethyl radicals combine with zero activation energy, this plot yields an activation energy of 37.0 kcal. per mole for the decomposition of the ethyl radical at 630 mm pressure. Also shown in Figure 34 are points interpolated from the data of Lin and Back (22) for the same pressure. These authors had observed an activation energy of 32.7 kcal. per mole for a study at temperatures of 550 and 640°C. Figure 34 shows that the absolute values of their rate-constant ratio are in remarkably good agree-

Figure 24

An Arrhenius plot of $k_4/k_{3a}^{1/2}$ at a pressure of 630 mm.

△ : data of Lin and Back (22).

○ : this work.

The activation energy is 37.0 kcal. per mole.

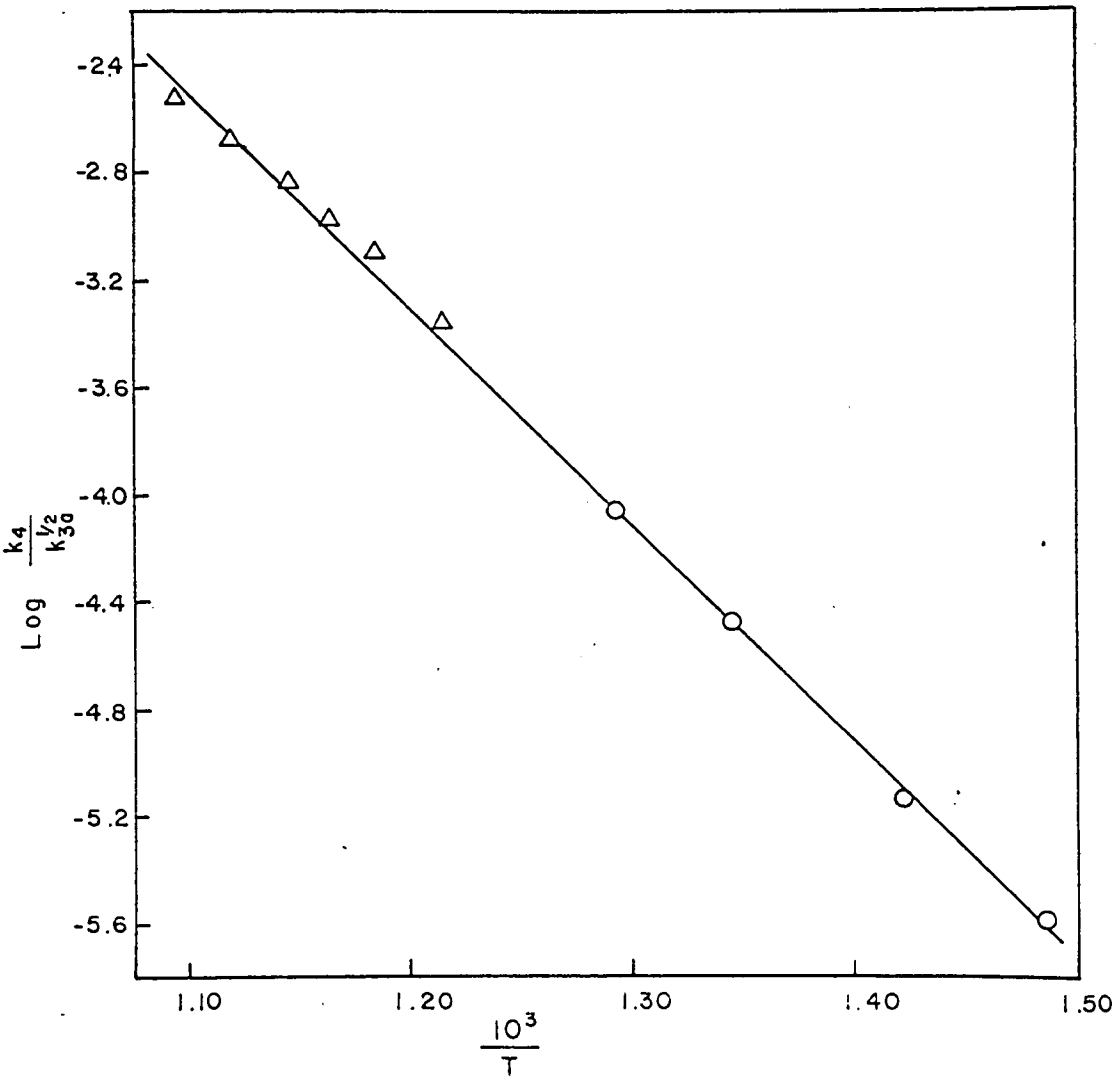
-2.4
-2.8
-3.2
-3.6
-4.0
-4.4
-4.8
-5.2
-5.6
Log $\frac{k_4}{k_{3a}^{1/2}}$
1.10
1.20
1.30
1.40
1.50
$\frac{10^3}{T}$

ment with the present results, with the extension of the line which gave E_4 = 37.0 kcal. per mole cutting through the middle of their data.

The Arrhenius parameters corresponding to the high pressure limit are of more thermodynamic and kinetic interest. Figure 35 shows a Lindemann plot of the reciprocal of the rate constant against the reciprocal of concentration for the data at 500°C. For lower 1/[M] values the typical deviation from linearity is observed and extrapolation to obtain the intercept is seen to be difficult, since the data approach the $k_{3a}^{1/2}/k_4$ axis almost asymptotically. In Figure 35 the square root of the reciprocal of concentration has also been plotted against the reciprocal of the rate constant as suggested by Schlag and Rabinovitch (42). This second method of plotting yields a curve which approaches the rate constant axis more satisfactorily. The intercept has been taken such that both plots were satisfied. From the intercepts of Lindemann plots at each of the four temperatures studied, values of $k_4^\infty / k_{3a}^{1/2}$ were obtained, and Figure 36 shows an Arrhenius plot of the results. The value of k_{3a} has been taken as 2.0×10^{13} cc mole^{-1} sec^{-1} with zero activation energy (43), (39). This value, combined with the slope and intercept of the Arrhenius plot of Figure 36 gives

$$k_4^\infty = 3.5 \times 10^{14} e^{-40,900/RT} \text{ sec}^{-1}$$

The low-pressure limiting rate constant for k_4 has been

Figure 35

Plots used to evaluate k_4^∞ and k_4^0 at 500°C.

o : The usual Lindemann plot of k^{-1} vs $[M]^{-1}$.

x : A plot of k^{-1} vs $[M]^{-1/2}$.

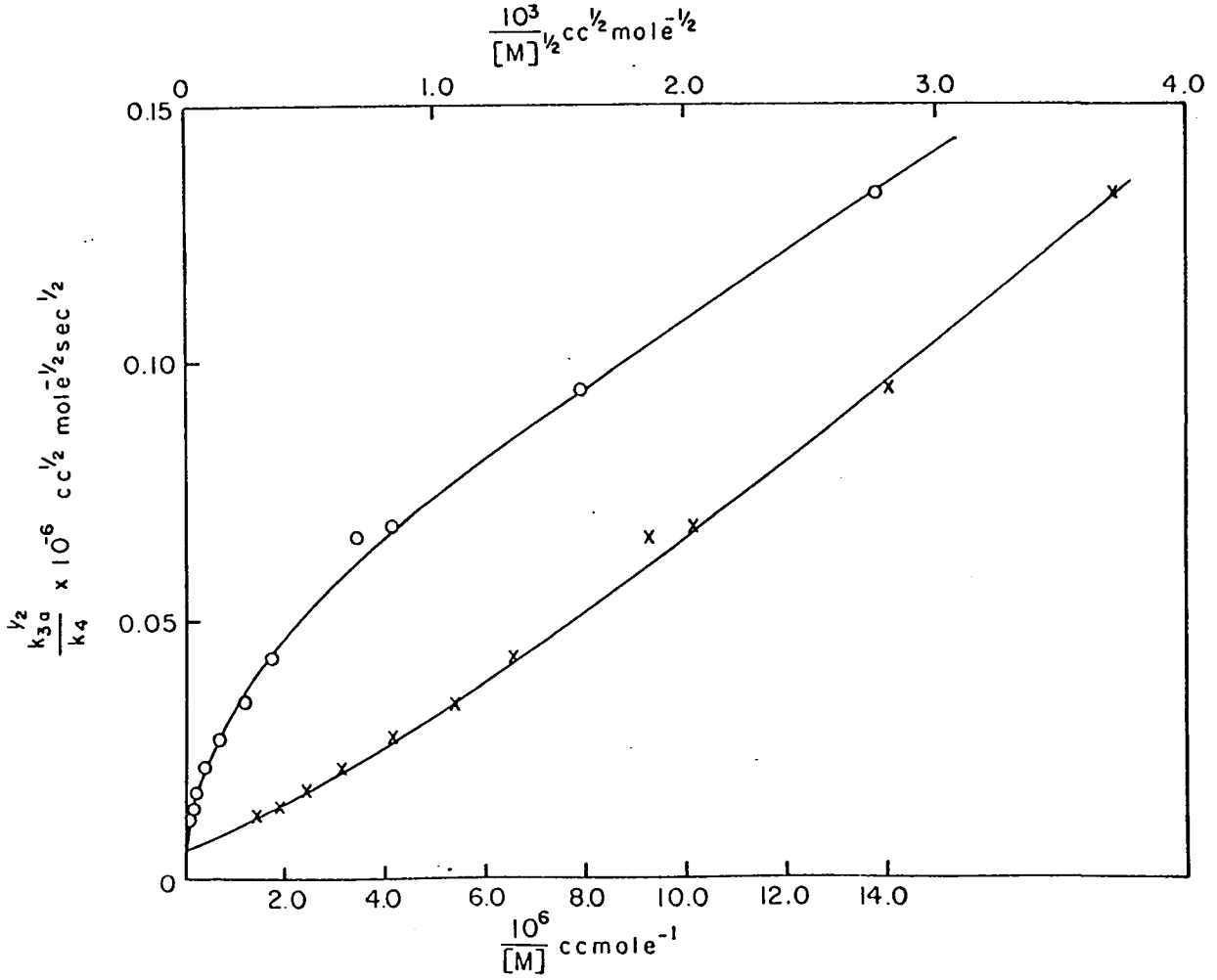
$\frac{10^3}{[M]^{1/2}}$ cc$^{1/2}$ mole$^{-1/2}$
0
1.0
2.0
3.0
4.0
0.15
0.10
0.05
0
$\frac{k_{3a}^{1/2}}{k_4}$ x 10^{-6} cc$^{1/2}$ mole$^{-1/2}$ sec$^{1/2}$
2.0
4.0
6.0
8.0
10.0
12.0
14.0
$\frac{10^6}{[M]}$ ccmole^{-1}

Figure 36

An Arrhenius plot of $k_4^{\infty}/k_{3a}^{1/2}$.

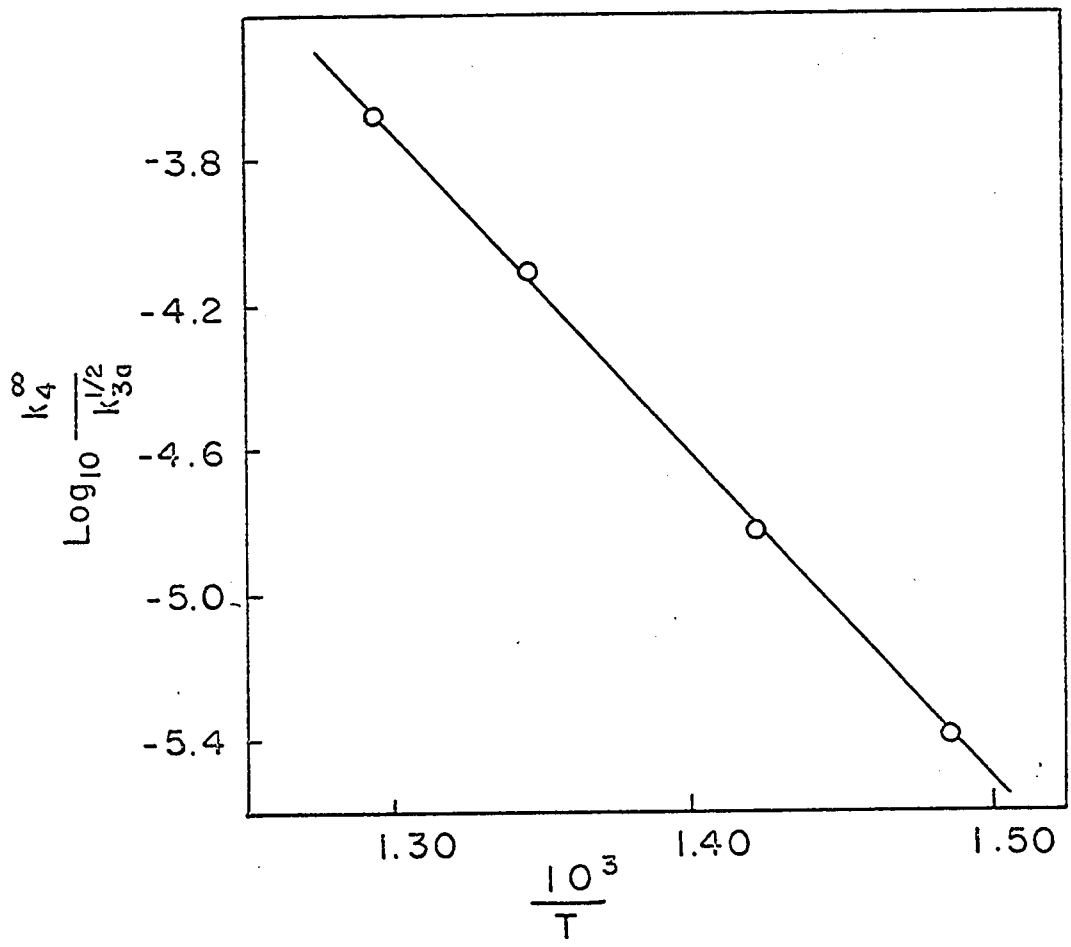
-3.8
-4.2
-4.6
-5.0
-5.4
$\log_{10} \frac{k_4^s}{k_{3a}^{1/2}}$
1.30
1.40
1.50
$\frac{10^3}{T}$

evaluated from the slopes of the Lindemann plots and an Arrhenius plot is shown in Figure 37. The slopes were quite well defined at higher temperatures, but at 400° the slope was not uniquely defined so that the point corresponding to 400° has been weighted less in assigning the slope of the Arrhenius plot. The low-pressure second-order rate constant is given by

$$k_4^o = 6.8 \times 10^{17} e^{-31800/RT} \text{ cc mole}^{-1} \text{ sec}^{-1}$$

In estimating the Kassel parameter s in their work, Lin and Back (17) concluded that this low-pressure rate constant was best described by:

$$k_4^o = 1.4 \times 10^{17} e^{-31800/RT} \text{ cc mole}^{-1} \text{ sec}^{-1}.$$

The extrapolated values of the intercepts and the slopes of the Lindemann plots are shown in Table VIII along with the logarithms of the calculated rate-constant ratios.

The limits of error for E_4^∞ and E_4^o are not easily assessed since the slope and the intercept can only be defined within certain limits. E_4^∞ has a lower limit of 37 kcal. per mole since this value was observed at 630 mm where the decomposition of the ethyl radical is well into its pressure-dependent region. The quoted value for E_4^∞ = 40.9 kcal. per mole is probably valid to ± .5 kcal. per mole. The value of E_4^o = 31.8 kcal. per mole could readily have limits of ± 2 kcal. per mole.

Figure 37

An Arrhenius plot of $k_4^0/k_{3a}^{1/2}$.

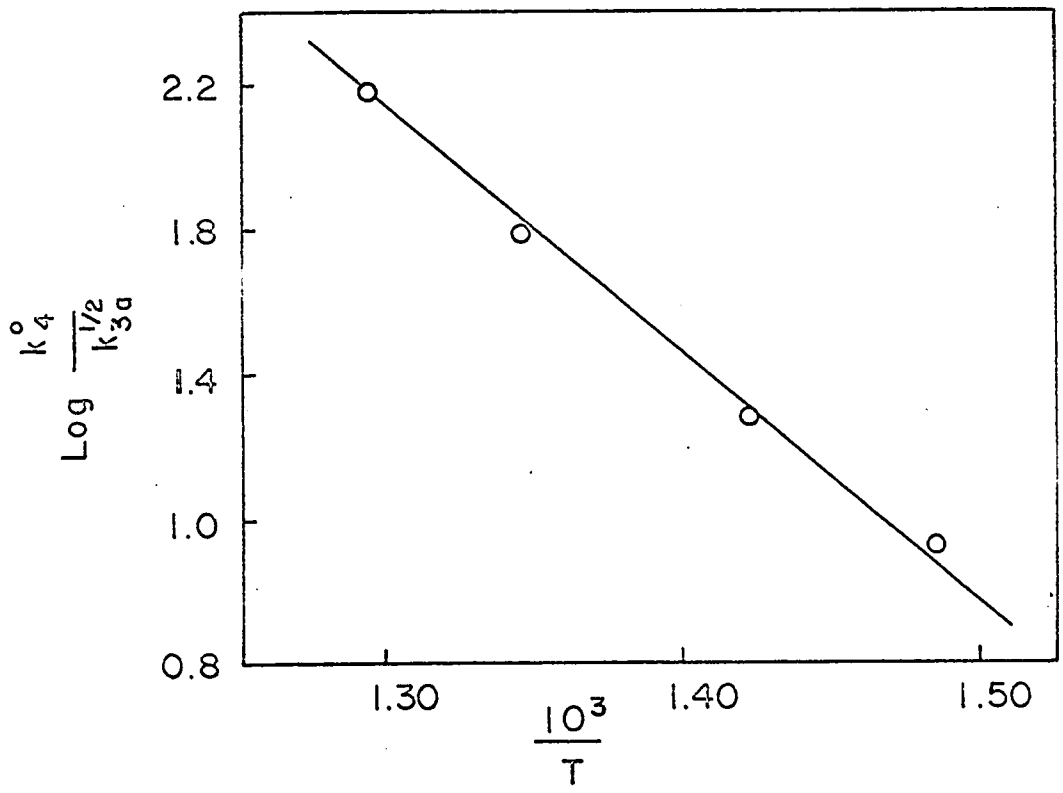
2.2
1.8
1.4
1.0
0.8
1.30
1.40
1.50
$\frac{10^3}{T}$
$\text{Log } \frac{k_4^\circ}{k_{3a}^{1/2}}$

TABLE VIII

Intercepts and Slopes from the Lindemann Plots

Temp. °C	$\frac{k_{3a}^{1/2}}{k_4^{\infty}} \times 10^{-6}$ $cc^{1/2}\ mole^{-1/2}\ sec^{1/2}$	$\log \frac{k_4^{\infty}}{k_{3a}^{1/2}}$	$\frac{k_{3a}^{1/2}}{k_4^{o}}$ $cc^{-1/2}\ mole^{1/2}\ sec^{1/2}$	$\log \frac{k_4^{o}}{k_{3a}^{1/2}}$
400	0.20	-5.398	0.119	0.924
430	0.068	-4.832	0.0523	1.282
470	0.013	-4.114	0.0163	1.788
500	0.0048	-3.682	0.00666	2.177

Homogeneity of Reactions

A separate aspect of the present study concerns the homogeneity of reaction conditions involved in the mercury-photosensitized decomposition of ethane. For all runs so far described the concentration of mercury in the reaction zone was controlled by a spiral trap immersed in a bath at -30°C; the trap was part of the tubing leading to the reaction vessel. The rate of initiation was also studied as a function of the mercury concentration in the reaction vessel, with the concentration of mercury taken as the equilibrium vapor pressure of mercury for the temperature of the bath on the spiral trap. The trap temperature was varied from -30°C to +20°C and a number of runs were conducted at 300°C where no chain reaction will be occurring. At these temperatures, the rate of initiation is given by the rate of hydrogen production. Figure 38 shows the rate of initiation as a function of mercury concentration. It is seen that for higher concentration of mercury, the rate of initiation reaches a maximum. We interpret this maximum to correspond to complete absorption of the resonance line. Associated with complete absorption there should be a concentration gradient of Hg $^3P_1$ ranging from very high near the incident face of the reaction vessel to very low at positions near the dark face of the reaction vessel. Completely homogeneous production of Hg $^3P_1$ would be obtained only when a small fraction of the incident light is absorbed.

Figure 38

The rate of initiation of the mercury-photosensitized decomposition of ethane at 300°C as a function of the mercury vapor pressure in the reaction vessel.

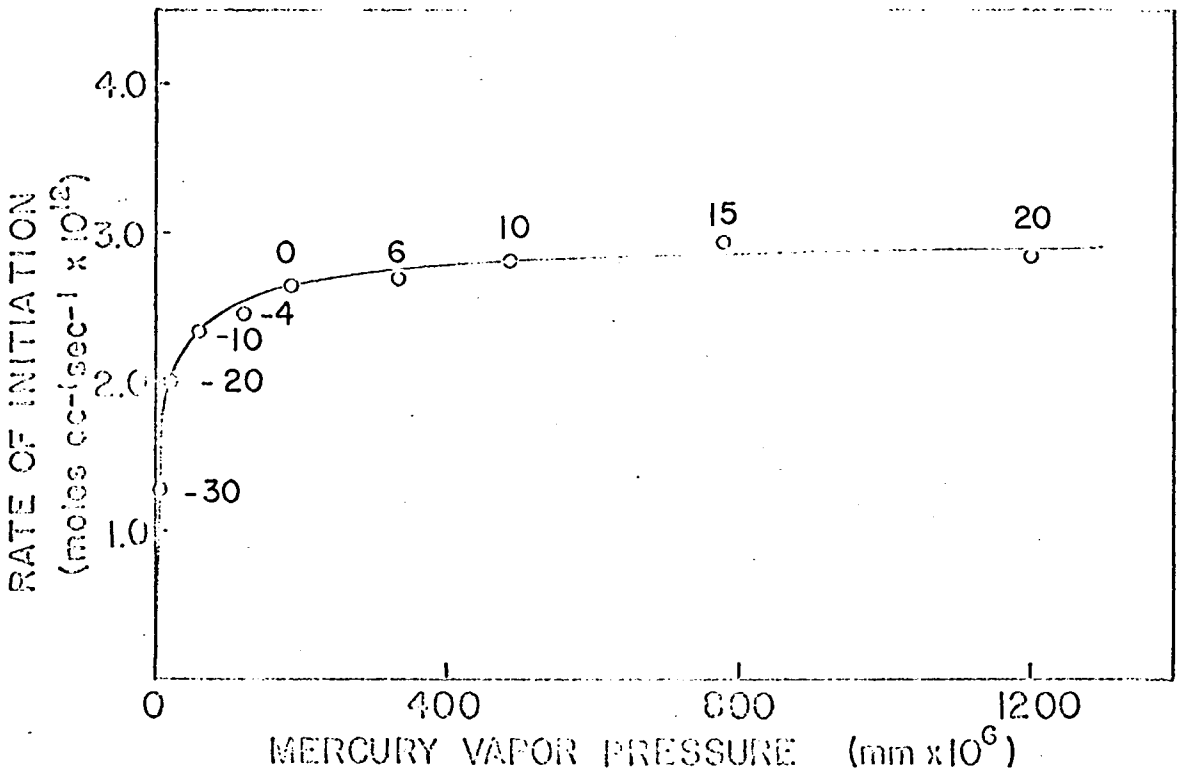
RATE OF INITIATION
(moles cc⁻¹sec⁻¹ x 10¹⁸)
4.0
3.0
2.0
1.0
0
400
800
1200
MERCURY VAPOR PRESSURE (mm x10⁶)
-30
-20
-10
-4
0
6
10
15
20

For -30°C the rate of initiation has been reduced by a factor of 2 and should represent fairly homogeneous reaction conditions. Similar effects observed in the mercury-photosensitized decomposition of dimethyl ether have been described in previous chapters.

DISCUSSION

With the value of k_4^∞ established it is possible to apply the Kassel equation to calculate the expected pressure dependence of the rate constant and to evaluate the s parameter of the Kassel-Rice-Ramsperger theories. The collisions which energize the ethyl radical will usually involve an ethyl radical and an ethane molecule. Thus $\frac{2M_A M_B}{M_A + M_B}$ was taken as 29.558 and the collision diameter for the collision of an ethyl radical with an ethane molecule was taken as 5.0 A. This collision diameter which is greater than the 3.35 A used by Purnell and Quinn (37) is a value obtained from the viscosity data of ethane and has been used previously in the literature (44,45,46). Kassel integrals have been evaluated for various s values at 500°C and the theoretical pressure dependence is compared with the experimental pressure dependence in Figure 39. It is seen that s = 8 is consistent with the experimental pressure dependence. The s value, which is interpreted as the number of normal modes which contribute to the energization of the species decomposing, is slightly higher than reported by Purnell and Quinn (37) or by Lin and Back (17). The higher

Figure 39

A double logarithm plot of $k_4/k_{3a}^{1/2}$ against pressure for experimental points at 500°C and for the curves calculated from the Kassel equation with s = 7, 8 and 9.

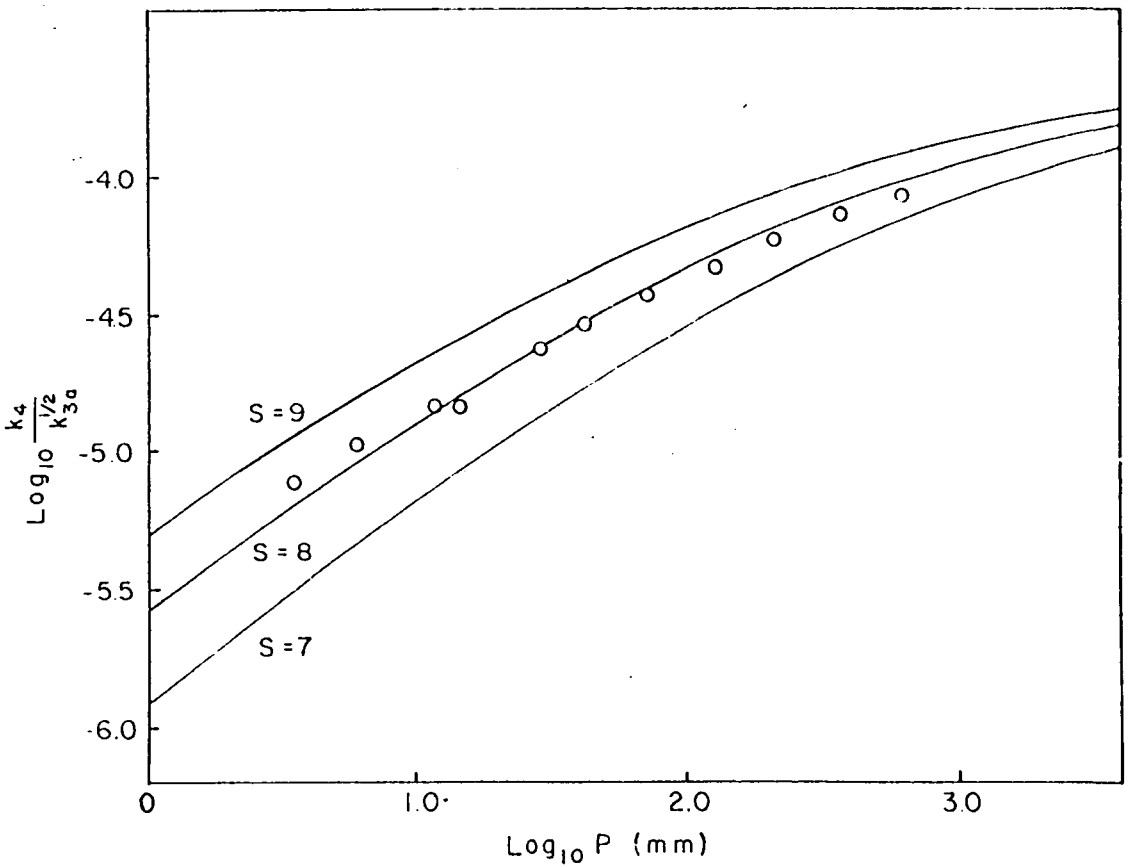
-4.0
-4.5
-5.0
-5.5
-6.0
S = 9
S = 8
S = 7
0
1.0
2.0
3.0
$\text{Log}_{10} \frac{k_4}{k_{3a}^{1/2}}$
Log_{10} P (mm)

s value results from the frequency factor which was found to be considerably greater than the value 10^{13} assumed by Purnell and Quinn. The higher activation energy found in the present work and the larger collision diameter used, would both tend to decrease the s value slightly from the value found by Purnell and Quinn. It may be noted that s = 8 or 9 was observed for the thermal decomposition of the methoxymethyl radical in Chapter III.

Another evaluation of the number of modes contributing to energization is provided by the equation

[12] $$E^{\infty} - E^{o} = (s - 3/2)RT$$

which comes from the Hinshelwood expression for the rate of energization. From the values E_4^{∞} = 40.9 kcal. per mole and E_4^{o} = 31.8 kcal. per mole one obtains s = 8, in agreement with the conclusion from the Kassel equation.

Thermochemistry

With a value of E_4^{∞}, and with a knowledge of the activation energy of the back reaction, E_{-4}, it is possible to calculate the bond dissociation energy of ethane and the heat of formation of the ethyl radical. The activation energy for the addition of a hydrogen atom to ethylene has been reported to be 1.9 kcal. per mole by Yang (47). For the thermochemical discussion we will consider the equations:

[13] $C_2H_6 \longrightarrow C_2H_5 + H$

[4] $C_2H_5 \longrightarrow C_2H_4 + H$

[14] $C_2H_6 \longrightarrow C_2H_4 + 2H$

At a given temperature T the enthalpy change of reaction [4] can be expressed as

[15] $$\Delta H_4^0 (T) = E_4^\infty - E_{-4} + RT$$

where the coefficient of RT is unity since two species are produced from one in the reaction. Also the enthalpy change of reaction [4] at temperature T is related to the enthalpy change at 0°K by

[16] $$\Delta H_4^0 (T) = \Delta H_4^0 (0^0) + \int_0^T \Delta C_p dT$$

ΔH_4^0 (T) was evaluated from [15] and then, with this value, ΔH_4^0 (0°) was found to be 36.2 kcal. per mole from [16], where it has been assumed that the heat capacity of the ethyl radical is the same as that of ethane. The thermochemical data used are those of Rossini et al. (48).

The enthalpy change of reaction [14] at 0°K, ΔH_{14}^0 (0°), is calculated as 134.3 kcal. per mole. The enthalpy change of reaction [14] is the sum of $\Delta H_4^0 + \Delta H_{13}^0$, and hence ΔH_{13}^0 (0°) is 98.1 kcal. per mole. The enthalpy change of the reaction [13] at 0°K is the bond dissociation energy of ethane; thus $D(C_2H_5\text{-}H)$ = 98.1 kcal. per mole. The heat of formation of ethyl radical at 0°K is found to be 30.0 kcal. per mole from the relation

[17] $$\Delta H_f^0(C_2H_5)_{0^0} = \Delta H_{13}^0(0^0) + \Delta H_f^0(C_2H_6)_{0^0} - \Delta H_f^0(H)_{0^0}.$$

The results of analogous calculations for 298, 500 and 800°K are shown in Table IX along with the values obtained for 0°K.

TABLE IX

Thermodynamic Quantities at Various Temperatures for Reactions [4] and [13]

T°K	$(\Delta C_p^\circ)_T T^*$	ΔH_4°	ΔH_{13}°	$\Delta H_f^\circ(C_2H_5)$
		(kcal. per mole)		
0	0	36.2	98.1=D	30.0
298.16	2.2	38.4	98.5	26.2
500	3.3	39.5	98.9	24.1
800	4.5	40.7	99.3	21.9

$$^*(\Delta C_p^\circ)_T T = \int_o^T \Delta C_p^\circ dT$$

REFERENCES

1. R. A. Marcus, B. de B. Darwent and E. W. R. Steacie, J. Chem. Phys., 16, 987 (1948).
2. R. F. Pottie, A. G. Harrison and F. P. Lossing, Can. J. Chem., 39, 102 (1961).
3. A. F. Trotman-Dickenson, J. Chem. Phys., 19, 261 (1951).
4. S. W. Benson and D. V. S. Jain, J. Chem. Phys., 31, 1008 (1959).
5. D. J. McKenney and K. J. Laidler, Can. J. Chem., 41, 1984 (1963).
6. A. Shepp, J. Chem. Phys., 24, 939 (1956).
7. A. F. Trotman-Dickenson and E. W. R. Steacie, J. Chem. Phys., 19, 329 (1951).
8. G. Pilcher, A. S. Pell and D. J. Coleman, Trans. Far. Soc., 60, 499 (1964).
9. F. D. Rossini et al., Selected Values of Chemical Thermodynamic Properties, National Bureau of Standards, Circular 500, (1952).
10. S. Toby and K. O. Kutschke, Can. J. Chem., 37, 672 (1959).
11. A. R. Blake and K. O. Kutschke, Can. J. Chem., 37, 1462 (1959).
12. G. B. Kistiakowsky and E. K. Roberts, J. Chem. Phys., 21, 1637 (1953).

13. K. U. Ingold and F. P. Lossing, J. Chem. Phys., 21, 1135 (1953).

14. K. U. Ingold, I. H. S. Henderson and F. P. Lossing, J. Chem. Phys., 21, 2239 (1953).

15. R. E. Dodd and E. W. R. Steacie, Proc. Roy. Soc., (London) Ser. A, 223, 283 (1954).

16. S. Toby and B. H. Weiss, J. Phys. Chem., 68, 2492 (1964).

17. M. C. Lin and M. H. Back, Can. J. Chem., 44, 2357 (1966).

18. E. K. Gill and K. J. Laidler, Proc. Roy. Soc., (London) Ser. A, 250, 121 (1959).

19. P. B. Ayscough and E. W. R. Steacie, Proc. Roy. Soc., (London) Ser. A, 234, 476 (1956).

20. F. O. Rice and K. F. Herzfeld, J.A.C.S., 56, 284 (1934).

21. K. H. Anderson and S. W. Benson, J. Chem. Phys., 36, 2320 (1962).

22. M. C. Lin and M. H. Back, Can. J. Chem., 44, 505 (1966).

23. This thesis, Chapter VI.

24. H. Hershenson and S. W. Benson, J. Chem. Phys., 37, 1889 (1962).

25. M. F. R. Mulcahy and D. J. Williams, Austral. J. Chem., 17, 1291 (1964).

26. S. W. Benson, The Foundation of Chemical Kinetics, McGraw-Hill Book Co., New York, 1960, p.390.

27. R. H. Martin, F. W. Lampe and R. W. Taft, J.A.C.S., 88, 1353 (1966).

28. S. Marantz and G. T. Armstrong, private communication.

29. This thesis, Chapter III.

30. K. A. Kobe, A. E. Ravier and S. P. Vohra, J. Chem. Eng. Data., 1, 50 (1956).

31. M. Miyoshi and R. K. Brinton, J. Chem. Phys., 36, 3019 (1962).

32. J. W. Warren, Nature, 165, 810 (1950).

33. F. H. Field and J. L. Franklin, Electron impact phenomena and the properties of gaseous ions, Academic Press, 1957, p.114.

34. C. E. Moore, Atomic Energy Levels, Vol. III, National Bureau of Standards, Circular 467, (1958).

35. F. P. Lossing, private communication.

36. This thesis, Chapter VII.

37. J. H. Purnell and C. P. Quinn, Proc. Roy. Soc., (London) Ser. A, 270, 267 (1962).

38. S. Bywater and E. W. R. Steacie, J. Chem. Phys., 19, 326 (1951).

39. J. A. Kerr and A. F. Trotman-Dickenson, J. Chem. Soc., 1611 (1960).

40. B. C. Roquitte and J. H. Futrell, J. Chem. Phys., 37, 378 (1962).

41. C. P. Quinn, Proc. Roy. Soc., (London) Ser. A, 275, 190 (1963).

42. E. W. Schlag and B. S. Rabinovitch, J.A.C.S., 82, 5996 (1960).

43. A. Shepp and K. O. Kutschke, J. Chem. Phys., 26, 1020 (1957).

44. A. F. Trotman-Dickenson, J. R. Birchard and E. W. R. Steacie, J. Chem. Phys., 19, 163 (1951).

45. B. S. Rabinovitch and D. W. Setser, Advances in Photochemistry, Vol. 3; W. A. Noyes Jr., G. S. Hammond and J. N. Pitts Jr., Ed., Interscience, New York, 1964, p.76.

46. S. W. Benson, The Foundations of Chemical Kinetics, McGraw-Hill, New York, 1960, p.155.

47. K. Yang, J.A.C.S., 84, 719 (1962).

48. F. D. Rossini et al., Selected values of physical and thermodynamic properties of hydrocarbons and related compounds, American Petroleum Institute, Carnegie Press, 1953.

APPENDIX I

A Table of Original Data for the Mercury-Photosensitized Decomposition of Dimethyl Ether

Run #	Temp. °C	Time min	Pressure mm	v_{CH_4}	$v_{C_2H_6}$	v_{MEE}	v_{dimer}	v_3
40	200	20	26.2	0.7831	0.1411	0.7284	2.631±	1.7937
41	200	10	13.4	0.3795	0.1305	0.6862	2.871	1.3267
42	200	10	47.0	1.2149	0.0884	0.8785	2.445	2.2702
43	200	10	4.0	0.1581	0.1245	0.6476	1.627	1.0547
44	200	10	256.2	3.5110	0.0974	0.6396	3.504±	4.3454
45	200	10	184.3	2.7610	0.080±	0.7631±	3.017	3.6841
46	200	10	40.8	0.9595	0.1325	0.8183	2.359	2.0428
47	200	15	4.9	0.1666	0.1158	0.6908	1.412	1.0890
48	200	10	12.7	0.3599	0.1757	0.7380	1.486	1.4493
49	200	10	25.0	0.6911	0.1205	0.8365	1.978	1.8186
50	200	10	75.0	1.9851	0.1155	0.6373	2.530	2.6534

Appendix I (continued)

Run #	Temp.	Time	Pressure	ν_{CH_4}	$\nu_{C_2H_6}$	ν_{MEE}	ν_{dimer}	ν_3
51	200	10	130.6	2.2580	0.1206	0.7570	2.781	3.2560
52	200	10	42.3	0.9994	0.1054	0.7580	2.199	1.9682
53	200	5	612.	5.1928	n.f.	0.4157±	3.765	5.6085±
54	200	5	589.	4.8193	tr.	0.6787	3.404	5.498 ±
55	200	5	424.0	3.9618	0.0904±	0.9237	3.293	5.0663
56	248	5	40.0	8.1968	1.237	2.171	0.8543	12.842
57	248	5	12.6	2.8464	1.114	1.787	0.5341	6.861
58	248	5	186.0	25.542	0.8434	1.914	1.345	29.143
59	248	5	5.8	1.362	0.9438	1.185	0.4458	4.4546
60	248	5	26.5	5.1867	1.084	1.956	0.7189	9.3107
61	248	5	9.3	2.0301	0.9960	1.418	0.4745	5.5401
62	248	5	17.5	3.5482	1.179	1.691	0.5462	7.5972
63	248	5	99.5	15.668	0.9478	1.649	0.9639	19.213
64	248	2.5	346.0	35.269	0.6265	1.952	1.867	38.474
65	248	2.5	640.	54.418	0.6345	1.803	2.831	57.490

Appendix I (continued)

Run #	Temp.	Time	Pressure	v_{CH_4}	$v_{C_2H_6}$	v_{RE}	v_{dimer}	v_3
66	248	5	61.0	10.735	0.7532	1.699	0.7473	13.940
67	300	2.5	51.0	36.169	3.000	0.9076	tr.	43.077
68	300	2.5	20.0	16.256	3.012	1.139	tr.	23.469
69	300	2.5	99.5	63.655	3.080	1.502	tr.	71.317
70	300	2.5	7.5	6.856	2.602	0.9076	tr.	12.967
71	300	2.5	14.5	12.714	2.900	1.0723	tr.	19.586
72	300	2.5	33.0	25.490	3.040	1.1566	tr.	32.727
73	300	1.0	233.4	150.90	3.283	3.213	tr.	160.68
74	300	5/6	397.0	223.49	1.807	3.747	tr.	230.85
75	300	2.5	3.4	3.8711	1.944	0.5923	tr.	8.3414
76	300	2.5	57.5	40.771	2.811	1.305	tr.	47.698
77	300	2.5	5.5	5.3767	2.510	0.7510	tr.	11.148
78	200	10	10.0	0.3068	0.1305	0.6998	1.6265	1.2676
79	200	10	5.5	0.2229	0.0753	0.6928	1.360	1.0663

Appendix I (continued)

Run #	Temp.	Time	Pressure	v_{CH_4}	$v_{C_2H_6}$	v_{MEB}	v_{dimer}	v_3
80	225	7.5	62.6	4.8410	0.4779	1.3708	2.236	7.1676
81	225	7.5	40.7	3.4545	0.5622	1.5033	1.968	6.0822
82	225	7.5	5.7	0.7033	0.5154	0.9465	1.138	2.6806
83	225	7.5	9.5	1.0289	0.5127	0.9933	0.9572	3.0476
84	225	7.5	3.2	0.3956	0.2972	1.0330	0.7631	2.0730
85	225	7.5	24.5	2.4458	0.5783	1.3628	1.0977	4.9652
86	225	7.5	95.5	6.9368	0.4351	1.2999	1.794	9.1069
87	225	7.5	157.8	9.5007	0.3307	0.9170	2.062	11.079
88	225	7.5	14.5	1.4632	0.5569	1.3722	1.124	3.9492
89	225	7.5	69.2	5.3892	0.4645	1.4257	1.693	7.7439
90	225	7.5	35.6	3.2013	0.5274	1.6560	Lost	5.9121
91	225	7.5	43.6	3.9850	0.5877	1.5060	1.580	6.6664
92	270	4	41.2	17.196	2.184	1.9277	0.4134	23.492
93	270	4	12.4	5.4809	1.9528	1.5587	0.1914	10.945
94	270	4	5.4	2.9064	1.4659	1.1973	0.1797	7.0355

Appendix I (continued)

Run #	Temp.	Time	Pressure	v_{CH_4}	$v_{C_2H_6}$	v_{MEA}	v_{dimer}	v_3
95	270	4	22.8	9.9465	2.0382	1.6817	0.3396	15.705
96	270	4	61.0	22.1860	1.9955	2.0206	0.3891	28.198
97	270	4	94.7	33.208	1.9880	2.0030	0.5751	39.187
98	270	4	7.0	3.9217	1.6114	1.2036	0.1707	8.3481
99	270	4	146.0	44.277	1.6114	2.2641	0.5068	49.764
100	270	5	3.5	1.8622	1.2811	0.9056	0.1201	5.3300
101	270	3	157.0	47.189	1.5428	2.4506	0.4193	52.725
102	270	4	29.5	11.559	1.9578	1.6817	0.3100	17.156
103	270	3	301.6	74.833	1.0375	2.5736	0.9227	96.638
104	270	4	174.0	51.104	1.5989	2.1837	0.7457	56.486
105	248	6	3.0	0.8565	0.7547	0.9622	0.2564	3.3281
106	248	5	30.3	6.5783	1.2610	2.1305	0.4773	11.231
107	248	5	34.5	7.1793	1.2610	2.0643	0.5572	11.7656
108	248	5	32.2	7.0084	1.3112	2.0241	1.797 ±	11.655
109	248	5	30.7	6.6416	1.2691	2.0040	0.9490	11.184

Appendix I (continued)

Run #	Temp.	Time	Pressure	v_{CH_4}	$v_{C_2H_6}$	v_{MEE}	v_{dimer}	v_3
110	248	5	8.0	1.9798	1.1064	1.2008	0.5392	5.3934
111	248	5	27.0	4.5365	0.9739	1.4157	0.5363	7.9000
112	248	6	3.8	1.0911	0.8066	1.0509	0.3738	3.7552
113	225	7.5	237.4	11.5795	0.2195	lost	1.981	13.337
114	225	7.5	412.4	15.556	0.1138	1.1017	2.062	16.885
115	225	7.5	2.8	0.3150	0.2677	0.7195	0.2712	1.5699
139	248	10	26.7	6.1355	1.1396	1.8283	0.4749	10.243
140	248	10	28.5	6.4107	1.0914	1.6376	0.4819	10.231
141	225	20	30.0	3.0599	0.4478	0.8579	0.2610	4.8134
142	225	15	86.5	7.7979	0.4384	0.9481	0.6225	9.6228
143	225	20	15.2	1.6952	0.4443	0.7831	0.2058	3.3669
144	225	20	8.0	0.9441	0.3765	0.7219	0.2234	2.4190
145	225	20	3.9	0.4882	0.2771	0.3887	0.1055	1.4311

Appendix I (continued)

Run #	Temp.	Time	Pressure	ν_{CH_4}	$\nu_{C_2H_6}$	ν_{AEE}	ν_{dimer}	ν_3
146	225	10	126.0	9.2476	0.2610	0.9739	0.4819	10.744
147	225	15	56.2	5.3681	0.4665	1.0345	0.3916	7.3356
148	270	10	39.3	13.384	1.0321	0.6466	tr.	16.095
149	270	20	24.2	8.7952	1.0654	0.5156	0.02749	11.442
150	270	20	35.9	12.691	lost	0.6054	0.0268	15.496
151	270	20	30.3	11.175	1.1235	0.5996	0.0465	14.022
152	248	20	28.8	6.1847	0.8052	0.7048	0.09543	8.4999
153	248	20	51.2	9.2018	0.6475	0.5868	0.1057	11.084
154	248	20	19.2	4.2174	0.7550	0.6616	0.08248	6.3890
155	200	20	29.2	0.8994	0.1401	0.6822	0.4669	1.8618
156	200	20	17.6	0.5228	0.1576	0.6325	0.4669	1.4705
157	200	20	48.7	1.4517	0.1245	0.5266	0.5823	2.2273
158	200	20	66.6	1.8000	0.1305	0.5038	0.6727	2.5648

Appendix I (continued)

Run #	Temp. °C	Time min	Pressure CO_2 mm	Mercury Trap °C	Pressure mm	v_{CH_4}	$v_{C_2H_6}$	v_{MEE}	v_{dimer}	v_3
117	248	10	59.3		11.0	2.0178	0.6024	0.4985	0.0823	3.7211
118	248	15	97.5		11.0	1.6153	0.4498	0.2744	0.0335	2.7893
119	248	30	279.0		10.0	0.8932	0.2296	0.0363	0.0157	1.4387
120	248	15	36.7		5.2	0.9935	0.4632	0.4726	0.0757	2.3925
121	248	30	107.0		5.1	0.7019	0.2871	0.0897	0.0191	1.3658
122	248	15	104.8		27.5	4.3615	0.6178	0.6406	0.1090	6.2377
123	248	20		-10	22.4	5.5873	1.0582	1.3770	0.2234	9.0807
124	248	10		-20	32.5	6.9578	0.9116	0.9568	0.1064	9.7378
133	248	15		-20	32.5	7.7644	1.0863	1.3461	0.2444	11.283
134	248	15		-20	35.8	8.5676	1.0291	1.1272	0.2075	11.753
135	248	5		-20	37.4	8.8111	1.2410	1.3042	0.1955	12.597
136*	248	10		0	32.7	3.6181	0.3795	0.4383	0.0654	4.8154
137	248	20		-30	34.7	7.8815	0.8659	1.0562	0.1648	10.6695
138*	248	20		0	40.5	4.8594	0.3835	0.5170	0.1129	6.1434

Appendix I (continued)

Run #	Temp.	Time	Pressure CO_2	Mercury Trap	Pressure	v_{CH_4}	$v_{C_2H_6}$	v_{MEE}	v_{dimer}	v_3
159	225	20		-20	36.0	3.7446	0.5351	0.9142	0.5120	5.7290
160	225	20		-10	37.0	3.8553	0.5231	1.3765	0.7882	6.2780
161	225	15		+10	36.5	2.5179	0.3414	0.9880	1.653	4.1887
162	225	15		+20	36.1	1.7770	0.2349	0.8916	1.928	3.1384
163	225	15		0	36.6	3.3988	0.4799	1.3012	1.272	5.6598
164	225	15		+15	37.0	2.1127	0.2564	1.2048	1.774	3.8303
165	225	15		+ 6	36.0	2.6503	0.3762	1.1499	1.519	4.5526
166	225	20		-30	37.0	3.5517	0.4006	0.7839	0.2058	5.1368

All rates are quoted in moles cc^{-1} sec^{-1} x 10^{12}.
Runs 40 to 122, 136, 138 to 140 inclusive were conducted with 0°C for the mercury saturator trap.
Runs 141 to 158 inclusive were conducted with -30°C for mercury saturator trap.
!: indicates a possible error in the measurement.
n.f.: not found.
tr.: trace quantities found.
*: a wire gauze was used to reduce light intensity.

CLAIMS TO ORIGINAL RESEARCH

1. The pressure dependence of the first-order rate coefficient for the unimolecular decomposition of the methoxymethyl radical was studied over the pressure range 3 to 600 mm Hg. Addition of inert gas, CO_2, confirmed the pressure dependence. Kassel integrations were carried out and fitted to the results.

2. The limiting high-pressure and low-pressure Arrhenius parameters for the thermal decomposition of the methoxymethyl radical were deduced from a temperature and pressure study.

3. The pressure dependence of the second-order rate coefficient for the combination of methyl radicals was examined in the mercury-photosensitized decomposition of dimethyl ether.

4. The combination of a methyl radical with a methoxymethyl radical to form methyl ethyl ether was studied over the pressure range 3 to 600 mm. The second-order rate coefficient for this reaction was found to be pressure-dependent. Kassel integrations were carried out for the reverse reaction and fitted to the observed pressure dependence of the combination reaction.

5. The enthalpy of formation of the methoxmethyl radical was deduced from kinetic measurements on the

pyrolysis of 1,2-dimethoxyethane. The heat of formation was independently checked by appearance potential measurements on CH_3OCH_3 and CH_3OCH_2Cl which were combined with kinetic measurements on the thermal decomposition of CH_3OCH_2Cl.

6. The pressure dependence of the first-order rate coefficient for the unimolecular decomposition of the ethyl radical to give ethylene and a hydrogen atom, was studied over the pressure range 4 to 650 mm. The Kassel equation was applied and fitted to the experimental data.

7. The high-pressure and low-pressure rate constants for the thermal decomposition of the ethyl radical were determined from a temperature and pressure study of this reaction.

8. The homogeneity of Hg $^3P_1$ production in a mercury-photosensitized reaction was examined as a function of the mercury concentration.